DETERMINING THE MECHANISM OF CK2.3 SIGNALING IN CELLS ISOLATED FROM PATIENTS DIAGNOSED WITH OSTEOPOROSIS

by

Hilary Weidner-Durbano

A dissertation submitted to the Faculty of the University of Delaware in partial fulfillment of the requirements for the degree of Doctor of Philosophy in Biological Sciences.

Summer 2020

DETERMINING THE MECHANISM OF CK2.3 SIGNALING IN CELLS ISOLATED FROM PATIENTS DIAGNOSED WITH OSTEOPOROSIS

by

Hilary Weidner-Durbano

Approved: _____

Velia M. Fowler, Ph.D.
Chair of the Department of Biological Sciences

Approved: _____

John A. Pelesko, Ph.D.
Dean of the College of Arts and Sciences

Approved: _____

Douglas J. Doren, Ph.D.
Interim Vice Provost for Graduate and Professional Education and
Dean of the Graduate College

I certify that I have read this dissertation and that in my opinion it meets the academic and professional standard required by the University as a dissertation for the degree of Doctor of Philosophy.

Signed: _____

Anja Nohe, Ph.D.
Professor in charge of dissertation

I certify that I have read this dissertation and that in my opinion it meets the academic and professional standard required by the University as a dissertation for the degree of Doctor of Philosophy.

Signed: _____

Liyun Wang, Ph.D.
Member of dissertation committee

I certify that I have read this dissertation and that in my opinion it meets the academic and professional standard required by the University as a dissertation for the degree of Doctor of Philosophy.

Signed: _____

Donna S. Woulfe, Ph.D.
Member of dissertation committee

I certify that I have read this dissertation and that in my opinion it meets the academic and professional standard required by the University as a dissertation for the degree of Doctor of Philosophy.

Signed: _____

Robert A. Sikes, Ph.D.
Member of dissertation committee

I certify that I have read this dissertation and that in my opinion it meets the academic and professional standard required by the University as a dissertation for the degree of Doctor of Philosophy.

Signed: _____

Jessica E. Tanis, Ph.D.
Member of dissertation committee

ACKNOWLEDGMENTS

I would like to thank both the NIH and the Department of Biological Sciences at the University of Delaware for my funding in the pursuit of my degree. None of this would be possible without the funding and support granted from both institutions. I am extremely thankful to my advisor Dr. Anja Nohe who helped me grow not only as a researcher, but as a person. She imparted both independence and confidence in myself throughout my career at UD, and for that I will be forever grateful. I cannot even begin to summarize how many times I barged into her office or called her on the phone panic-stricken. She always knew what to say and how to guide me through the troubling times that are sprinkled throughout Graduate school. I cannot count how many times she told me to "stop freaking out." When I first met with her she gave me my choice of projects, and while cancer research always interested me, the passion and love she instilled in me for studying osteoporosis and potential therapeutics, made my choice quite easy. I could not be more elated with my project and how it progressed.

I would like to thank my committee members Dr. Robert Sikes, Dr. Donna Wolf, Dr. Liyun Wang, and Dr. Jessica Tanis for their continued support and guidance. Dr. Liyun Wang gave me the remarkable opportunity to complete my rotation in her lab. Unfortunately, due to COVID19 closures and unexpected shutdowns, the overall goal of my rotation project shifted. She did not hesitate to formulate a plan and provide me with a "virtual project" to complete. Dr. Sikes helped me fine tune my approach to all things PCR related when I was facing difficulties, as well as providing constructive, but vital criticism during my committee meetings. He

helped me expand my horizons as a researcher. Dr. Woulfe gave me consistent advice on how to speak or write about science related topics, which in turn made me conscious of my love for both writing and communicating science. When Dr. Tanis joined my committee later, she was just as helpful in offering feedback. She gladly joined my committee without pause, for which I am grateful. I would also like to thank Dr. Randy Duncan, who was a former member of my committee and a fellow bone biologist. His expertise guided me through the difficulties of studying bones. University of Michigan is fortunate to have him. Thank you to Dr. Mark Eskander, Debbie Dibert, and Sean McTague for collaborating with us and providing our specimens to us so readily. You made the trips to Christiana Care a breeze.

I would like to thank Dr. Melinda Duncan and Dr. Erica Selva for guiding our department and helping answer my numerous questions. Thank you Dr. Selva for ensuring I had funding through the last portion of my degree. It means the world to me. I would also like to sincerely thank Betty Cowgill, Jim Farmer, and Jaime Quesenbury for their continued support throughout the pursuit of my degree. Betty always knew the answers to my many questions – having her in the department is a true blessing. There is no one in the department who does not think highly of her. Both Jim and Jaime helped me trouble shoot and repair many pieces of broken equipment and kept our lab sane throughout the McKinly fire incident. I am certain that without them my project would not have been possible. The department would simply not function without all of them.

I would like to thank all of my former lab members: Dr. Hemanth Akkiraju, Aprana Swarup, Prashanth Moku, Lauren Harper, Caitlin Deung, Ryan Kabrick, Dr. Vrathasha Vrathasha, Lora Schell, Ryan Wood, and Semaj Kelly. Each of them taught

me so many things. I do not know where I would be without them. I would also like to thank my current lab members: John Nguyen, Danny Halloran, Brian Heubel, and Victoria Stone. You have made coming to lab so much fun. I will miss working with each of them in our lab. John has offered so much support throughout this process. I do not know if I would have been able to complete western blots without him. Canada is very lucky to have him. Danny has become such a close friend of mine. I know our friendship will last a lifetime. He is an amazing scientist and even better friend. I know that his future is bright and he will be doing great things! Brian has been one of the most eager researchers I have ever met and the lab is lucky to have him.

I would like to sincerely thank all of my family and friends who have stood by my side and encouraged me throughout this process. Mom and Dad, you have supported me my entire life. I would not be in the position that I am in today without your sacrifices and unconditional love. I am so blessed to come from such a loving and supportive family. Thank you mom, for always being a phone call away, and always dropping everything just to talk with me. She is truly my best friend; I do not know what I would do without her. Dad, thank you for your constant advice and encouragements, without them I would not gotten through this experience. I love you both so much.

Thank you to my brother Zachary and my grandparents for their unconditional love and support. Zachary, you have faced so many challenges in your lifetime and you have overcome them all. I could not be more proud of the computer scientist you have become. My grandparents: Jeannette, Edward, Diane, and Earl have always believed in me. I cherish all the time I have gotten to spend with them. Edward,

Buddy, is no longer with us – however he has always been such a strong influence in my life. He helped me become the woman that I am today.

Last, but certainly not least, I would like to thank my husband, Mike. I am not sure anyone could have put up with me and my anxiety ridden self as much as he did. Coming home to you every day made the bad days good, and the good days even better. I could not be more fortunate to have you in my life and as my husband. You are one of the most compassionate and loving people I have ever met. Your praise and solace gave me what I needed to obtain this degree. You are my rock.

I could go on, with many more thank you notes to more of my family and friends. However, if I do, I fear my acknowledgments may be as long as my dissertation. Please know, that even if you are not mentioned above, you have helped me complete this degree, and I will always be so grateful.

TABLE OF CONTENTS

LIST OF TABLES

LIST OF FIGURES

ABSTRACT

Bone is an extremely important organ as it provides structure, protects other internal organs, anchors muscles to assist in locomotion, and supports mineral homeostasis. Two major cell types found within bone that are responsible for its maintenance are osteoblasts (bone building cells) and osteoclasts (bone resorbing cells). However, there are many different bone diseases in humans where bone becomes unhealthy or the critical balance between osteoblasts and osteoclasts may become disrupted. The most common bone disease in humans is osteoporosis (OP), which is characterized by low bone mineral density. Current therapeutics treating OP have a laundry list of negative side effects, and a majority can be taken only for a limited number of years, with drug holidays interspersed throughout their use. Therefore, there is a need to develop new therapeutics that target both osteoblasts and osteoclasts to treat this debilitating bone disease.

Bone morphogenetic protein 2 (BMP2) is a potent growth factor that is known to activate both osteoblasts and osteoclasts. Recently, many studies have showed a lack of BMP2 response in OP patients. While BMP2 may not be an effective or ideal treatment for OP, its signaling pathway is still of interest since it controls both osteoblasts and osteoclasts. The Nohe lab has extensively studied this protein and its signaling pathway. They previously discovered a novel interaction between the BMP type Ia receptor (BMPRIa) and an interacting protein called casein kinase II (CK2). Several CK2 phosphorylation sites were discovered on BMPRIa and corresponding blocking peptides (named CK2.3, CK2.2, and CK2.1) were designed to further

elucidate their function. The peptides are hypothesized to bind to CK2 and block the interaction with BMPRIa at that site. Previously, CK2.3 has been shown to increase osteoblast activity and decrease osteoclast activity in a variety of animal models and cell lines. CK2.3's effect on primary human cells has not yet been investigated.

In this study, I investigated BMP2 and CK2.3's effect on isolated osteoblasts from human femoral heads obtained from patients undergoing hip arthroplasty surgery at Christiana Care Hospital in Newark, DE. The patients were diagnosed with either OP or osteoarthritis (OA), however prior to experimentation the clinical diagnosis was confirmed through single photon absorptiometry by X-raying the femoral heads. After confirmation, cells were extracted from the femoral heads and stained for osteoblast specific markers osteocalcin (OC) and alkaline phosphatase (ALP) to determine if the extracted cell population was mature osteoblasts. The cells also were assessed for mineralization potential through a von Kossa assay after stimulation with either BMP2, CK2.3 or left unstimulated (US). Cells extracted from OA patients had increased their mineralization significantly after both BMP2 and CK2.3 stimulation. Cells extracted from OP patients only significantly increased their mineralization after CK2.3 stimulation. Cells from OP patients did not respond to BMP2 stimulation. Next, the cells were stained again for osteoblast specific markers following BMP2 and CK2.3 stimulations. CK2.3 significantly increased fluorescent intensity of the osteoblast specific markers, while BMP2 did not.

BMPRIa levels were investigated in a variety of models using both *in vitro* and *in vivo* approaches. Increase fluorescent expression was observed in MMA embedded bone slices of OP patients when compared with control patients. Explants from both OP or control patients were stimulated as mentioned previously. In control explants

both BMP2 and CK2.3 stimulation significantly increased BMPRIa and CK2 expression when compared to US. In OP explants only CK2.3 significantly increased expression of these two proteins, while BMP2 significantly decreased BMPRIa and CK2 expression. Steady state mRNA levels also showed a decrease in *BMPRIa* after BMP2 stimulation. The consequences of this decrease in expression could be causing an overall decrease in BMD; therefore, downstream signaling proteins like pSMAD and pERK were investigated. Both BMP2 and CK2.3 did not change the immunofluorescent or protein expression of pSMAD. CK2.3 significantly increased expression of pERK in both the fluorescent and protein expression studies, indicating that CK2.3 still acts through ERK signaling in humans. BMP2 significantly decreased expression of pERK in both experiments, indicating that this lack in response may be due to aberrant BMP signaling.

Previously, CK2 was discovered to bind and phosphorylate ERK in several cell lines. Since CK2.3 is known to act through this signaling pathway, and directly binds and mediates CK2 activity, this could be a possible explanation as to how CK2.3 induces a response in cells derived from OP patients, while BMP2 does not. Therefore, this was investigated through a fluorescent colocalization study. No significant changes in colocalized pixel distribution was discovered between pSMAD and CK2. CK2.3 significantly increased pixel colocalization between CK2 and pERK, when compared with BMP2 and US cells, indicating a potential mechanism of action. Given the research presented here, CK2.3 continues to be a unique potential therapeutic for the treatment of OP. It is critical to continue exploring this mis-regulation in BMP signaling, as well as to further delineate the exact mechanism of CK2.3.

Chapter 1

INTRODUCTION

1.1 Bone, a Dynamic Organ

Human bone is a specialized organ that is changing constantly. Maintaining healthy bones is critical as it provides structure, protection of internal organs, locomotion through anchoring and attachment of muscles, and mineral homeostasis(1). The tensile strength of bone is comparable to cast iron, however, bone itself is much more flexible and dynamic as it responds to mechanical and hormonal stimuli(2-4). Approximately 10% of human bone is remodeled per year, and as a result the entire human skeleton is regenerated every ten years(5). Mis-regulation in bone maintenance can lead to increased bone porosity. An extremely common, debilitating bone disease, osteoporosis, is characterized by this disruption in regulation(6). To further understand the causes of osteoporosis, the structure of bone and different types of bone must be discussed and understood.

1.1.1 The Structure and Types of Bone

The human skeleton can be categorized into five major types of bone and they are classified based upon their shape. There are short (carpals, tarsals), flat (sternum, ribs), long (femur, tibia), irregular (vertebrae, facial bones), and sesamoid bones (patella). Each type has a general function including support, leverage, protection of internal organs, points of attachment for muscles, tendon protection, and stability(7). All bone is comprised of four layers of bone tissue; the periosteum, compact/cortical

bone, spongy/cancellous/trabecular bone, and bone marrow. The periosteum is the outermost layer of bone tissue, which surrounds and protects the bone tissue with a strong fibrous network. The periosteum network is comprised of two layers: the fibrous layer made up of fibroblast cells and the osteogenic layer made up of progenitor bone cells(7). Cortical or compact bone is the outer dense shell and makes up approximately 75-80% of total skeletal mass. The mass of cortical bone matrix per unit of volume is greater than that of cancellous or spongy bone. Since cortical bone has a higher density and lower porosity, it is less flexible than cancellous bone. The structure of the whole skeleton is determined by the contribution of cortical bone, which creates a dense, but highly organized structure.

As seen in Figure 1.1, cortical bones are comprised of circular structures known as osteons, which is where bone remodeling takes place. Within osteons there are spaces called lamellae which are connected through small channels termed canaliculi. Haversion canals are tubes located in the center of osteons. They contain blood vessels which helps deliver nutrients and cells necessary for bone remodeling.

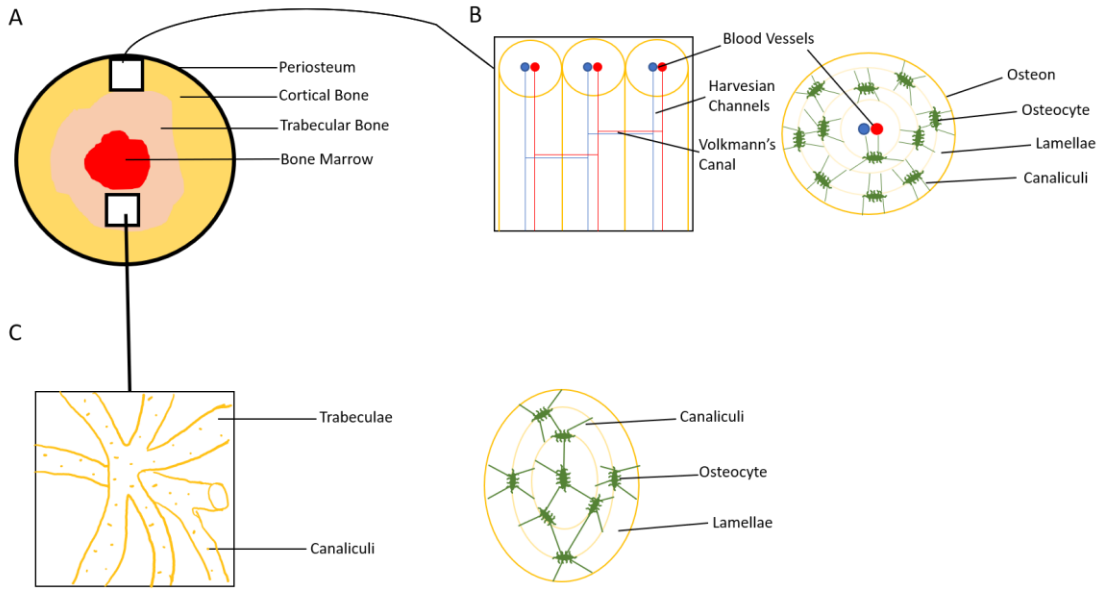

Figure 1.1 **Molecular Dynamics of Bone Tissue.** (A) A cross section of bone with its four major layers. (B) Schematic of cortical bone organization. (C) Schematic of trabecular bone organization.

Osteons are connected to each other through Volkmann's canals, which connects blood vessels. In long bones, like the femur, cortical bone forms the shaft of the bone or the diaphysis, however proximal to the diaphysis is the metaphysis where the cortical bone begins to thin and cancellous bone can be found. In short bones there are thinner layers of cortical bone and more cancellous bone(2, 7). Cancellous bone is composed of plates and rods of trabeculae and it makes up approximately 25-30% of total skeletal mass. Structurally, cancellous bone has lamellae that are arranged parallel to the trabecular surface, Figure 1.1C. Thin, microscopic canals connect lamellae to one another and the bone surface, called canaliculi. Small spaces between lamellae are termed lacunae. There are half osteons or hemiosteons that are indicative of previous sites of bone remodeling. The hemiosteons border marrow cavities and are

separated from the rest of the trabeculae by a cement line. The cement line is the boundary between osteons and the bone matrix not currently undergoing bone resorption. It is located along the bottom region of a bone remodeling center. In cancellous bone, bone remodeling takes place on a longer surface than it does in cortical bone (Haversion canals) and since it takes place next to marrow cavities a central vascular channel is not needed(8). How bone is created or resorbed is dependent on the various types of bone cells contained within it.

1.1.2 Bone Cells and their Functions

On the cellular level, bone is comprised of four different cell types which are responsible for the bone remodeling process. Since bone is a mineralized soft connective tissue, the bone remodeling cycle is an extremely intricate process which old or damaged bone is replaced by new bone, and it occurs through the coordination of four cell types: osteoclasts, osteoblasts, osteocytes, and bone lining cells(9, 10). They all come together to form the basic multicellular unit (BMU), which can be seen in Figure 1.2(11).

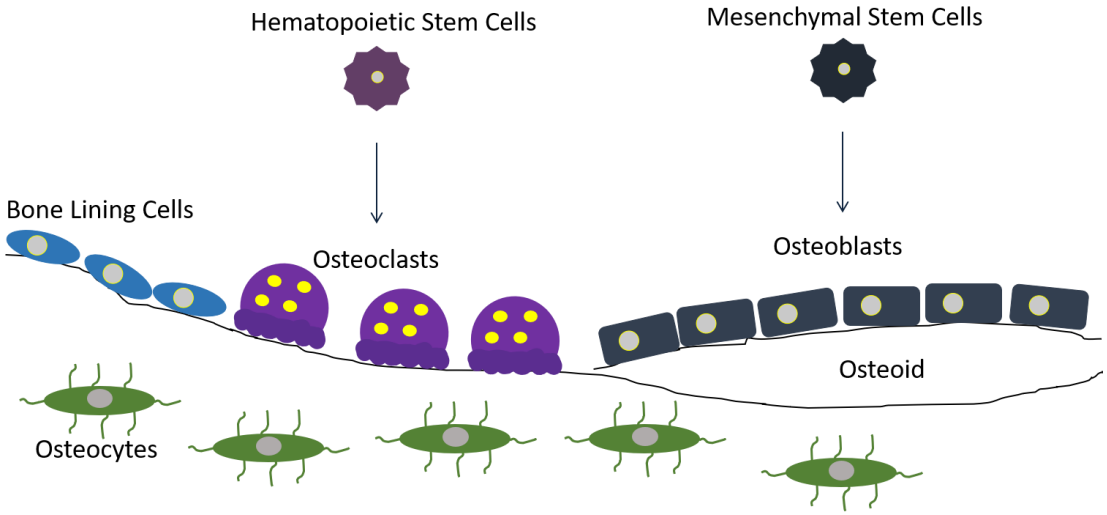

Figure 1.2 **A Schematic of the Bone Remodeling Cycle**. Osteoblasts build new bone while osteoclasts resorb back old or damaged bone. Osteoblasts can terminally differentiate into bone lining cells or osteocytes. Osteoblasts originate from mesenchymal stem cells (MSCs) and osteoclasts originate from hematopoietic stem cells (HSCs).

This coordination is both responsible and necessary for fracture healing, skeletal adaptation to mechanical use, and for calcium and mineral homeostasis(12).

1.1.2.1 Osteoclasts

Osteoclasts are terminally differentiated multinucleated cells derived from HSCs under the influence of several important growth factors such as macrophage colony-stimulating factor (M-CSF), and receptor activator of nuclear factor kappa β ligand (RANKL)(10). Both of which are secreted by osteoprogenitor cells (osteoblasts, osteocytes or stromal cells) and promote the activation of transcription factors and gene expression in osteoclasts(13). M-CSF binds to its receptors on osteoclast precursor cells, which stimulates their proliferation and inhibits apoptosis. RANKL binds to the RANK receptor, also located on osteoclast precursors and pushes

them to differentiate further into multinucleated osteoclasts. However, osteoblasts also produce a decoy receptor known as osteoprotegerin (OPG), which binds directly to RANKL preventing it from binding to RANK and promoting osteoclastogenesis(14). Osteoclasts are formed through the fusion of mononuclear precursor cells. They are responsible for resorbing back old or damaged bone during the initial phases of the bone remodeling cycle, and as mentioned before, are an integral part of the BMU(9, 15). Bone resorption involves the dissolution and degradation of the organic bone matrix through the osteoclast producing and secreting acid and proteolytic enzymes. They are also responsible for transporting and shuttling the degraded bone products through themselves(15).

In order to effectively conduct bone resorption the osteoclasts must polarize and reorganize their cytoskeletons into four separate types of domains on their membrane, which can be seen in Figure 1.3. (10).

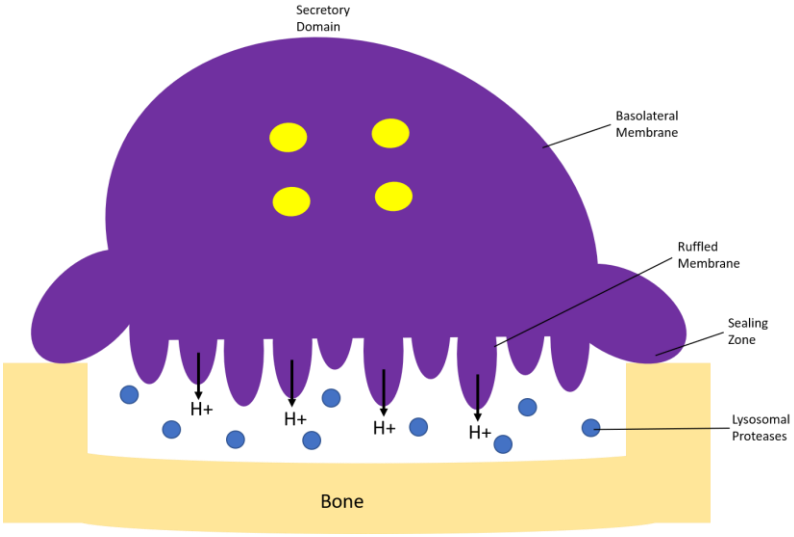

Figure 1.3 **Diagram of an Osteoclast**. The osteoclast is a multinucleated cell from the HSC lineage. When active, it contains four different membrane regions: secretory, basolateral, ruffled, and the sealing zone. The ruffled membrane is responsible for excreting protons and lysosomal proteins to help degrade the bone surface. The sealing zone is to help protect the outer regions of bone not currently undergoing resorption.

They are the sealing zone, ruffled border, basolateral, and functional secretory domains. The sealing zone and the ruffled border are in direct contact with the bone matrix, whereas the basolateral domain is located peripheral to the matrix and the functional secretory domain is located on the opposite side of the bone matrix(15). The polarization of the membrane occurs with the rearrangement of the actin cytoskeleton, where a thick constant zone of highly dynamic podosomes (known as the F-actin ring) is formed. This zone is formed to provide an isolated area of membrane which becomes the ruffled membrane domain of the osteoclast. This only occurs when the osteoclast is in direct contact with the mineralized bone matrix through the attachment of $\alpha_V\beta_3$ integrin and CD44, which binds to noncollagenous

bone matrix proteins containing the RGD sequence (bone sialoprotein, osteopontin, and vitronectin)(16).

The ruffled border itself is formed by microvilli and is separated from the surrounding bone tissue by the clear or sealing zone of the membrane(10). These zones are domains that are devoid of organelles and are located adjacent to the mineralized bone matrix. Within the ruffled membrane there are vacuolar-type H^+-ATPases, which helps to acidify the resorption lacuna (or Howship lacuna) and dissolve the hydroxyapatite crystals found within the mineralized bone matrix(15). Dissolving the hydroxyapatite and collagen releases a large amount of calcium, phosphate, and other peptide fragments (like osteocalcin, osteopontin, and osteonectin(15). This peptide fragments can be released into the extracellular fluid or become transcytosed through the osteoclast to the functional secretory domain. Osteocalcin, osteopontin and osteonectin may be released from the matrix as active petides (or may become activated) where they are responsible for promoting osteoblast recruitment/differentiation, promoting bone formation, regulating calcium, or organizing mineral/collagen components within the matrix(17). Protons and enzymes are secreted through the ruffled membrane of the osteoclasts into the Howship lacuna to promote degradation. Secreted enzymes include tartrate-resistant acid phosphatase (TRAP), cathepsin K, and matrix metalloproteinase-9 (MMP-9). Once dissolved, the products are then either endocytosed across the ruffled border and transported internally to the functional secretory domain of the osteoclast, where they are exported or released into the extracellular fluid under the sealing zone of the osteoclast(10, 15).

1.1.2.2 Osteoblasts

Osteoblasts stem from the MSCs lineage and are located along the bone surface. They are cuboidal in shape and are known for their bone forming capacity. They have abundant rough endoplasmic reticulum with dilated cisternae, large Golgi apparatuses with multiple Golgi stacks, and vesicles/vacuoles containing fibular structures(18, 19). When osteoblasts become polarized, they secrete osteoid, or unmineralized, uncalcified, unmatured bone, toward the bone matrix, Figure 1.4.

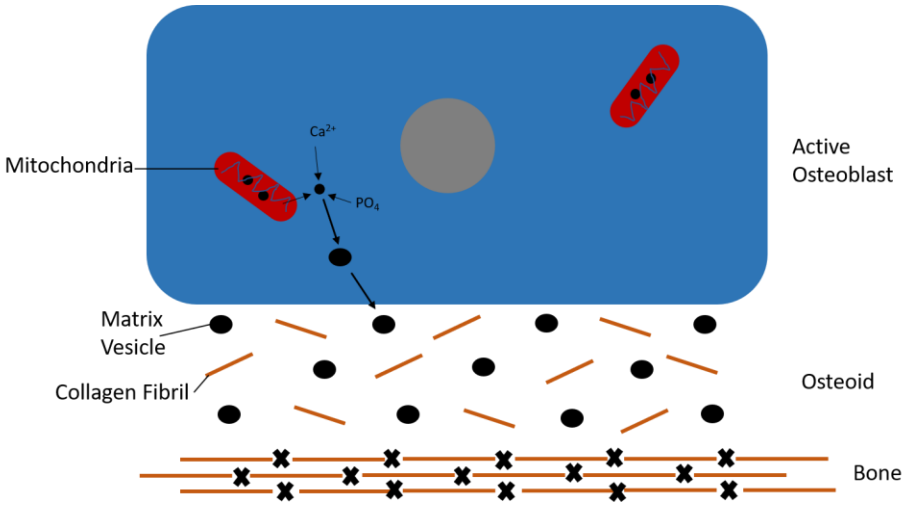

Figure 1.4 **Active Osteoblast Schematic.** Osteoblasts release matrix vesicles containing calcium and phosphate molecules, which continue to influx into the vesicles until the vesicles itself bursts. The mature hydroxyapatite crystals (indicated with an X) are deposited onto the ends of the collagen fibrils.

The osteoid also is important because it houses and stores several crucial growth factors necessary for osteoblast differentiation. Those growth factors include bone morphogenetic proteins (BMPs) and members of the wingless (Wnt) pathways(18, 19). These crucial growth factors are released upon osteoclast mediated bone

resorption and lead to the recruitment/differentiation of osteoblasts, the bone forming cells. Other genes responsible for differentiating MSCs into osteoblasts are runt-related transcription factor 2 (Runx2), distal-less homeobox 5 (Dlx5), and osterix (Osx)(18). Runx2 is known as the master regulator of osteoblast differentiation and regulation because it is responsible for upregulating other osteoblast specific genes like osteonectin (OCN), alkaline phosphatase (ALP), bone sialoprotein (BSP), collagen type I AI (COL1A1), and osteocalcin (OC)(20). Once progenitor osteoblasts express Runx2 and COL1A1 they are considered pre-osteoblasts and will begin to proliferate and induce ALP activity. Pre-osteoblasts become mature osteoblasts when they express Osx and secrete COL1A1, BSP or other bone matrix proteins. The morphology of the cells also begin to become larger and more cuboidal as the cells differentiate into mature osteoblasts(18, 20).

Mature osteoblasts are responsible for synthesizing and mineralizing new bone. This process occurs in two major steps: the deposition of organic matrix and mineralization of bone. The deposition of the organic matrix occurs when osteoblasts secrete collagen proteins (type I collagen, noncollagenous proteins (OCN, OC, BSP, and osteopontin), and proteoglycans (decorin and biglycan), which form the organic bone matrix(10, 11). Type I collagen is a polymeric protein that initially is secreted in the form of a precursor form of collagen. This contains peptide extensions at the amino and carboxyl ends, which eventually are removed proteolytically and collagen begins to take on a three-chained form. These collagen molecules assemble themselves into collagen fibrils which become interconnected with each other through the formation of pyridinoline cross links. Collagen proteins are expressed ubiquitously in vertebrates and other multicellular organisms as they are responsible for

maintaining their structural integrity. Collagen fibrils also define the shape of the tissues in which they are located. The organization of these collagen fibrils are not only thermally stable, but allow for condensed organization that leads to increased structural support. As other non-collagenous proteins are produced, they also are incorporated into collagen fibrils themselves, which gives shape to the organic and unmineralized bone matrix(21).

Mineralization of the organic bone matrix is the second step of bone formation, which takes place in two additional phases. The first phase is known as the vesicular phase and involves matrix vesicles (MVs) produced by osteoblasts. The MVs are released from the apical membrane of the osteoblast and they are approximately 30-200nm in length. Once released MVs combine with the organic bone matrix where they bind to proteoglycans and other organic components. Within the MVs are calcium ions that become immobilized through the binding the negatively charged sulfated proteoglycans. The proteoglycans become degraded through the secretion of osteoblast enzymes, where the immobilized calcium is released from the MVs through channels formed by annexin proteins. Phosphate containing compounds also are located in MVs and are degraded into phosphate ions by ALP. This occurs through decreasing pyrophosphate levels and increasing inorganic phosphate levels, which ultimately promotes mineralization. The phosphate and calcium ions nucleate when inside the MVs, which form a compound called hydroxyapatite crystals, $Ca_{10}(PO_4)_6(OH)_2$. Pyrophosphate is a small molecule found within the extracellular matrix and is a known hydroxyapatite crystal nucleation inhibitor through direct binding. Increasing levels of pyrophosphate inhibits mineralization, while decreasing levels of pyrophosphate promote mineralization(22). The fibular phase, or the second

phase of bone mineralization, occurs when the calcium and phosphate ions become supersaturated inside the MVs, which leads to the rupturing of the MVs. The hydroxyapatite crystals are then released into the surrounding matrix and the bone is considered mature and mineralized(23).

Once osteoblasts have matured and produced bone matrix they undergo one of three fates. Osteoblast can undergo apoptosis, or programmed cell death, though it is believed that a low percentage of osteoblasts go through this process. A majority of osteoblasts will either be further differentiated into bone lining cells or become embedded in the matrix where they become osteocytes(21).

1.1.2.3 Osteocytes

Osteocytes are the most abundant cell type found within the bone; they make up approximately 90-95% of the total bone cells. In addition, they have the longest ranging lifespan of bone cells, and can stay viable for up to 25 years(24). Older osteocytes are typically not involved in bone remodeling due to their location within bone and distance to the bone surface. Eventually older osteocytes will undergo apoptosis and will leave behind an empty lacunae space(25). Osteocytes are defined by their morphology and location rather than their function, which is different and unique when compared with other bone cells. They have extremely important functions in the bone, and as stated previously, they are embedded within the mineralized bone matrix. They are located within the lacunae, surrounded by mature mineralized bone matrix and have a dendritic morphology, but the type of bone they are located within defines their exact shape. Osteocytes tend to be rounder or more circular when found in trabecular bone, while in cortical bone they tend to be more elongated(26).

There are four major stages of osteoblast to osteocyte differentiation: osteoid-osteocyte, preosteocyte, young osteocyte, and mature osteocyte. As the osteocyte differentiates the cytoplasm of the osteoblast begins to form into processes, which are long extensions of the cytoplasm. Before being completely encased into the bone matrix the size of organelles (the prominent rough endoplasmic reticulum and Golgi apparatuses) decrease and the nucleus to cytoplasm ratio begins to increase, which ultimately leads to a decrease in protein synthesis (27). The proteins being downregulated are OCN, BSP, ALP, and collagen type I while dentine matrix protein 1 (DMP1) and sclerostin (osteocyte specific markers) are expressed highly(28).

The cytoplasmic processes can be as numerous as up to 50 per cell and extend into and cross the tiny tunnels within the lacunae or canaliculi, which originate from the lacuna space(10). The processes also can connect to other osteocytes through structures known as gap junctions as well as other bone surface cells (osteoblasts and bone lining cells). These extensions form the lacunacanalicular system and facilitates the intracellular transport of small signaling molecules like prostaglandins and nitric oxide (NO). The lacunacanalicular system is located in close proximity to the vasculature within the bone matrix, which helps to supply the osteocyte bone network with oxygen and other essential nutrients(29). Cell to cell communication is achieved through the interstitial fluid that flows between the osteocyte processes and the canaliculi. Osteocytes act as mechanosensors because their interconnected network has the capacity to detect mechanical pressures, which helps adapt the bone to everyday stimuli. Osteocytes help to orchestrate bone remodeling through regulating both osteoblast and osteoclast activity(26). Osteocyte apoptosis has been linked to

chemotactic signaling for osteoclast recruitment and activity. Osteoclasts have been shown to engulf and absorb apoptotic osteocytes(30).

The osteocytes are able to be effective mechanosensors due to their location within the bone matrix, their shape and spatial arrangement that promotes the translation of mechanical stimuli into vital biochemical signals, a process called the piezoelectric effect(31). There are three possible mechanisms that have been proposed in the literature as to exactly how the piezoelectric effect occurs within osteocytes(10, 31). The first involves a protein complex formed by a cilium and its associated proteins, polycystins 1 and 2, which signal for osteoblast/osteocyte mediated bone formation. These polycystins located within the cilium can be associated with other cells or the ECM. They have been implicated in acting as mechanosensors, sensing flow induced calcium signaling (32). The second potential mechanism involves osteocyte cytoskeleton components that include focal adhesion protein complexes and various actin-associated proteins (paxillin, vinculin, talin, and zyxin). Osteocytes will produce secondary messengers, like adenotriphoshate (ATP), NO, Ca^{2+}, and prostaglandins, when they sense a mechanical stimulus. Osteocytes sense mechanical stimulus through the movement of the interstitial fluid surrounding their processes within the canaliculi. The osteocytes sense the movement with the fluid and release the aforementioned secondary messengers, which can ultimately signal for bone remodeling or BMU recruitment(33). Finally, the last potential mechanism is the general thought that osteocytes have a mechanosensitive function due to their location to the intricate canalicular network, allowing them to be in contact with various bone cells, like bone lining cells(10).

1.1.2.4 Bone Lining Cells

Bone lining cells are another form of terminally differentiated osteoblasts and they exhibit a quiescent flat shape. They also cover the bone surfaces that are not currently undergoing bone remodeling. Important morphological characteristics of bone lining cells are a thin and flat nucleus, and their cytoplasm extends along the bone surface. Some bone lining cells can possess processes that extend into the canaliculi and gap junctions between adjacent bone lining cells and osteocytes(34).

The secretory action of bone lining cells depends on their physiological bone cell status. Interestingly they can re-acquire secretory activity through enhancing their size and adapting a cuboidal morphology that mimics the morphology they previously possessed when they were osteoblasts(35). The actual function of bone lining cells is not well understood, but they are thought to be involved in preventing the direct interaction between osteoclasts and the bone surface. This will help indicate where bone resorption should take place during the bone remodeling process. In addition they have been implicated in osteoclast differentiation because they secrete OPG and RANKL, crucial osteoclast differentiation markers(11).

These four major cell types are all responsible for upholding the bone remodeling cycle, and ensuring that old or damaged bone is resorbed back and replaced by new bone. How this is coordinated depends on the age of the individual and whether or not they are undergoing development. This dictates the type of bone growth that will occur. There are two different types of bone growth, and they are discussed in the following section.

1.1.3 Types of Bone Growth During and After Development

In order to create new bone for development a template must be present. Without a template, bone growth would be unorganized and inefficient. There are three derivatives from which skeletal development stems: the cranial neural cells, somites, and the lateral plate mesoderm, which give rise to the flat bones in the skull, clavicle, cranial bones; axial skeleton; and long bones respectively(36). The developmental template is often cartilage derived from the embryonic mesoderm or from the undifferentiated mesenchyme. The bone development process, or ossification, begins between the sixth and seventh week of development and continues until early adulthood or age 25. There are two types of ossification: endochondral ossification and intramembranous ossification. Both types of ossifications begin with the mesenchymal tissue precursors, however, as development continues the way in which those precursors transition into bone differ between the two processes (37).

1.1.3.1 Endochondral Ossification

This process of ossification involves the replacement of the hyaline cartilage with bone when the MSCs from the mesoderm differentiate into chondrocytes, as seen in Figure 1.5(38).

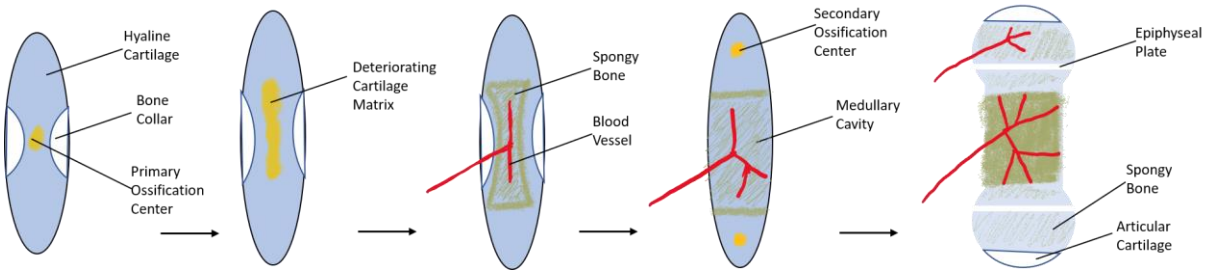

Figure 1.5 **Endochondral Ossification.** This process occurs during development. First, there is a formation of bone collar around hyaline cartilage. Then the cartilage matrix begins to deteriorate and the creation of an internal medullary cavity which eventually becomes invaded by periosteal blood vessels. Spongy bone formation also occurs around the same time. Secondary ossification centers begin to appear in the epiphyses of the bone, and they also become invaded by blood vessels. The invasion of blood vessels helps to increase the production of spongy bone. Finally, the ossification centers become mature spongy bone, the articular cartilage and epiphyseal growth plate also form.

This type of ossification is responsible for the formation of the vertebrate appendicular and axial skeleton during development (39). These chondrocytes proliferate and grow rapidly, from a proliferation center, and secrete an extracellular matrix (ECM) which forms the blueprint for bone ossification. Chondrocytes near the center of the proliferation center undergo hypertrophy, and as this is occurring collagen X and fibronectin become added into the ECM, which ultimately allow for calcification to take place. Calcification of the chondrocyte ECM stops nutrient delivery to hypertrophic chondrocytes, causing chondrocyte apoptosis. Once chondrocytes have undergone apoptosis there is more space within the ECM allowing for blood vessels invasion, causing enlarged spaces which will eventually combine to form the medullary cavity. Osteoblasts create a thickened region of cortical bone in the diaphyseal region of the periosteum. This creates the primary ossification center.

Bone replaces the cartilage in the diaphysis while cartilage continues to proliferate at the ends of long bones, increasing bone length. The proliferative areas then form the epiphyseal plates providing longitudinal growth of bones immediately after birth and into early adulthood. The epiphyseal growth regions will eventually become the secondary ossification centers. As development continues both the primary and secondary areas of ossification encroach on the remaining cartilage, turning it into bone once the skeleton fully matures, except for the articular cartilage surfaces (38).

1.1.3.2 Intramembranous Ossification

This type of ossification involves the direct conversion of mesenchyme to bone. It is responsible for the formation of craniofacial skeleton. This process begins when the neural crest derived MSCs differentiate into osteoblasts, as seen in Figure 1.6.

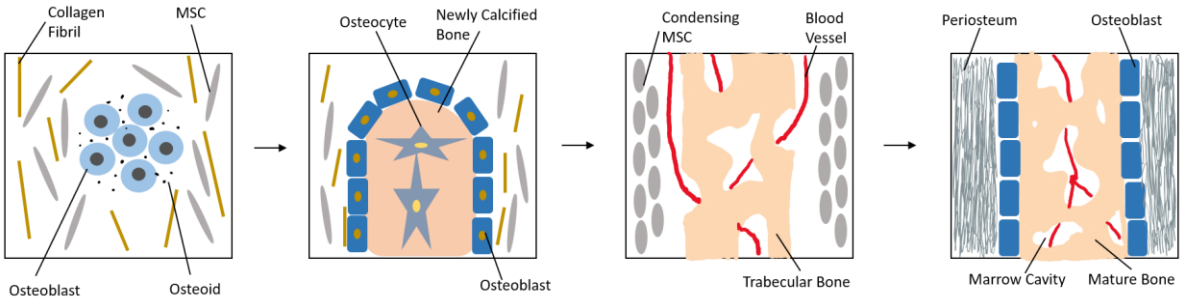

Figure 1.6 **Intramembranous Ossification.** An ossification center will appear in the fibrous connective tissue membrane, where MSCs and collagen fibrils are located. Centrally located MSCs will differentiate into the osteoblasts in a cluster, where osteoid will be deposited. Second, the bone matrix will begin to mature and grow, as the number of osteoblasts grow. Eventually the matrix will be mineralized, and some osteoblasts will become entrapped in the matrix where they terminally differentiate into osteocytes. Third, the surrounding MSCs will condense around the growing bone matrix, and blood vessels will begin to invade the matrix. Finally, the bone collar of the compact bone shell will form, trabecular bone will thicken, and the condensed MSCs will become the periosteum.

During development osteoblasts will gather into a group or ossification centers where the osteoblasts will secrete the unmineralized, immature bone, osteoid. The osteoid will begin to become mineralized or mature and bind calcium and phosphate ions, thereby hardening the surface and entrapping osteoblasts within the matrix itself. Once entrapped the osteoblasts will differentiate into osteocytes. Non-entrapped osteoblasts will continue to secrete osteoid around blood vessels, which forms the trabecular or cancellous bone. The blood vessels will eventually become the red bone marrow found within the spaces or lacunae of trabecular bone. MSCs at the surface will become the periosteum, enveloping, and protecting the bone. MSCs at the inner surfaces will differentiate into osteoblasts, secrete their own osteoid matrix and form organized layers of cortical bone (40).

Bone formation is a critical process, however continued maintenance and homeostasis are just as crucial. Old or damaged bone needs to be effectively replaced or resorbed, both of which occur in different processes. This becomes even more critical to study as we continue to think about bone health and managing the debilitating bone disease, osteoporosis. As mentioned briefly above, bone fractures are extremely common in those diagnosed with osteoporosis, therefore the types of bone fracture healing will be discussed in the following section.

1.1.4 Bone Fractures and Fracture Healing

While bones are structurally sound and strong, they often experience trauma, breaks, and fractures. There are five fractures that are most commonly seen in the clinic and they are compound, transverse, oblique, comminuted, segmental, compression, and greenstick, Figure 1.7.

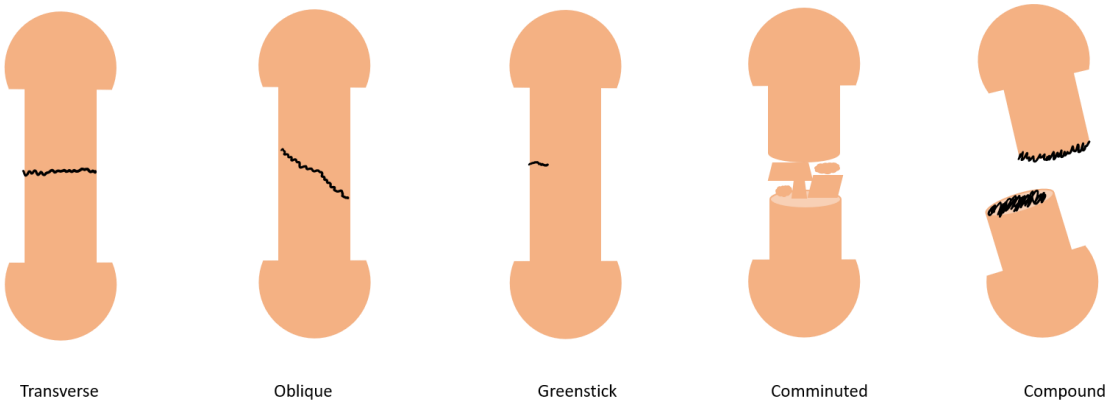

Figure 1.7 **Diagram of Fracture Types**. Schematic representing the five major types of fracture seen in the clinic. The type of fracture depends on the magnitude and direction of crack in the bone.

The differences between these types of fractures are determined by the pattern the fractures exhibits. For example, transverse fractures are horizontal line fractures, while oblique fractures are angled. Segmental fractures are created when there are two breaks in the bone, creating a floating bone segment and comminuted fractures have three or more breaks. Greenstick and stress fractures do not involve a complete split or break in the bone, instead there are tiny or hairline cracks in the bone. Compression fractures are when the bone is crushed, and fragments of the bone are wider or flatter. Stable fractures are a complete break in the bone, however the broken ends of the bone do not come out of alignment. In a displaced fracture the broken bone fragments are not in alignment. Once broken bone pierces through the skin and muscle the fracture is known as a compound fracture(41, 42).

The process of fracture healing utilizes the same processes in bone development and since a majority of the time the fractured bone will return to its prior non fractured state this whole process is considered a type of tissue regeneration. However, the fracture healing processes may fail as the fracture sites could heal in an unfavorable anatomical position, which delay the healing process as well as potentially causing the development of nonunions(43). There are lots of different processes involved in the fracture healing response, which include an immune response, remodeling system response, and developmental system or ontogeny responses(44).

1.1.4.1 Indirect Fracture Healing

The most common form of fracture healing is indirect or secondary fracture healing. This process consists of both endochondral and intramembranous ossification(45). This does not depend on rigid stability or immobilization of the

fracture site. In fact, it can be enhanced through micromotion, however excess motion would be detrimental to the fracture healing process, causing a nonunion(46). The major indirect fracture healing steps are outlined in Table 1.1.

Table 1.1 Indirect Bone Healing Steps

Step #	Process	Timeline	Description
1	Hematoma formation and inflammatory response	First 24 hours - 7 days	Hematoma coagulates between the broken bones and form a template for callus formation.
2	MSC recruitment, fibrin rich granulation tissue formation, and endochondral/intramembranous ossification	7 - 9 days	Recruitment of MSCs to hematoma granulation tissue so both methods of ossification can begin to take place.
3	Blood vessel invasion and vascularization, and replacement of the cartilage callus with a bony callus	3 - 4 weeks (possibly years)	Blood vessels help guide where to send additional cells and nutrients. Cartilaginous callus will be replaced by a bony callus through hypertrophic chondrocytes and the subsequent calcification and mineralization.

Once trauma has occurred a hematoma is formed at the fracture site/s. This hematoma consists of peripheral and intramedullary blood as well as bone marrow cells. This formation causes an inflammatory response, which causes the hematoma to coagulate in between the broken bone fragments, helping to form a template for callus formation(47). The acute inflammatory response lasts from 24 hours to seven days and involves the secretion of the following factors: tumor necrosis factor alpha (TNF-α), interleukin -1 (IL-1), IL-6, IL-11, and IL-8(45, 48). These factors recruit inflammatory cells and the factors also promotes angiogenesis. IL-6 is an important secretion factor because it is known to not only stimulate angiogenesis, but also stimulates vascular endothelial growth factor (VEGF) production and promotes the differentiation of both osteoblasts and osteoclasts(49).

After the inflammatory response, MSCs need to be recruited to the fracture sites because they need to proliferate and differentiate into osteoblasts and osteoclasts. MSCs can be recruited from the surrounding soft tissue, the bone marrow, and from systemic circulation(50, 51). As mentioned previously BMPs are located within the bone matrix and signal for MSC recruitment/differentiation. Similarly, both BMP2 and BMP7 play critical roles in promoting the recruitment of MSCs to these fracture sites(52, 53). After hematoma formation and the recruitment of MSCs a fibrin rich granulation tissue forms where endochondral ossification begins to occur between the fracture segments or ends(43). This callus formation will give increased strength and stability to the fracture site(54). This process occurs seven to nine days post trauma(44). Intramembranous ossification also occurs simultaneously to endochondral ossification. Intramembranous ossification takes place subperiosteally adjacent to the distal and proximal ends of the fracture, beginning to generate a hard callus, further increasing stability(43, 48). When MSCs are recruited a molecular cascade is induced that produces matrix with collagen I and collagen II, as well as production of some vital signaling molecules like BMP2, BMP5, and BMP6(53).

The next step in this process is vascularization of the fracture site, which further recruits necessary cells and nutrients to these sites(55). This is completed through two pathways: angiopoietin dependent pathway and VEGF pathway(56). Eventually the cartilaginous callus formed needs to be replaced by a bony callus. This is completed through chondrocytes undergoing hypertrophy and calcification of the cartilaginous matrix previously laid down by the chondrocytes. This calcified matrix will become mineralized, lending the callus to now become even more structurally sound and stable(47). Next a second resorptive and remodeling phase will be induced

because the hard callus needs to be further remodeled into lamellar bone structure with a central medullary cavity so that the full biomechanical and structural properties of bone are restored. BMP2 has been shown to be highly expressed during this phase(43). This process can occur three to four weeks post trauma but may take years to fully complete(45). As humans age the bone healing process slows, and decreased BMP2 levels have been associated with increased risk of developing osteoporosis. Other researchers have found a decreased response to BMP2 stimulation in MSCs and osteoblasts from OP patients, again pointing to the importance and potency of BMP2.

1.1.4.2 Direct Fracture Healing

Another type of fracture healing is direct fracture healing. This type is not as common as indirect fracture healing because it involves complete stability, no gap formations, and often requires surgical intervention to achieve these requirements. This will take place through direct remodeling of the lamellar bone and the entire process may take place in a few months to years following bone trauma(43). There are two methods of direct fracture healing: contact healing, which requires the ends of the broken bones to be placed into direct contact with one another and gap healing, which does not require direct contact of the broken bone fragments(57).

Now that bone dynamics of bone maintenance, remodeling, homeostasis, and fracture healing have been discussed, the next topics will focus on the molecular signaling related to bone maintenance as this plays an integral part in proper and healthy bone preservation. The most widely studied group of proteins related to bone, are BMPs, which are extensively discussed in the next section.

1.2 Bone Morphogenetic Proteins

BMPs are the largest subfamily group of the Transforming Growth Factor Beta (TGFβ) superfamily. They are conserved highly phylogenetically and were discovered initially from bone extracts. They were discovered due to their ability to direct ectopic bone formation within the stomach pouch, quadriceps, and erector spinae muscles(58); however, they also are involved in a vast multitude of developmental processes. They also are extremely important for human health and viability, in that BMP knockout mice were embryonically lethal(59, 60). Based on sequence similarity and functions BMPs could be divided into 4 subgroups, with approximately 13 currently discovered BMPs(61, 62). They are synthesized as 400-500 amino acid precursors, which contain an N-terminal signal peptide (responsible for directing secretion), a prodomain (responsible for proper protein folding), and C-terminal mature peptide sequence(63). Active BMPs have 50-100 amino acids with seven cysteines, six of which form three intramolecular disulfide bonds (or cysteine knots). The seventh cysteine is responsible for dimerization with another monomer through forming a covalent disulfide bond(64). Some BMPs, however, do not follow this categorization, but still seem to be biologically active(63).

Once BMPs are cleaved at their primary cleavage site, their respective prodomains remain loosely associated with the BMP protein. The prodomain is crucial not only for correct protein folding, but continued association with the prodomain helps direct the protein complex to the microfibril elements within the extracellular matrix. BMPs are typically bound to fibrillins in the extracellular matrix through binding of the prodomain. Both BMP2 and BMP4 prodomains, however, have been shown to either disassociate or fall off in transition. Since prodomains are critical for BMP protein direction and anchoring to the extracellular matrix, both BMP2 and

BMP4 undergo different processes. Both of these molecules have secondary cleavage sites within their prodomains that are tissue specific. This generates long or short prodomains that dictate whether the mature protein is released as soluble (short) or tethered/anchored (long)(65).

BMPs are found throughout the human body, and their actions depend on the bioavailability of these molecules. For example, BMPs 1-7 have been found within matrix vesicles of growth plate chondrocytes, indicating and supporting that they are found within the mineralizing matrix of bone(66). BMPs also are found in almost every type of body fluid. BMP2 and BMP4 are found in high levels within the serum because they have been shown to be active in their soluble forms(67). The bioavailability of BMPs also depends on the presence of known antagonists to BMP signaling and activation. There are currently over 15 BMP antagonists, which help to regulate levels of active BMPs. They are classified into three subgroups based on the size of their cysteine knots(68). The regulatory methods of these antagonist have been hypothesized to act in three possible ways. They may inhibit through interaction of the seventh cysteine residue on BMPs, which affects the dimerization of the BMP protein. They also could inhibit through blocking BMP receptor activation by masking the epitopes responsible for receptor binding on the BMP molecule. Finally, they may compete for receptor binding itself. Some antagonists may also be considered agonists and they would also be classified as competitive activators of the receptor system(69).

At the cell membrane BMPs bind and interact with their respective BMP receptors or BMPRs in order to produce a signaling assembly(62). BMPs are known to activate both SMAD dependent and SMAD independent signaling cascades which affect gene transcription. Activation of the signaling cascade is due to the bound and

dimerized serine/threonine kinase receptor complex, which include a type I receptor and a type II receptor(70). However, activation is completely dependent on the BMP ligand binding to the type I receptor(62). BMPRs have a short extracellular domain with 10-12 cysteine residues, a single transmembrane domain, and an intracellular serine/threonine kinase domain. There are five known BMP type I receptors and three known type II receptors. The type I receptors have a higher affinity for ligand binding(64). This differs from typical TGFβR activation, as they signal through a network of receptors. Normally, the type II TGF-β receptor (TβRII) dimerizes with another type II receptor with a pair of type I receptors(71).

Of the 13 BMPs discussed above, the most critical and potent is BMP2. BMP2 has been the most widely studied in relation to bone formation. Its activity and subsequent signaling cascade is discussed in the following section.

1.3 BMP2 and its Signaling

BMP2 is responsible for inducing lineage specific determination for osteoblasts, osteoclasts, adipocytes, and chondrocytes. It was discovered and identified in 1965 by Marshall Urist(72). It also was discovered that it is critical to development and continually expressed into adulthood as it induces both intramembranous and endochondral ossification as well as cartilage formation(60, 73, 74). It has been responsible for osteoblast and osteoclast differentiation as well as bone remodeling. BMP2 is released from the bone matrix during bone resorption mediated by osteoclasts to signal for the differentiation and recruitment of preosteoblasts to the remodeling site. Mice lacking BMP2 developed bones with reduced width and increased risk of spontaneous fracture(18, 19). Since BMP2 is multifunctional and has increased osteogenic capabilities it was approved by the FDA for healing of spinal

fusions. It is administered in tapered or cylindrical cages for this purpose(75-77). However, there are a lot of post-surgical complications, including, radiculitis, vertebral osteolysis, increased microfracture incidence, hematoma and seroma formation. Many of these post-surgical complications are so severe that they require patients to undergo corrective surgery. Therefore, use of BMP2 to treat skeletal diseases or complications may not be ideal given its multifaceted response(78-83).

The BMP2 gene is located on chromosome site 20p12 (84, 85). Once the gene is transcribed and translated it becomes functionally active as a crosslinked homodimer through proteolytic cleavage by proprotein convertase subtilisin/kexin type 5 (PCSK5) at its C terminus(86). BMP2 that is functional and activated has 115 amino acids and is released from the cell where it can bind to BMPRs. BMP2 can bind to two receptors, a type I receptor and type II receptor. Type I receptors include BMP type Ia (BMPRIa), BMP type Ib (BMPRIb), and activin receptor type I receptor (ActRI)(87, 88). Type II receptors include BMP type II (BMPRII), activin receptor type IIa (ActRIIa), and activin receptor type IIb (ActRIIb)(62, 64). These receptors can be localized in caveolae, clathrin coated pits (CCPs), and lipid rafts located on the plasma membrane and are expressed in osteoblasts and osteoclasts, indicating how critical they are for bone remodeling and homeostasis(73). BMP2 preferentially binds to BMPRIa/b where it binds at the beta4beta5 loop, which oligomerizes with BMPRII, or BMPRIb to a lesser extent. However, the signaling pathways subsequently activated depend on which type I receptor BMPRII oligomerizes with (89, 90). Phosphorylation and activation of BMPRIa leads to adipogenesis, chondrogenesis, and osteogenesis while phosphorylation and activation of BMPRIb leads to apoptosis and cell death(91, 92). BMPRs can be found in different domains within the plasma membrane. BMPRs

can also be found oligomerized together in preformed complexes or become oligomerized upon ligand binding. For example, SMAD signaling occurs when BMP2 binds to preformed heteromeric complexes, whereas SMAD independent signaling occurs when BMP2 binds to BMPRIa and BMPRII is recruited to that complex, seen in Figure 1.8(70, 93, 94).

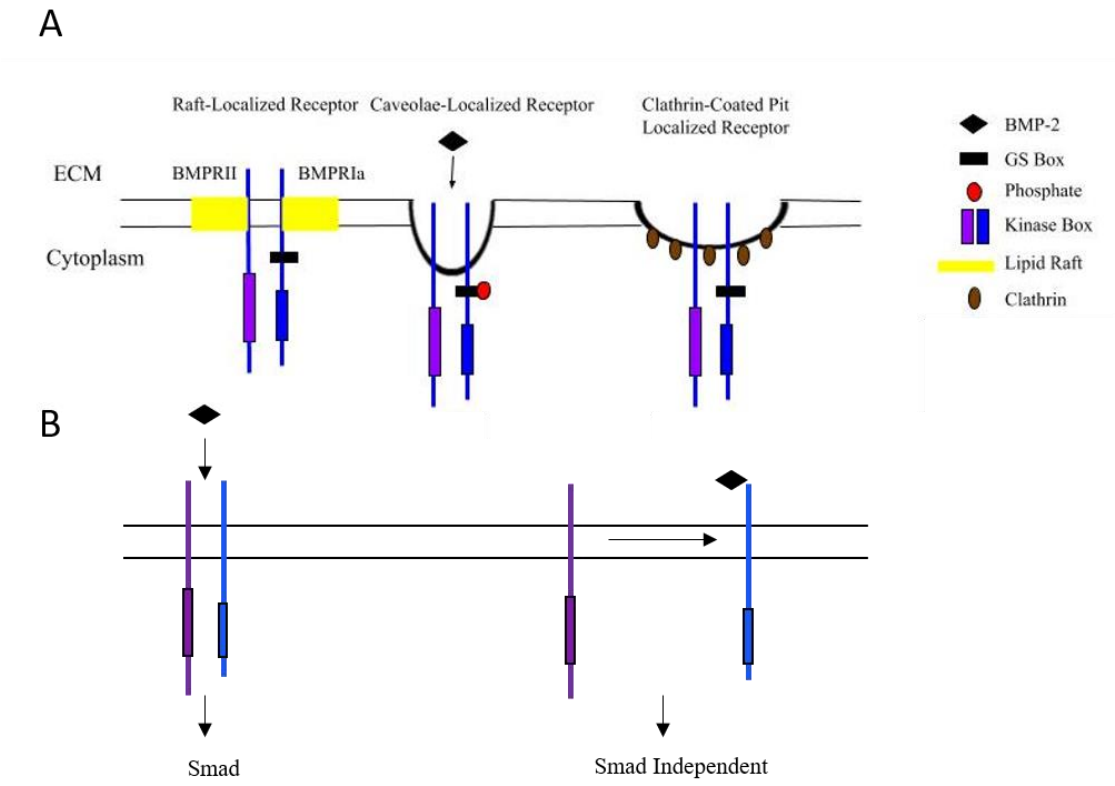

Figure 1.8 **BMPR Plasma membrane Dynamics.** (A) BMPRs can exist in several different domains within the plasma membrane (lipid rafts, caveolae, and CCPs). (B) They can also exist as preformed complexes or they may stand alone and be recruited together once a ligand (BMP2) binds preferentially to BMPRIa, thus recruiting BMPRII and inducing Smad independent signaling.

Canonical BMP signaling, or SMAD dependent signaling occurs when BMPRIa phosphorylates SMAD 1/5/8, recruiting SMAD4 (a regulatory SMAD). This bound complex will translocate into the nucleus and acts as a transcription factor for osteogenic genes like *RUNX2* and *OSX*(95, 96). Non canonical or SMAD independent

signaling occurs when BMP2 binds to BMPRIa, recruiting BMPRII. BMPRII phosphorylates BMPRIa at the GS box and MAPK signaling becomes activated, which activates extracellular signal related kinase (ERK), phosphatidylinositol-2 kinase (PI3K), and the TAB/TAK1 pathways. Each of these signaling events activates NF-kβ and p38 leads to differentiation of osteoblast precursors into osteoblasts, except for the TAB/TAK1 pathway, seen in Figure 1.9(62, 97, 98).

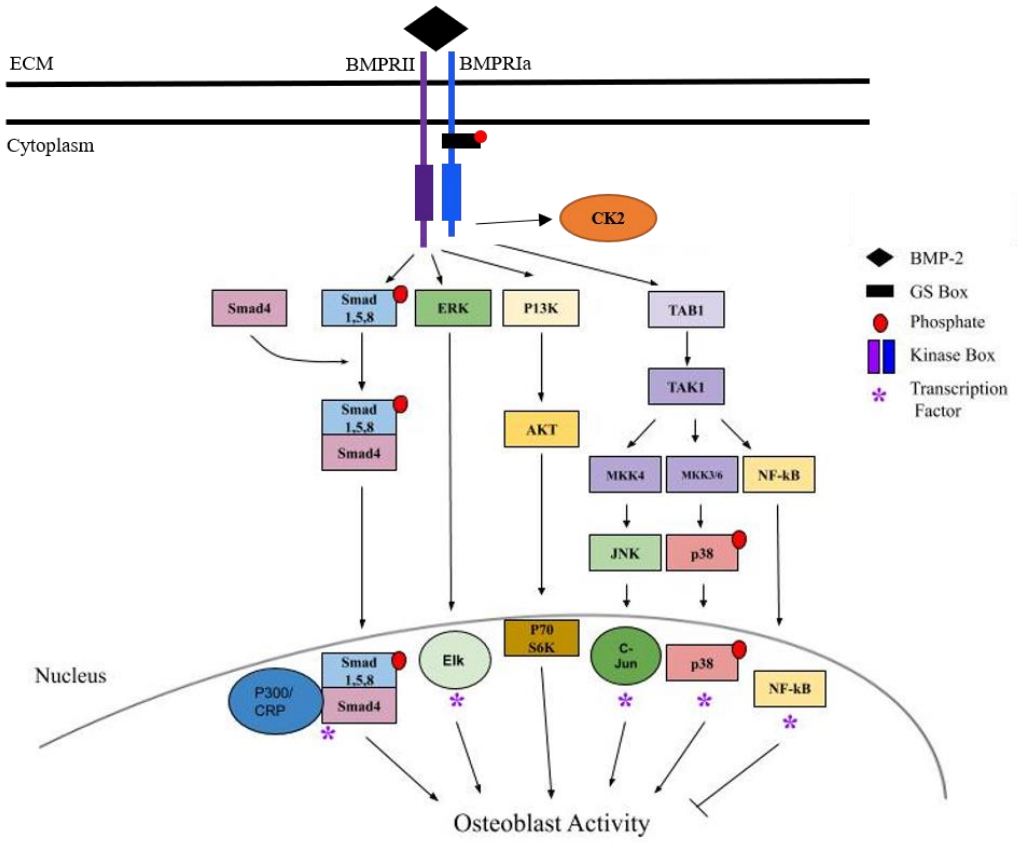

Figure 1.9 **BMP2 Signaling Schematic.** BMP2 will bind to its two corresponding receptors, BMPRIa and BMPRII. This binding activates several signaling cascades through the activation and phosphorylation of the GS box. In addition, CK2 also is phosphorylated, activated and released from BMPRIa. The most notable BMP signaling cascade is the Smad signaling cascade, shown on the left. Smad independent signaling involves the activation of Erk, PI3K, and the TAB1/TAK1 pathways. All of these pathways influence osteoblast activity.

The area in which the BMPRs are localized will dictate how they are endocytosed or activated. BMP2 has been shown to preferentially bind to BMPRIa aggregates localized in caveolae, but like previously mentioned BMPRs can be found in CCPs and lipid rafts(99-102). The BMP2 and BMPR complex becomes endocytosed into the

cell, but the exact fate of the complex is unknown. The complex could be recycled back up to the membrane or degraded through lysosomal degradation, but how this occurs and what dictates the complex endocytic pathway needs to be further investigated(103-106).

New areas within BMP signaling dynamics continue to be discovered. In previous years the Nohe lab had discovered the novel interaction between BMPRIa and an interacting protein kinase called CK2, which is a known substrate modifier to a large variety of other proteins. CK2 and its role in BMP signaling will be discussed in the following section.

1.4 Casein Kinase 2 and its Role in BMP Signaling

CK2 is a highly and ubiquitously expressed protein found in eukaryotic organisms. It exists in tetrameric form which consists of two catalytic subunits and two regulatory subunits(107-109). In humans there are three isoforms of the catalytic subunit which include CK2α, CK2α', and CK2α''. There is only one regulatory subunit isoform, which is CK2β(110, 111). The tetrameric complex may consist of various combinations of these isoforms. CK2 is known for its ability to phosphorylate serine or threonine residues proximal to acidic amino acids(112). While it preferentially phosphorylates serine and threonine residues, it also can act as a dual specificity kinase by activating and phosphorylating tyrosine residues, but less favorably(113). This expands the amount of substrates with which CK2 can interact, and there are currently over 300 known CK2 substrates(114).

Interestingly, CK2 is a key regulator of the BMP pathway. Without BMP2 bound to its receptors, CK2 associates with BMPRIa at three phosphorylation sites and prevents activation of downstream effector proteins. Once BMP2 binds to its

receptor/receptors, CK2 is released and upregulation of osteogenesis is observed(97, 115, 116). When inhibiting CK2's interaction at the three phosphorylation sites, activation of downstream proteins are affected(97). To further study each phosphorylation site, mutants of BMPRIa at each of those sites were constructed. The phosphorylation sites are: AA 213-217, AA 324-238, and AA 475-479(115). The mutations were completed by exchanging a serine residue for an alanine residue and those mutations led to an induction of osteogenesis, adipogenesis, chondrogenesis respectively(116). Blocking peptides were constructed that correspond with each of the phosphorylation sites, and the peptides are named CK2.1, CK2.2, and CK2.3. These peptides bind to CK2 and prevent its interaction with BMPRIa at that particular phosphorylation site. Peptides led to increased chondrogenesis (CK2.1), adipogenesis (CK2.2), and osteogenesis (CK2.3). This indicates that the phosphorylation sites on BMPRIa control the activated signaling pathways for BMP2 induced signaling(97, 100, 103, 115-118).

CK2 may be involved in the shuffling and recycling of BMPRs, but this function is still unknown. CK2 has also been shown to interact with ERK, a downstream protein of the BMP pathway, and aid in its nuclear translocation, which subsequently activates vital osteogenic specific genes(119). Therefore, peptide mediation of CK2 could increase CK2 and ERK colocalization and activation, but this also remains unknown and needs to be explored further.

BMPs, their subsequent signaling, membrane dynamics, and novel interactions have been discussed and outlined, however it is important to note, all the previous statements relate to a normal, healthy individual. Many abnormalities exist within

these aforementioned that topics can lead to various bone related diseases. Common bone diseases and their known causes (if any) are discussed in the following sections.

1.5 Major Human Skeletal Diseases

Unfortunately, the bone remodeling cycle and bone homeostasis can be disrupted in different ways. This leads to a variety of different skeletal diseases or disorders. Generally, these diseases or disorders occur before birth or later in life. A skeletal disease arising before birth is osteogenesis imperfecta, other developmental bone disorders are classified as sclerosing bone disorders like osteopetrosis or marble bone disease. Some rare bone disorders that can arise in children or adults are rickets/osteomalacia, and Pagets disease, which is a progressive disorder. Some more common skeletal disorders include osteoarthritis and osteoporosis, which greatly affect not only the American population, but also the world's population. These diseases are outlined in the following sections(120).

1.5.1 Developmental Bone Diseases

Osteogenesis imperfecta (OI) is the most common genetic and developmental bone disorder. It is inherited and causes the bone to be very brittle, breaking or fracturing very easily. There are a number of different forms of this disease and all are a result of different types of genetic defects or mutations. These defects cause OI to interfere with the production of collagen type I, which is an integral part of bone tissue as it is a major component. Most of these genetic variations are inherited, but some are not and can occur spontaneously. Most patients diagnosed with OI have low bone mass or osteopenia, and therefore exhibit an increased risk of fracture. There are four different types of OI: type I- is the most common and the mildest of the four, very few

fractures are seen; type IV- is the second mildest form of this disease, there can be some mild to moderate bone deformities with some patients showing dental problems or hearing loss; type III-is a more severe version of this disorder, patients experience frequent fractures, shortened statures, hearing loss and dental problems, and type II- is the most severe form of this disease where patients experience numerous fractures, and severe bone deformity that leads to death(120-122).

Other developmental bone diseases are sclerosing bone disorders, one of which is known as osteopetrosis or marble bone disease. This results from genetic defects that impair osteoclasts from resorbing back old or damaged bone. This causes bone to be very dense, however it is not structurally more durable. In fact, osteopetrosis bone is very brittle and structurally unsound, therefore fractures frequently occur. This disorder also poses some neurological issues, such as deafness or blindness, and anemia, which is due to the compression of nerves within the bone tissue(121).

1.5.2 Rare Bone Disorders

Two rare bone diseases that stem from the same deficiency are rickets (affecting children) and osteomalacia (affecting adults). These disorders are caused by a deficiency of Vitamin D. While rare, these two disorders can cause serious abnormalities. Rickets, in particular, is caused by a delay in calcium phosphate deposition in growing bones, which causes skeletal deformities. Skeletal deformities do not occur in osteomalacia, because it occurs in adults and longitudinal growth during development has stopped. However, it does cause an increase in fractures in weight bearing bones. Mostly these diseases are caused by reduced sun exposure (or reduced vitamin D), phosphate deficiency, and lastly inheritance (to a lesser extent)(123, 124). Chronic renal diseases also can put patients at risk for developing

both rickets and osteomalacia, in addition to renal osteodystrophy(125). Renal osteodystrophy is a complex bone disease that is characterized by increased parathyroid hormone (PTH) and delayed bone mineralization caused by the decreased kidney production of 1,25 dihydroxyvitamin D. Vitamin D_3 itself is produced within the skin from 7-dehydrocholesterol and UV radiation. Eventually the liver and kidneys will further process vitamin D into 25 hydroxyvitamin D (OHD), which is the main circulating form of vitamin D. 25 OHD will become further metabolized within the kidney into 1,25 dihydroxyvitamin D, which is the main hormonal form of vitamin D in the body(126). A decrease in hormonal vitamin D causes bone cysts to form through increased osteoclast resorption by excessive parathyroid hormone (PTH) production(127, 128). PTH is secreted by the parathyroid gland and is a key regulator of calcium homeostasis within the body. When extracellular calcium levels fall, PTH is released and signals for bone resorption to take place, in order to increase the extracellular calcium levels(129).

1.5.3 Paget's Disease

Paget's disease is a progressive and crippling disorder caused by dysregulation of bone remodeling. It is the second most common bone disease in humans. It can be transmitted, but it is more likely to be inherited. It also can be caused by environmental factors, but this is very rare. This mostly affects the spine, pelvis, legs, or skull – but all bones can be affected. There is increased bone resorption at the affected site, due to the increased number of osteoclasts, as well as their increased activity. Bone formation then increases, but the newly formed bone does not have structural integrity due to the disorganized structure of the newly formed bone. Patients who have Paget's also have larger bones, blood vessels, and connective tissue

within the bone marrow. This leads to deformities as well as an increased risk of fractures. This disease can also lead to neurological complications due to the compression of the nerves within the bone(130).

1.5.4 Osteoarthritis

A prevalent skeletal disorder not immediately related to bone deficiency, but rather cartilage deficiency is osteoarthritis (OA). It is known also as degenerative joint disease and involves, as the name implies, softening or loss of articular cartilage, subchondral bone sclerosis, cyst formation, and development of osteophytes. It is also the most common form of arthritis. When the joints of OA patients (where the cartilage is found) becomes painful, swollen, and hard to move. OA mostly affects the hips, knees, hands, lower back, and neck. It can start at any age, but most commonly affects individuals in their 50s or older. It is also more prominent in women than it is in men. OA starts gradually, and then worsens over time. It is diagnosed through an X-ray, magnetic resonance imaging (MRI), or joint aspiration. There are no treatments on the market that restore or reverse cartilage loss. Current therapeutics focus on managing the pain associated with the disease, as well as to slow its progression(131).

1.5.5 Osteoporosis

Osteoporosis (OP) is the most common bone disease in humans, millions of Americans are affected by this debilitating bone disease. Approximately one in two women and one in three men age 60 and older will be diagnosed with OP. As the aging population increases, so will the incidence and occurrence of OP. It is characterized by low bone mass or low bone mineral density (BMD), as well as the deterioration of the bone structure. This causes bones to be more brittle, thus causing

an increased risk of fracture that those diagnosed with OP exhibit. Individuals also have increased risk to develop multiple fractures, which can cause injuries that can be debilitating, leading to a decrease in physical and mental health capacities. OP can occur throughout the body (the most common form, also called generalized OP), but it can also occur in localized areas throughout the skeleton(120). There are two types of OP: primary OP and secondary OP. Each will be discussed below(132).

1.5.5.1 Primary OP

Primary OP is the most common type and it mostly affects the elderly. It is sometimes referred to as age related OP or post-menopausal OP, as women are at a greater risk of developing primary OP(132). Younger children and adults can also have primary OP, but it is very rare. This is termed idiopathic primary OP, as the cause of this particular version of OP is not known(120). Age related primary OP is two to three times more likely to affect women than men, which is due to women having two phases of age-related bone loss, while men only have one. The two phases of bone loss that women experience is: a rapid phase which begins at menopause and lasts approximately four to eight years after menopause ends; the slower, continuous phase lasts throughout the remainder of life. Men mostly lose bone through the slower continuous phase. This slower phase accounts for 20-25% loss of both cortical and trabecular bone, while the rapid phase results in an additional 5-10% loss of cortical bone, and a 20-30% loss of trabecular bone(133). The rapid phase of bone loss is mostly due to estrogen loss in women, but also can occur in men. When women undergo menopause there is a swift decline in estrogen production. This decrease in estrogen causes a decrease in the activation of estrogen receptors found within bone cells, which causes an increase in osteoclast activity leading to bone resorption and a

decrease in osteoblast activity or bone formation. This causes thinning of the cortical bone shell and decreases integrity within the trabecular bone structure.(134).

The slower phase of bone loss is caused by some additional factors like: age-related impairment of bone formation, decreased calcium and vitamin D consumption, lower amount of physical activity, and loss of the positive effect of estrogen on calcium balance within the intestines as well as calcium storage within the kidneys(133). Calcium imbalance then causes a detrimental cycle within the bone as well as the body, especially if there are lower amounts of calcium consumed. Calcium levels continue to fall due to lack of calcium within the kidneys and inevitable, but continued loss through stool and urine. This causes serum levels of calcium to fall, which in turn triggers parathyroid hormone (PTH) levels to rise. PTH signals for osteoclast resorption in order to release calcium back into the serum to make up for the original loss. This vicious cycle leads to more and more bone being resorbed back, and less bone being formed, leading to OP(120).

In men, age related OP is attributed to sex steroid deficiency. Testosterone is the major sex hormone in men, however some of it is converted to estrogen through an aromatase enzyme. This conversion to estrogen is to provide more calcium regulation, and to protect bones. However, as mentioned before, men can also experience a decrease in estrogen (as well as testosterone). This is from an increase in a sex binding hormone called globulin. This protein binds to both estrogen and testosterone creating a complex that renders both sex hormones inactive. The inactivity of these hormones causes a decrease in bone formation and increases bone resorption through the effect of calcium malabsorption, eventually increasing PTH levels(135).

1.5.5.2 Secondary OP

Secondary OP is observed as a byproduct of another treatment or pre-existing condition. This type of OP can affect both young and old. Those diagnosed often experience greater levels of bone loss when compared to individuals of the same age, gender, and race(135, 136). Some diseases that cause secondary OP are idiopathic hypercalcemia and cystic fibrosis. This is due to calcium and vitamin D malabsorption, delayed puberty, and a decrease in sex hormones(137). It can also be caused by Turner's, Kallman's, and Klinefeter's syndromes due to sex hormone deficiency during adolescence that those diagnosed with these syndromes exhibit(133). Primary hypothyroidism is common in post-menopausal women, which again increases the chances of women to develop OP. Primary hypothyroidism causes increased secretion of PTH, leading to increased osteoclast activity(138). Many neurological disorders also cause secondary OP due to their effects on decreased mobility or balance. Interestingly, this also includes patients who have had a stroke, or spinal cord and brain injuries(139). Some psychiatric disorders have been linked to secondary OP, including depression and anorexia nervosa. It is important to note that it is not known whether or not having low BMD causes depression or vice versa(140).

There are also some therapeutics that cause secondary OP. The main treatment that is known to cause OP, and that has been studied extensively is glucocorticoids. There is even a name associated with this type of secondary OP, glucocorticoid induced OP. Glucocorticoids are used to treat inflammatory conditions like arthritis, asthma, and chronic lung disease. They cause large reductions of bone formation as well as possibly increasing bone resorption. It is a large concern in the health care community, and providers are prescribing this treatment only to those patients who absolutely need it. They also are urged to prescribe glucocorticoids at the lowest

possible effective dosage, for the shortest amount of time. It also is recommended to administer this treatment locally, whenever possible in order to decrease the amount of bone loss in patients(141).

1.6 Diagnosis and Treatment Options for OP

Currently osteoporosis is diagnosed through a central DXA (Dual Energy X-ray Absorptiometry) scan of the total hip, femoral neck, and lumbar spine, which then determines the T-score. The T-score shows how much the bone density of the patient is higher or lower than a healthy, 30-year-old adult. The lower the T-score value, the lower the patient's BMD. It is recommended that female patients 65 years and older and male patients 70 years and older obtain regular bone screenings through DXA. If a patient has a T-score below -2.5, they are diagnosed with OP(142).

The current treatments on the market for OP are not ideal, in that they produce several unwarranted side effects. Additionally, not all medications are approved by the FDA for every type of OP(143). Current therapeutics approved by the FDA are highlighted in Table 1.2.

Table 1.2 Current Osteoporotic Therapeutics Approved by the FDA

Treatment	Type	Side Effects
Bisphosphonates	Antiresorptive	Osteonecrosis of the jaw, atypical femoral fracture, upper gastrointestinal discomfort
Selective estrogen modulators (SERMs)	Antiresorptive	Hot flashes, vaginal bleeding, venous thromboembolisms, stroke
RANKL Inhibitor	Antiresorptive	Hypersensitivity, serious infections, musco-skeletal pain, hypercholesterolemia
Calcitonin	Antiresorptive	Rhinitis, back pain, severe bone pain, liver cancer
Synthetic PTH	Anabolic	Hypercalcemia, gout, osteosarcoma
Sclerostin Inhibitor	Anabolic	Myocardial infarction, stroke, fever, joint pain, increased heart rate

Treatments can be grouped into two categories, antiresorptive and anabolic. A majority of the treatments on the market are antiresorptive, because they focus on decreasing bone resorption (144). The most common treatment prescribed or the first line of treatment for primary OP are bisphosphonates. They can be oral tablets, effervescent tablets, or in some cases an injection. The oral tablets are the most common form of bisphosphonates, which are recommended to be taken alone, first thing in the morning, on an empty stomach. This is a major inconvenience as these patients are typically in the older generation, and the main side effect is upper gastrointestinal discomfort. Bisphosphonate injections are not a typical way to administer this drug, as the major benefit is the oral tablet delivery method. All other treatments highlighted in the table are injections, which is a major drawback for some patients, increasing the popularity and use of bisphosphonates. Bisphosphonates can only be taken for a maximum of five years, after which it is recommended to take a drug holiday as the risks far outweigh the benefits(145).

There are very few anabolic therapeutics on the market, they include synthetic PTH and sclerostin inhibitor (144). Synthetic PTH can be taken only for a maximum of two years, after this time period the negative effects far outweigh the positive effects, due to the increased risk of the development of osteosarcoma, which has been observed in rats (146).There are two forms of synthetic PTH available, teriparatide and abloparatide. Teriparatide was the first anabolic treatment approved for OP and is suggested as a treatment for those at a higher risk of fracture or those with previous fragility fractures(145). Abloparatide was the second anabolic treatment approved for OP in 2017 and it is also used for women at higher risk for fractures and for patients who are intolerant to other therapies(147). Both synthetic therapies mimic the physiological actions of PTH in stimulating new bone formation through stimulating osteoblast activity when administered in intermittent small doses(148). Both therapies also have extended side effects that include dizziness, nausea, fatigue, upper abdominal pain and vertigo(143). The newest treatment available is sclerostin inhibitor, romosozumab, which is a humanized monoclonal antibody that inhibits sclerostin(149). It was approved by the FDA in 2019 and is administered through two consecutive injections, once a month. It is only recommended to take this treatment for one year, after the initial year the beneficial anabolic effects decrease(150). Since it is newly approved, there are no long-term studies or side effects that are known. Current known side effects include myocardial infarction, stroke, cardiovascular death, fever, joint pain, trouble breathing, and increased heart rate(151). There is no treatment that focuses on decreasing osteoclast activity, while also increasing osteoblast activity. Therefore, there is a great need to better understand what is causing this disease, so better therapeutics can be developed. BMP2 is a growth factor that increases bone

growth (or osteoblast activity) (49) and decreases bone resorption (or osteoclast activity) (152-155). Human recombinant BMP2 (rhBMP2) is approved by the FDA for the healing of long bone fractures. However, the long term use of BMP2 is linked to increased osteoclastogenesis, therefore it is not a viable treatment for OP (152). While BMP2 is not an ideal treatment for OP, further investigation of the BMP pathway could elucidate new mechanisms or new potential therapeutics.

1.7 BMP Signaling in OP

Many studies point to the link of aberrant BMP2 signaling in OP. For example, in 2003, a linkage analysis of a large number of extended OP families in Iceland, using a phenotype that combines osteoporotic fractures and BMD measurements, showed linkage to Chromosome 20p12.3 (multipoint allele-sharing LOD, 5.10; p value, 6.3×10^{-7}) (156). Since then, researchers are still trying to determine if polymorphisms in the BMP2 gene may be implicated in OP. For example, in the Rotterdam study, which used a large cohort, BMP2 Ser37Ala and Arg190Ser polymorphisms or haplotypes were not associated with parameters of OP. On the other hand, polymorphisms of BMP2 rs967417 and rs79417223 are associated with osteoporotic fracture. The rs967417 TG/TT genotype might be a protective factor for osteoporotic fracture, while rs79417223 GG genotype might increase the risk of osteoporotic fracture (157). Several researchers reported that the BMP signaling pathway is affected in cells, serum levels and bone specimens of patients with OP (158-166). Some researchers looked into serum or blood levels of BMP2, ALP, SMAD4, pSMAD1, and OC(159,

160). While the findings were interesting, as OP patients who obtained a severe fracture had significantly lower BMP2 and SMAD4 levels, looking into circulating SMAD levels is not indicative of the BMP cellular signaling cascade. Other research groups looked into MSCs isolated from OP patients as compared to normal, healthy patients. They discovered that there was a significant decrease in pERK activation (assessed through a western blot) following BMP2 stimulation. Interestingly, when observing pSMAD1/5/8 protein levels, they found no significant differences following BMP2 stimulation(161). Moreover, while MSCs from OP patients have decreased SMAD1 levels, RUNX2 mRNA expression is controversial with one author citing no change and another suggesting upregulation in response to BMP2 (161, 163, 164). Interestingly another research group found that stimulation of MSCs with BMP2 showed an upregulation of pSMAD1/5/8; however this upregulation did not increase expression of RUNX, OC, DLX5 and ALP (161, 163, 165). However, osteoporotic MSCs had increased gene and protein levels of BMPRIa when compared to MSCs derived from control patients, which indicates a potential disparity in the BMPRIa signaling pathway or receptor distribution. Recently a publication suggests OBs from 30% of donors of spongy bone did not respond to BMP2 (166). These cells upregulated BAMBI, and SOST was downregulated (166). In order to determine if OBs isolated from OP respond to BMP2, we stimulated explant cultures from femoral heads obtained after hip arthroplasty and determined the effect of BMP2 on OB activity and mineralization. As our published data showed, OBs isolated from POP did not respond to BMP2 (158). Moreover, BMPRIa was upregulated in POP. These

results are similar to previous reports on BMPRIa expression in BMSCs of POP (165). Taking data obtained from patients diagnosed with OP (167) and the data obtained from animal experiments (100, 168) confirming the positive effect of BMP2 on osteogenesis, osteoblast activity and bone formation (169-171), BMP2 should be a powerful treatment for OP. However, BMP2 failed in the clinic as a treatment for fractures due to an array of side effects and general lack of effectiveness (172). None of the treatments for OP affect BMP signaling pathways, which is aberrant in POP. Therefore, new therapeutics need to be designed in order to address this BMP signaling issue.

1.8 CK2.3, a Potential Novel OP Therapeutic

Looking into the BMP pathway, the Nohe lab shows an interacting protein, CK2 that associates with BMPRIa, through an immunoprecipitation of BMPRIa (97). CK2 is ubiquitously expressed and has over 300 phosphorylation substrates (173). It consists of two catalytic subunits (an α and an α1) and two regulatory β subunits (114). The β subunits help with CK2 assembly and docking to the various CK2 substrates, while the catalytic subunits favor serine and threonine residues (174). Three potential CK2 phosphorylation sites located on BMPRIa were discovered through a prosite search. Novel peptides were designed to mimic those sites (97). The peptide sequence contains the antennaepedia homeodomain, which aids in cellular uptake of the peptide, and several amino acid residues flanking each end of the phosphorylation site sequence, to aid in the peptides binding to the corresponding CK2

binding site. These peptides are hypothesized to bind to CK2 and inhibit its interaction at that particular site on BMPRIa. The peptide that blocks site 3 (which correspond to amino acids SLKD) on BMPRIa (at position 213-217) is known as CK2.3 (175). CK2.3 induces bone growth and mineralization in both an *in vivo* and *in vitro* mouse model (115, 117, 118). It was unclear if the same phenotype would occur in cells extracted from patients diagnosed with OP. To test this, cells were extracted from human femoral heads and assessed for mineralization through a Von Kossa assay. The femoral heads were collected from patients diagnosed with both OP and OA from Christiana Care Hospital in Newark, DE. The extracted cells were treated with BMP2 or the Nohe lab's novel peptide (and potential osteoporosis therapeutic) CK2.3. Cells extracted from OA patients responded to both BMP2 and CK2.3. It was observed that osteoporotic patients did not respond to BMP2 but still responded to CK2.3(158). Under normal conditions, when BMP2 binds to its two dimerized receptors, BMPRIa and BMPRII, the type II receptor phosphorylates the type I receptor at the GS box, and a signaling cascade is induced. Both SMAD dependent and SMAD independent signaling is activated. However, under osteoporotic conditions it is not known what occurs. When BMP2 is introduced in this scenario, an osteogenic signaling cascade is not induced. CK2, the interacting protein, could not be released from the type I receptor in this situation, causing further unknown complications. CK2.3 stimulation is hypothesized to rescue this mechanism, by releasing CK2 from BMPRIa, and inducing, either SMAD dependent activation, ERK (SMAD independent) activation, or both. CK2.3 has previously been shown to act through the ERK signaling pathway,

and the SMAD signaling pathway (to a lesser extent) in isolated mouse cells, and C2C12 cells, outlined in Figure 1.10 (116).

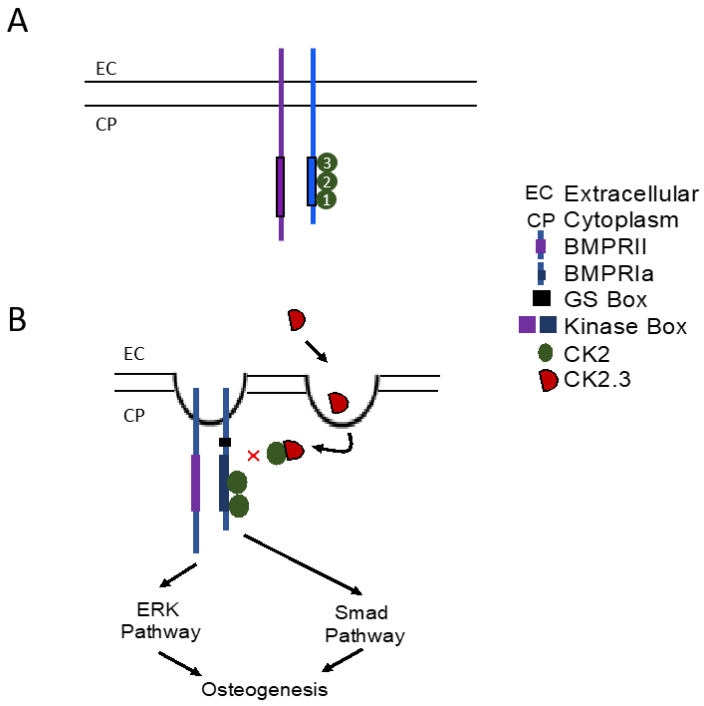

Figure 1.10 **CK2 and BMPRIa Phosphorylation Sites**. (A) Potential CK2 phosphorylation sites on BMPRIa, labeled with numbers corresponding to the respective sites. Mimetic peptides were designed that mimic the CK2 phosphorylation site and have synonymous residues from BMPRIa flanking both sides. Each peptide corresponds to a different CK2 phosphorylation site, CK2.1 with site 1, CK2.2 with site 2, and CK2.3 with site 3. (B) CK2.3 has been shown to increase osteoblast activity in a variety of cell lines and animal models. Recently, it was discovered to be uptaken into the cell through caveolae, where it binds to CK2 and increases osteogenesis through the Smad and Erk signaling pathways.

Whether CK2 interacts with SMAD or ERK directly in cells isolated from patients diagnosed with OP to induce a signaling response is not yet known. CK2 interaction

and phosphorylation of ERK is shown in HeLa cells, therefore the possibility of interaction between CK2.3 and ERK is plausible (119).

1.9 Hypothesis and Aims

The linkage between OP and aberrant BMP signaling needs to be further elucidated. In addition, CK2's potential interaction with downstream BMP signaling partners also need to be further elucidated. CK2.3 could rescue aberrant BMP signaling through the direct mediation of CK2 with ERK or SMAD. Taking all of this together the following hypothesis and aims were proposed and completed.

Hypothesis: Mature osteoblasts isolated from patients diagnosed with OP have an altered BMP signaling pathway.

Aim 1: Elucidate the difference between BMP2 and CK2.3 stimulation in osteoblasts isolated from human femoral heads.

Aim 1a: Establish primary osteoblast extraction and culture methodology from human femoral heads.

Aim 2a: Determine the mineralization response to both BMP2 and CK2.3 stimulations.

Aim 2: Clarify the signaling pathways utilized by BMP2 and CK2.3 in cells extracted from OP patients.

Aim 2a: Define the regulation of BMP receptors with CK2.

Aim 2b: Determine CK2.3's effect on BMP signaling.

Chapter 2

MATERIALS AND METHODS

2.1 Subjects

Following institutional review board (IRB) exemption from Christiana Care Hospital, Newark, DE, (10 April 2013) human femoral heads were obtained after being extracted from patients undergoing hip arthroplasty surgery (DDD# 602228). The patients were diagnosed with osteoporosis or osteoarthritis (or control). A total of 86 femoral heads were collected, of which 68 (aged 37–92) were from patients diagnosed with OP and 18 (aged 56–86) were from patients diagnosed with OA; all femoral heads were isolated from female patients.

2.2 X-raying Femoral Heads

The femoral heads were X-rayed posterior to anterior with a Nomad Pro Veterinary Handheld X-ray System. A penny was positioned in the X-ray to verify that the distance between the handheld X-ray and the femoral head remained constant. After the radiographs were obtained, the pixel intensity (PI) of each femoral head was calculated.

2.3 Calculation of BMD

The radiographs were analyzed and measured in ImageJ. The PIs of two background regions of interest (ROI) were measured using the “Measure” function of ImageJ (NIH, Bethesda, MD, USA). They were then subtracted from the PI of the

bone intensity ROI to obtain the BMD. PI is a measurement of a gray-level value on a scale of 0 (black) to 255 (white) and has been shown to correspond with bone density (mineralized) or BMD in several other studies (176, 177). This type of quantification of BMD is called single photon absorptiometry (SPA) as the X-ray penetrates through the sample in a single-photon ray and is reflected onto a detector (178).

2.4 Calculation of TMD

Microcomputed tomography scans were taken and analyzed through a SCANCO MicroCT 35 device. A total of 1000 X-ray images were obtained at a range of 180° at different angles, with a filtered back-projection algorithm used to determine the "brightness value" of each voxel. The voxels' "brightness value" was converted to density measurements through a conversion scale determined by several "brightness values" of metal rods of a known density. The trabecular volumes were manually defined, and the TMD reported is the averaged density of voxels within that particular ROI. A trabecular ROI from the image stack was defined by manually contouring the trabecular bone roughly for an irregular anatomic region a few pixels from the cortical bone for 16 slides and interpolating that to 231 slides. The microCT scans were treated with a Gaussian filter to remove background noise, and the ROIs were then subjected to auto thresholding, with the threshold for trabecular bone to be 35% maximal brightness. Several standard morphological measures of cortical and trabecular bone were reported for the contoured trabecular and cortical ROIs. TMD measured the averaged density of all voxels, including voids within the volume defined by the contours (or ROI).

2.5 MMA Embedding

Preserved femoral heads from patients diagnosed with either OP or OA were aged 58-95(11 total patients) and 41-66 (7 total patients), respectively. Using a modified embedding protocol from Akkiraju and colleagues (179), femoral heads were fixed in 10% Neutral Buffered Formalin (NBF). Once fixed the bones were cut down the midsagittal plane, and an area of trabecular bone was removed from the interior region of the bone. The bone fragments were washed with 1x PBS at room temperature (RT). They were then subsequently dehydrated using a series of ethanol dilutions. The ethanol dilution series started with a 70% ethanol incubation for 8-16 hours, 90% ethanol incubation for 8-16 hours, 95% ethanol incubation for 8-16 hours, two changes of 100% ethanol for 8-16 hours each, two changes of 100% isopropanol for 8-16 hours each, and two changes of methyl salicylate for 4 hours each. Once completely dehydrated samples were infiltrated with methyl methacrylate (MMA) I (750 mL MMA, 140 ml N-butyl pthalate) for 48 hours at RT. Next, they were infiltrated with MMA II (750 mL MMA, 140 mL N-butyl pthalate, and 9 grams of dry benzoyl peroxide) for 48 hours at 4°C. Last, the samples were infiltrated with MMA III (750 ml MMA, 140 mL N-butyl pthalate, 17.75 grams of dry benzoyl peroxide) for 48 hours at 4°C. Samples were embedded in glass vials, and once hardened samples were placed in a 40°C oven for seven days in order to fully solidify the samples. Once fully solid samples were removed from the glass vials by breaking the glass with a rubber mallet. They were then trimmed and sectioned using a diamond wafering blade (Buehler) using an IsoMet low speed Saw (Buehler, Lake Bluff, IL). The sections were then sanded down using Carbimet Abrasive discs (Buehler) sand paper.

2.6 Antigen Retrieval and Immunostaining of Embedded Samples

Cut and sanded MMA samples with approximately 200-600μm thickness were placed in a Xylene solution for one minute to dissolve back the plastic resin. They were then placed in a prewarmed (37°C) testicular hyaluronidase solution (47 mL 0.1M potassium phosphate, 3 mL 0.1M sodium phosphate, and 0.025g testicular hyaluronidase) for 30 minutes. The samples were washed with 1x PBS three times following the incubation. Samples were then blocked with 3% Bovine Serum Albumin (BSA) for one hour at RT and then incubated with their designated primary antibodies overnight at 4°C. Primary antibodies included: BMPRIa goat polyclonal IgG as a 1:200 dilution (200 μg/mL, Santa Cruz Biotechnology, Dallas, TX, USA), and CK2α rabbit polyclonal IgG as a 1:200 dilution (200 μg/mL, Santa Cruz Biotechnology, Dallas, TX, USA). Following overnight incubation the samples were washed three times in 1x PBS for 15 minutes each and then incubated for the corresponding secondary antibodies for one hour at RT. Secondary antibodies include: Donkey anti goat IgG 488 as a 1:500 dilution (Life Technologies, Carlsbad, CA) and chicken anti rabbit IgG 568 as a 1:500 dilution (Life Technologies, Carlsbad, CA). The samples were washed three times with 1X PBS for 15 minutes each and then stained for the nucleus using Hoescht (bisbenzimide, Sigma-Aldrich, St. Louis, MO, USA Hoechst dye No. 33258, dissolved in H2O) for ten minutes and subsequently washed with 1X PBS. Embedded bone slices were imaged using Zeiss LSM 710 at the 20X/0.75 Plan Apochromat objective (Flour, Zeiss, Germany). After the images were collected pixel intensity was determined through the “Measure” function of ImageJ (NIH, Bethesda, MD, USA).

2.7 Explant Culture

Femoral heads were collected within 48 hours post extraction. The patients were diagnosed with either OP or OA (control) and were aged 79-87 (5 total patients) and 54-66 (4 total patients), respectively. Using nose pliers and DREMEL 4000 trabecular bone fragments (2 mm) were extracted from the interior of the bone, as shown in Figure 3.8. Once removed the samples were washed with 1X PBS, and then placed in a 100% antibiotic/antimycotic solution for ten minutes. Following this incubation samples were placed in a six well plate with DMEM and 10% FBS solution. Fragments were stimulated with 40nM of BMP2 and 100nM of CK2.3 as designated for five days, with media and re-stimulation occurring on the third day.

2.7.1 Viability Staining

In order to test the efficacy of utilizing a bone explant model, a cell viability assay was conducted. After the five day stimulation period, the bone fragments were stained for viable cells using CellTrace™ Calcein Red-Orange, AM (Thermo Fischer, Waltham, MA), 1µM solution was aliquoted directly into the media. This dye is readily taken up by eukaryotic cells with a retained cell membrane, indicating that the dyed cells are viable. A Hoescht nuclear stain (1µL of a 1:1000 dilution, directly into the media) was also used to determine the amount of live and dead cells present within a sample. After ten minutes, the media was aspirated and the samples were washed one time with 1X PBS. Two mL of PBS were aliquoted onto the samples while imaging. The samples were imaged using Zeiss LSM 710 at the 20X/0.75 Plan Apochromat objective (Fluor, Zeiss, Germany). The images were collected in z-stacks, ranging in size from 30-40 slices per sample for the entire sample. The images were analyzed using ImageJ (NIH, Bethesda, MD, USA) through the “Measure ” function,

slice by slice. Cells stained for Hoescht, Calcein, and Hoescht and Calcein were counted, slice by slice. This was completed to determine both the relative intensities of the stains and the number of cells stained per label in order to determine the percent cell viability throughout the entire explant sample.

2.7.2 Immunostaining of Explants

After stimulation the fragments were fixed with 4.4% Paraformaldhyde (PFA) overnight at 4°C. Following fixation the fragments were washed with 1X PBS five times and then the samples were blocked in 3% BSA for one hour at RT. The fragments were then incubated with primary antibodies overnight at 4°C. Primary antibodies include BMPRIa (same as above) and CK2α (same as above). After primary antibody incubation the fragments were washed in 1X PBS three times for 15 minutes each. They were then incubated with secondary antibodies (same as above) for one hour at RT. After incubation the fragments were washed with three changes of 1X PBS for 15 minutes each. The explants were also stained with Hoescht for 10 minutes at RT, and then washed one last time with 1X PBS. Approximately 1 mL of 1X PBS was aliquoted into the wells with the explants and the explants were imaged using Zeiss LSM 710 with the 20X/0.70W Plan Apochromat objective (Fluor, Zeiss, Germany). Images were collected as z-stacks, averaging approximately 30-40 slices per sample for the entire sample. Images were analyzed using the “Measure” function of ImageJ (NIH, Bethesda, MD, USA), slice by slice, in order to obtain the relative pixel intensities of each of the aforementioned stains. Pixel intensities were averaged for each stack and for each patient. This was completed in three OP patients and three OA/control patients.

2.8 Isolation of Primary Osteoblasts

In a sterile environment, femoral heads were selected from the trendline on the BMD versus age graph (Figure 3.2a) and then sliced down the midsagittal plane with an Arbor cut-off saw (Drill Master, 14 inch HP cut-off saw) or DREMEL 4000. Bone fragments of cancellous bone were extracted from the interior surface of the bone, washed once with 1X phosphate-buffered saline (PBS), and digested with a DMEM/collagenase (Dulbecco's Modification of Eagles Medium, Corning; Collagenase Type II, Worthington) solution for two days. The cellular suspension was filtered using a 70 µm cell strainer (BD Falcon), centrifuged to pellet, resuspended in fresh DMEM with no collagenase solution, and plated in a T25 flask. Cells were grown for seven days without a media change to ensure cell adhesion to the bottom of the flask. After the seventh day, fresh DMEM media was supplemented to the cells every four days in order to promote cell growth.

2.9 Immunostaining

Immunostaining for Osteoblast Specific Markers OC and ALP

Cells were isolated from three female osteoporotic patients whose ages were 60, 73, and 76. The cells were seeded in a 24-well plate at a density of 1×10^5 cells/cm^2 per well on glass coverslips (Thomas Scientific, Swedesboro, NJ). Once 90% confluent cells were serum-starved overnight and treated with 100 nm CK2.3, 40 nm BMP2, or left unstimulated (US). This was completed concomitantly with the Von Kossa experiments for the above three patients. After five days of treatment, cells were washed with 1X PBS and then fixed with acetone (Fischer Scientific, Waltham, MA) and methanol (Fischer Scientific, Waltham, MA). The samples were fluorescently labeled for one hour at RT for rabbit polyclonal IgG osteocalcin as a

1:200 dilution (200 μg/ml, Santa Cruz Biotechnology, Dallas, TX, USA), which was followed by Alexafluor chicken antirabbit as a 1:500 dilution (200 μg/ml, Life Technologies, Carlsbad, Ca, USA) and goat polyclonal IgG alkaline phosphatase as a 1:200 dilution (200 μg/ml, Santa Cruz Biotechnology), followed by Alexafluor 568 donkey antigoat IgG as a 1:500 dilution (200μg/ml, Life Technologies, Carlsbad, CA, USA). All antibodies were diluted in a 3% BSA solution. Bisbenzimide (Sigma-Aldrich, St. Louis, MO, USA Hoechst dye No. 33258, dissolved in H2O) was used as a nuclear stain for two and a half minute incubation. The coverslips were mounted using Airvol, as previously described [37,38]. Images were taken on Zeiss Axiophot with a 20X/0.75 Plan Apochromat objective (Fluor, Zeiss, Germany) and pixel intensity was determined through the "Measure" function of ImageJ (NIH, Bethesda, MD, USA).

Immunostaining for BMP Receptors, CK2α, and downstream signaling proteins

Cells were isolated from five female patients diagnosed with OP, aged 60-92. Cells were seeded at the same density and manner as above. After five days of treatment with either BMP2, CK2.3 or US, the cells were washed three times with 1X PBS and fixed with 4.4% (w/v) PFA for 15 minutes at RT. The cells were washed five times with 1X PBS, and then the membrane was permeabilized with 0.1% (w/v) saponin (Sigma Aldrich, St. Louis MO) for ten minutes on ice. The cells were washed again three times with 1X PBS. They were then blocked with 3% BSA for one hour at RT, and then they were incubated with the corresponding primary antibodies: BMPRIa (same as above), CK2α (same as above), pERK E-4 (mouse monoclonal antibody, 1:1000 dilution, 200ug/mL, Santa Cruz Biotechnology, Dallas, TX) , ERK 1/2 (p44/42

MAPK (ERK1/2) rabbit polyclonal antibody, 1:1000 dilution, Cell Signaling, Danvers, MA), pSMAD (phosphoSMAD1/5 rabbit monoclonal antibody, 1:1000 dilution, Cell Signaling, Danvers, MA), SMAD (SMAD 1/5/8 n-18 rabbit polyclonal antibody, 1:1000 dilution, 200ug/mL, Santa Cruz Biotechnology, Dallas, TX)). This incubation was followed by another hour incubation with the corresponding secondary antibodies at room temperature. They include: Alexafluor 488 chicken antirabbit IgG as a 1:500 dilution (200 μg/mL, Life Technologies, Carlsbad, Ca, USA), Alexafluor 568 donkey antigoat IgG as a 1:500 dilution (200μg/mL, Life Technologies, Carlsbad, CA, USA). All antibodies were diluted in a 3% bovine serum albumin (BSA) solution. Cells were stained for their nucleus using Hoescht for two and a half minutes. The coverslips were mounted using Airvol, as previously described(180, 181). Images were taken on Zeiss Axiophot with a 20X/0.75 Plan Apochromat objective (Fluor, Zeiss, Germany) and pixel intensity was determined through the "Measure" function of ImageJ (NIH, Bethesda, MD, USA).

Immunostaining for pERK/ pSMAD and CK2α pixel colocalization

Cells were isolated from five female patients diagnosed with OP, aged 60-92. Cells were seeded at the same density and manner as above. After five days of treatment with either BMP2, CK2.3 or US, the cells were washed three times with 1X PBS and fixed with 4.4% (w/v) PFA for 15 minutes at RT. The cells were washed five times with 1X PBS, and then the membrane was permeabilized with 0.1% (w/v) saponin (Sigma Aldrich, St. Louis MO) for ten minutes on ice. The cells were washed again three times with 1X PBS. They were then blocked with 3% BSA for one hour at RT, and then they were incubated with the corresponding primary antibodies: CK2α (same

as above), and pERK E-4 (same as above), or pSMAD1/5 (same as above). This incubation was followed by another hour incubation with the corresponding secondary antibodies at room temperature (the same antibodies listed above). All antibodies were diluted in a 3% bovine serum albumin (BSA) solution. Cells were stained for their nucleus using Hoescht for two and a half minutes. The coverslips were mounted using Airvol, as previously described(180, 181). Images were taken on Zeiss Axiophot with a 63X/1.4 Oil Plan Apochromat objective (Fluor, Zeiss, Germany). Two images were generated of each cell. The first image was of the entire cell, taken at zoom 1. A second image was taken of the same cell, but at zoom 10 within the cytoplasm of the cell so that pixel-pixel colocalization could be determined. Pixel-pixel colocalization was determined through the "Coloc 2" function of ImageJ (NIH, Bethesda, MD, USA).

2.10 Immunostaining Quantifications

2.10.1 OC and ALP, Explant, and MMA Analysis

Immunofluorescent images were quantified using ImageJ. Briefly, images were converted to 8 bits, and the threshold was then adjusted to the 2nd or negative control to eliminate nonspecific staining. Once converted, the images were black and white, which made it easier to calculate pixel intensity. Pixel intensity was calculated through the measure function of ImageJ and was averaged for BMP2-stimulated, CK2.3-stimulated, and US cells. Fluorescent staining intensity has been shown to be equivalent to the pixel intensity measured in ImageJ (NIH, Bethesda, MD, USA)(182).

2.10.2 BMPRIa and CK2α Analysis

Immunofluorescent images were quantified using ImageJ. Briefly, images were converted to 8 bits, and a threshold was used to adjust the images to the 2nd control. Total area of the stain was quantified using the "Analyze Particles" function of ImageJ (NIH, Bethesda, MD, USA) in order to measure the total amount of protein expressed.

2.10.3 pERK/ERK; pSMAD/SMAD; and, Cell Population Analysis

The total area of the stain was quantified as outlined above. Cells were counted when stained with specific proteins, and then divided by the number of cells in an image. The number of cells stained was then converted into a percentage and plotted to compare the number of cells expressing that specific protein.

2.10.4 pERK/CK2α and pSMAD/CK2α Colocalization Analysis

Immunofluorescence images were quantified for colocalization using ImageJ. Briefly images stained solely for pERK or pSMAD (green) and stained solely for CK2α (red) were converted to 8 bit. Background pixel intensity was measured using the "Measure" function, and was subtracted from the images using the "Subtract Background" function. The "Coloc 2" function of ImageJ was used, pERK or pSMAD was always assigned Channel 1 and CK2α was always assigned Channel 2. No ROI was selected since only the zoom10 images were used to quantify colocalization. The following parameters were used to quantify the degree of pixel colocalization: Costes threshold regression, Manders correlation, Ncoloc (or the number of pixels colocalized with one another), the point spread function (PSF) was set to 50, and Costes randomization was set to 10. The values reported here were the average Ncoloc per image set, Manders 1, and Manders 2. Ncoloc was averaged and is displayed in the

graph. The Manders coefficients are represented in the table. The Manders coefficients represent how much green (or pERK or pSMAD) colocalized with the red (CK2a), and how much red colocalized with the green, which signify Manders 1 and Manders 2, respectively. The closer the Manders coefficient is to 1, the more pixel to pixel colocalization is reported(183).

2.11 Von Kossa Assay

Cells used for these experiments were from five female OA patients aged 54-66 and five female OP patients, aged 82-95. Once cells from both patient populations were grown to confluency in a T25 flask, they were split onto a 24-well plated at the same seeding density of 1×10^5 cells/cm^2. Once 90% confluent, cells were serum-starved overnight and treated with either 100 nM CK2.3 or 40 nM BMP2 or left unstimulated (control). This was done concomitantly with the ALP/OC immunofluorescent population analysis. These concentrations were determined to be optimal for promoting osteogenesis (97). After five days, the assay was conducted as previously described (97). Briefly, cells were washed with 1X PBS, fixed with 4.4% (w/v) paraformaldehyde (PFA)(Acros, Fair Lawn, NJ) for 15 minutes, and assayed using 5% (w/v) silver nitrate (Sigma Aldrich, St. Louis, MO, USA) solution in order to determine phosphate deposits or mineralization. Ten images were taken of each well and quantified using ImageJ (NIH, Bethesda, MD, USA). Images were converted to 8 bits, and a threshold was set to the control and subsequently used for all treatments within an individual experiment. The surface area stained with silver (and represented mineralization) was quantified using the "Analyzing Particles" function of ImageJ (NIH, Bethesda, MD, USA).

2.12 Lysate Collection

Whole cell lysates were collected from five female OP patients aged 60-92. Cells were plated on a 6 well plate at a density of 1×10^5 cells/cm^2. Once 90% confluent, the cells were serum starved overnight and treated with either 40 nM BMP2, 100 nM CK2.3 or left US for five days. On the fifth day cells were washed with ice cold IX PBS and incubated with lysis buffer (containing 10 mM Tris pH 7.5, 50 mM NaCl, 1% Triton X-100, 60 mM octyl glucoside, 1 mM PMSF, 10 mg/mL each of leupeptin, aprotinin, soybean trypsin inhibitor, benzamidine-HCl, pepstatin, and antipain) for 1 hour, as previously described(26). Cells were then sonicated (30s, two times) and centrifuged at 14,000 G for 20 minutes to remove cellular debris. Protein concentrations were determined using a Promega Glomax plate reader following manufacturers protocols (Pierce™ BCA protein Assay Kit, Thermo Fischer, Waltham, MA).

2.13 Western Blot

Once protein concentration was determined, samples were normalized and loaded into a 12.5% SDS-Polyacrylamide gel. The gel was run for 90 minutes at 90V and then the protein extracts were transferred onto presoaked PVDF (Sigma-Aldrich, St. Louis, MO) membrane for one hour at 15V using a semi-dry transfer (BioRad, Hercules, CA). Once the protein had fully transferred, the membrane was blocked using 5%BSA in 1X PBST(PBS with 1% Tween (Sigma Aldrich, St. Louis, MO)) solution for one hour at RT. The membrane was then incubated with primary antibodies overnight at 4°C. Primary antibodies included: pSMAD 1/5 (Rabbit polyclonal IgG, Cell Signaling, Danvers, MA), SMAD (Rabbit polyclonal IgG, Santa Cruz Biotechnology, Dallas, TX), pERK (Mouse monoclonal IgG, Santa Cruz

Biotechnology, Dallas, TX), ERK (Rabbit polyclonal antibody, Cell Signaling, Danvers, MA), and β-actin (Rabbit polyclonal IgG, Proteintech, Chicago, IL). The membrane was then washed three times with 1X PBST for 15 minutes each. It was then incubated with secondary antibodies conjugated to horseradish peroxidase (HRP) for one hour at RT. Secondary antibodies included: Goat anti rabbit IgG-HRP (Abcam, Cambridge, UK) and rabbit anti mouse IgG-HRP (Abcam, Cambridge, UK). The membrane was again washed three time with 1X PBST for 15 minutes each. The membrane was then incubated with Chemiluminescence FemtoMAX™ Super Sensitive HRP Substrate (Rockland, Gilbertsville, PA) for two and a half minutes. Chemiluminescence was detected using a ChemiDoc (BioRad, Hercules, CA).

2.14 RNA Collection

RNA was collected from three female OP patients aged 76-92. Cells were plated in a six well plate at a density of 1×10^5 cells/cm^2. Once 90% confluent, the cells were serum starved overnight and treated with either 40 nM BMP2, 100 nM CK2.3, or left US for five days. On the fifth day the cells were washed with 1X PBS and 300 µL of TRIzol™ (Invitrogen, Carlsbad, CA) solution was added to each well. The lysate was pipetted up and down in the solution and then aliquoted into fresh centrifuge tubes. Chloroform (Fischer Scientific, Waltham, MA) was added to each tube, mixed well, and then incubated for ten minutes at RT. The samples were centrifuged for 15 minutes at 12,000 G at 4°C, which separates the solution into two phases: a top aqueous phase containing the RNA and a bottom phenol/chloroform phase. The top aqueous phase was removed and aliquoted into fresh centrifuge tubes. Isopropanol (Fischer Scientific, Waltham, MA) was added to each tube, and incubated for ten minutes at RT. They were then centrifuged for ten minutes at 12,000 G at 4°C,

which precipitates the RNA into a pellet. The supernatant was removed and the pellet was washed two times with 75% Ethanol (Fischer Scientific, Waltham, MA), vortexing between washes, and the pellet was then air dried for ten minutes at RT. The RNA was then re-suspended in 100 µL of RNase free water (Fischer Scientific, Waltham, MA).

2.15 Quantitative Reverse Transcription Polymerase Chain Reaction (RT-PCR)

Two step RT-PCR was performed with 2µg of RNA obtained and using a high capacity cDNA reverse transcription kit. In the second step the obtained cDNA was amplified through PCR using specific primers (Integrated DNA Technologies, Coralville, IA). The primer sequences used are as follows (1) *BMPRIa* (forward) *CAG CCT CCA GAC TCA CAG CAT* (reverse) *CGA GAC CCA TGA CTT AAG G. GAPDH* was used as the housekeeping gene, its primer sequences were (forward) *CAT GGC CTT CCG TGT TCC TA* (reverse) *CCT GCT TCA CCA CCT TCT TGA T*. The primer sequences have been used and verified in several publications(165, 184). The RT-qPCR used Fast SYBR™ Green Master Mix per the manufacturer's protocols (Thermo Fischer, Waltham, MA). Fold change in mRNA expression was processed using procedures outlined previously(185).

2.16 Statistical Analysis

BMD data were analyzed through linear regression analysis, and outliers were removed through Chauvenet's criterion. von Kossa, immunostaining, western blot quanitification, and RT-PCR data were analyzed through an ANOVA with a Tukey–Kramer post hoc test. Outliers were removed through Chauvenet's criterion, and error bars depict standard error of the mean.

Chapter 3

RESULTS

3.1 Femoral Head BMD and TMD Measurements from OP and OA Patients

SPA was used to measure BMD instead of micro CT due to time and cost constraints. To verify if our calculated BMD data was representative of our samples, Tissue Mineral Density (TMD) was calculated from the femoral neck of femoral heads from OP patients. Ten female OP patients TMD and BMD values were calculated and used, aged 56-86. TMD was determined through a microCT scan and all measurements are in mm Hg/cm (millimeters of mercury/centimeters). The TMD values were compared to the BMD values of the same patients and a positive correlation was observed (Figure 3.1a).

I obtained radiographs of each femoral head extracted from OA patients. Representative radiographs are shown in Figure 3.1b. The BMD of 25 female OA patients were analyzed and quantified. No decrease or increase of BMD was observed (Figure 3.1c). Therefore, I found no correlation between age and BMD in POA. I obtained 42 femoral heads from POP. They were X-rayed and their bone density was quantified. I found a negative correlation between age and BMD in POP. Representative radiographs are shown in Figure 3.1d and a graph of the BMD verse age can be seen in Figure 3.1e. This confirms that the femoral heads were osteoporotic.(186)

a

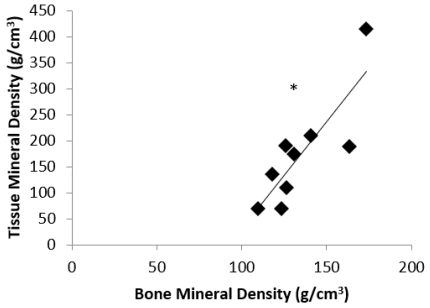
Tissue Mineral Density (g/cm³)
Bone Mineral Density (g/cm³)
0
50
100
150
200
250
300
350
400
450
*

b

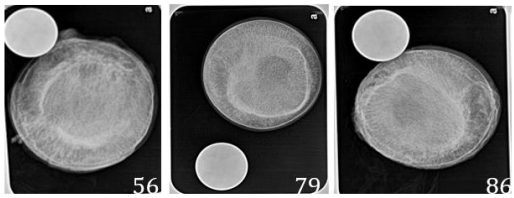
56
79
86

c

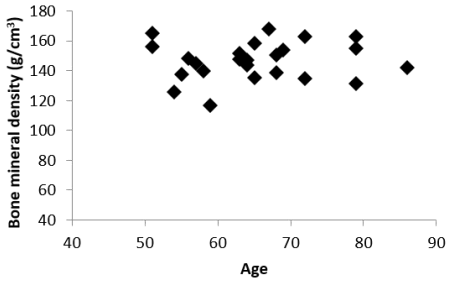
Bone mineral density (g/cm³)
Age
40
50
60
70
80
90
100
120
140
160
180

d

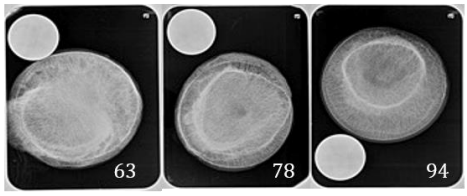
63
78
94

e

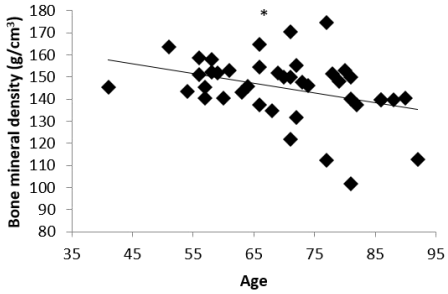
Bone mineral density (g/cm³)
Age
35
45
55
65
75
85
95
80
90
100
110
120
130
140
150
160
170
180
*

Figure 3.1. TMD measurements were calculated to determine and validate the BMD measurements and the corresponding trends observed. (a) A positive correlation was observed when comparing the microCT computed TMD measurements to the BMD measurements. Ten randomized femoral necks from OP patients were scanned through microCT in order to generate the computed TMD measurements. These measurements were then directly compared with the corresponding BMD measurements to validate any potentials trends between BMD and age. (b) X-ray images of three control extracted femoral heads. All patients were female and their age is labeled. X-rays were taken down the mid sagittal plane and a penny was used to verify consistency in distance between the handheld X–ray and specimen. (c) This was completed through Single Photon Absorptiometry (SPA), which utilizes a single-energy photon beam that passes through the bone to a detector, to quantify the patient's respective BMD. Femoral heads from 18 female OA patients were X-rayed, and their BMD was quantified. The data was then plotted and compared to increasing age and trends were observed. (d) Radiographs of three OP female's extracted femoral heads (age is labeled). (e) Extracted femoral heads from 35 female patients diagnosed with OP were X-rayed, and their BMD was quantified using SPA.

3.2 Successful Primary Cell Isolation and Culturing Method from Human Femoral Heads

Once the femoral head diagnosis was reaffirmed through X-ray and CTscans, mature osteoblasts were isolated. The human femoral heads were collected from Christiana Care Hospital in Newark, DE 48 hours post extraction (post hip arthroplasty surgery). They were collected from patients diagnosed with OP or OA. In a sterile cell culture environment, the femoral heads were sawed down the midsagittal plane, and fragments of trabecular bone were removed using nose pliers and were digested in a collagenase solution for two days at 37°C. After two days, the cellular suspension was strained and centrifuged. The pellet was re-suspended in fresh media

and plated in a culture flask. Plated cells were allowed to adhere to the flask for seven days without a media change. Subsequent media changes were conducted every four days. A schematic representing the cellular extraction process is shown in Figure 3.2.(186)

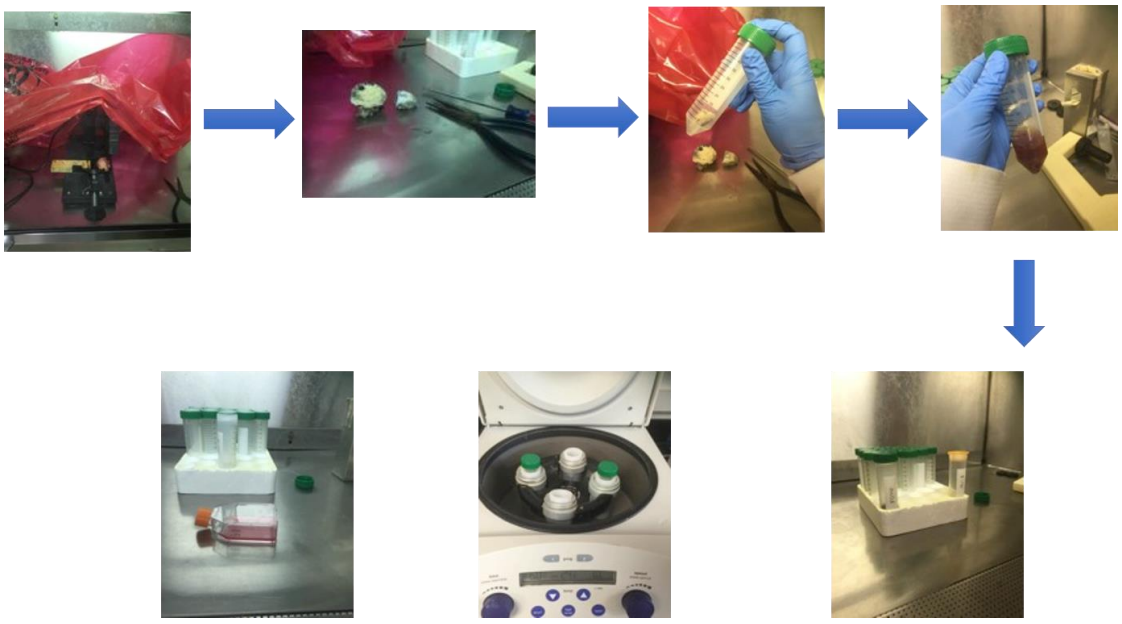

Figure 3.2. Primary cell extraction diagram. Schematic showing the steps involved in isolating primary osteoblasts from human femoral heads.

3.3 Cells Isolated from Digested Trabecular Bone Fragments Stain Positive for Active Osteoblast Markers

Most human, primary cell work in the bone field uses MSCs rather than mature bone cells. This is because MSCs are extremely easy to isolate, grow, and have a faster doubling time – thus a faster experimental turnaround time. There are some caveats to using strictly MSCs. Since they are being grown and differentiated *in vitro* there could be some discrepancies between how the cells react in culture, verse how

they would have reacted *in vivo*(187). Isolating and extracting mature osteoblasts is extremely time consuming and difficult, however, working with mature osteoblasts is more rewarding as it is more indicative of osteoblasts response *in vivo*(188). Mature osteoblasts phenotype were confirmed through fluorescently staining for osteoblast specific markers, ALP and OC. ALP is an early stage osteoblast marker, and OC is a late stage osteoblast marker. The primary cells were stained positive for both markers, (except the negative controls, or 2nd control), which can be seen in Figure 3.3. This confirmed that approximately 90% or more positively stained cells were osteoblasts and that mature osteoblasts were isolated from the femoral heads(186).

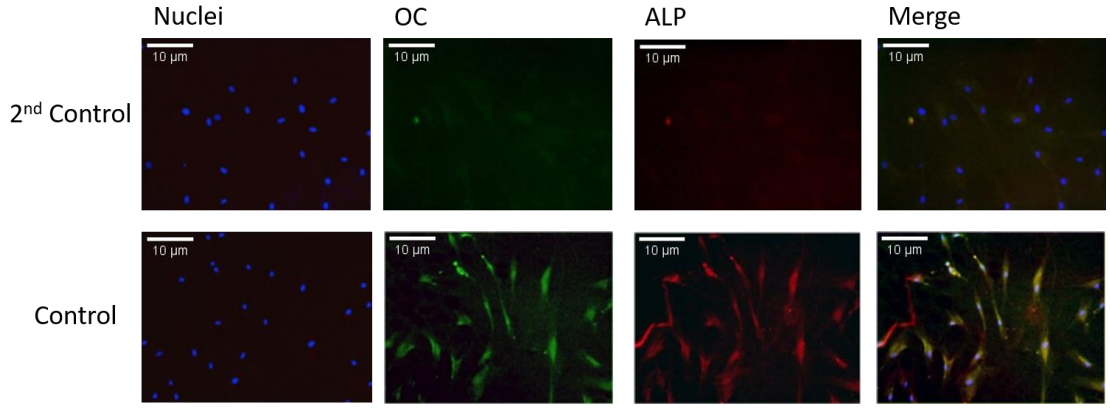

Figure 3.3. Osteoblast phenotype confirmed in isolated cells. Extracted cells were stained fluorescently for two osteoblast markers, ALP and OC.

3.4 Higher Basal Mineralization in OA Patient Cells when Compared with OP Patient Cells

Osteoblasts isolated from OA patients have a decreased mineralization when compared to cells isolated from normal patients. However, upon BMP2 stimulation the mineralization is shown to increase in OA osteoblasts, albeit not more than normal isolated osteoblasts [25]. I wanted to observe the mineralization potential of control or US cells from both the OA and OP populations. This was completed through a von

Kossa mineralization assay. The cells isolated from patients diagnosed with OA (aged 54-66) had a significant amount of mineralization deposits when compared with the cells isolated from patients diagnosed with OP (aged 60-82), seen in Figure 3.4. These data indicate that OA cells had a significantly higher basal mineralization level when compared to OP cells and suggested that they have different mineralization responses to BMP2(186).

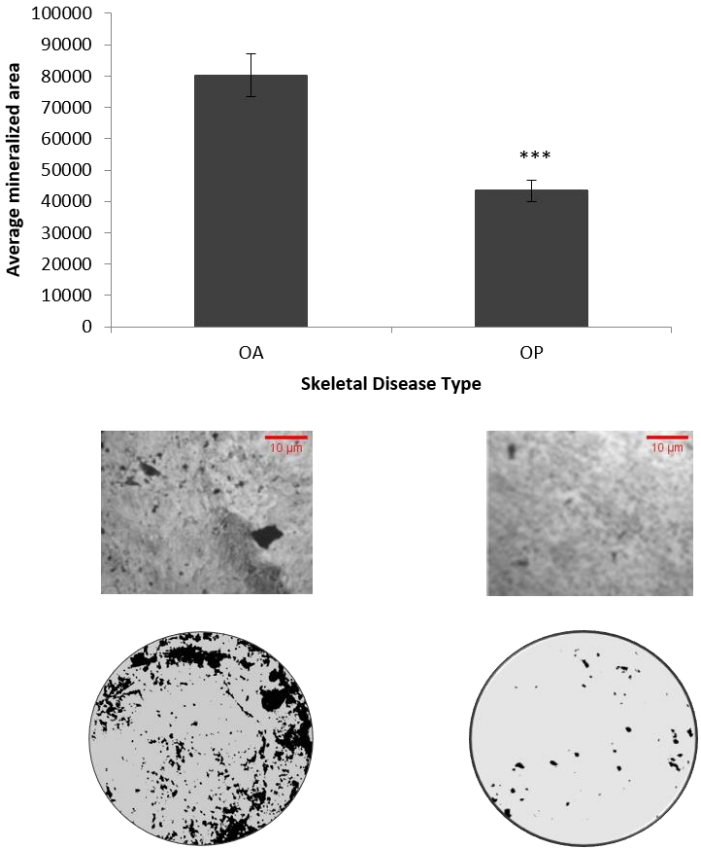

Figure 3.4. Basal level mineralization is higher in cells extracted from OA patients than OP patients. A von Kossa assay was used to determine mineralization potential between the two skeletal disease populations. Error bars represent standard error of the mean (SEM).

3.5 Cells from OP Patients do not Respond to BMP2 Stimulation

C2C12 cells, primary BMSCs and primary murine osteoblasts respond to BMP2 stimulation by increasing their mineralization [24]. However, these are all cells from mice, and it is unclear if mature human osteoblasts would have a similar response. A von Kossa assay was performed on the osteoblasts extracted from five female patients diagnosed with OA (aged 54-66) and five female patients diagnosed with OP (aged 60-80), to assess mineralization. The cells isolated from OA patients responded significantly when stimulated with BMP2 (Figure 3.5a), while OP cells showed no mineralization response with BMP2 stimulation when compared to the control (Figure 3.5b). This indicates a possible signaling disparity within the BMP pathway in cells extracted from OP patients(186).

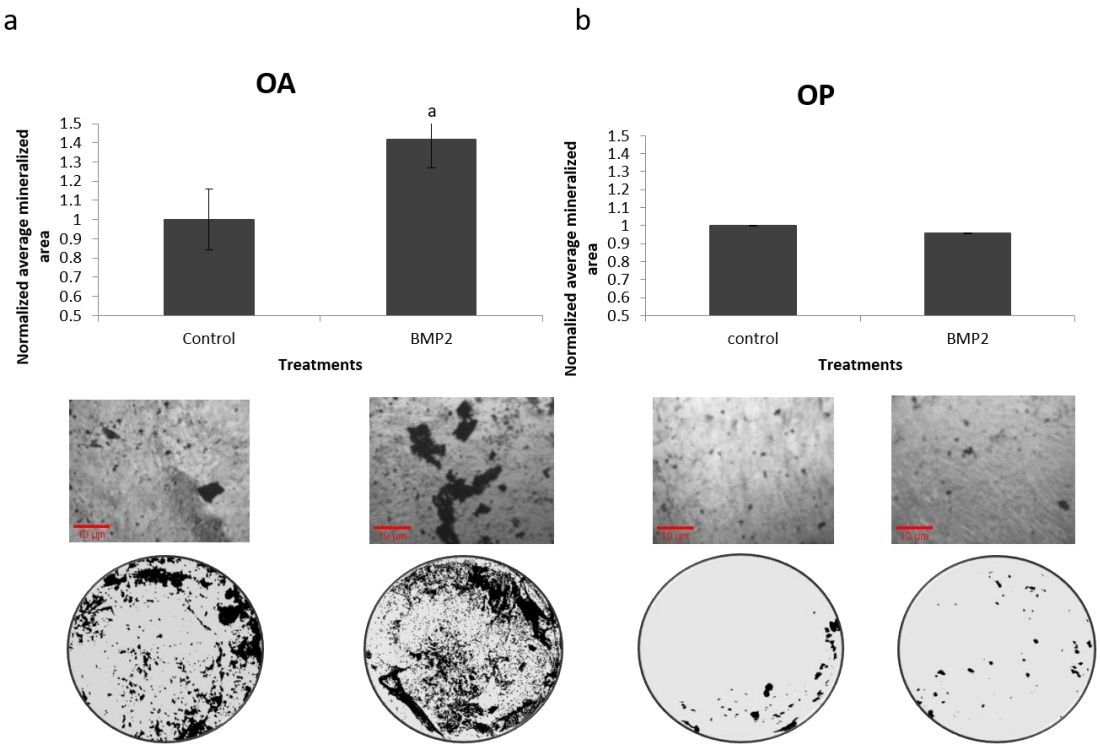

Figure 3.5. Cells isolated from OP patients do not mineralize in response to BMP2 stimulation. Mineralization was again assessed through a von Kossa assay. (A) Cells extracted from five female OA patients were analyzed and responded significantly to BMP2 stimulation when compared to US cells. (B) Cells extracted from five female OP patients were analyzed and showed no mineralization response when compared to the unstimulated ($p<0.05$). Error bars represent SEM.

3.6 Cells from Both OA and OP Patients Increase Mineralization in Response to CK2.3 Stimulation

A von Kossa assay was performed on the extracted osteoblasts from the same five female OA patients and cells extracted from five female OP patients to assess mineralization potential. The cells isolated from both significantly responded to CK2.3 stimulation (Figure 3.6a and b). CK2.3 has been shown to increase mineralization significantly in C2C12 cells, BMSCs, primary osteoblasts isolated from rodents [24],

and now primary osteoblasts from cells extracted from both OA and OP patients. While only cells extracted from OA patients responded to BMP2 stimulation, both cell populations responded to CK2.3 stimulation, showing that CK2.3 has an advantage over BMP2 by increasing osteoblast activity in OP cells(186).

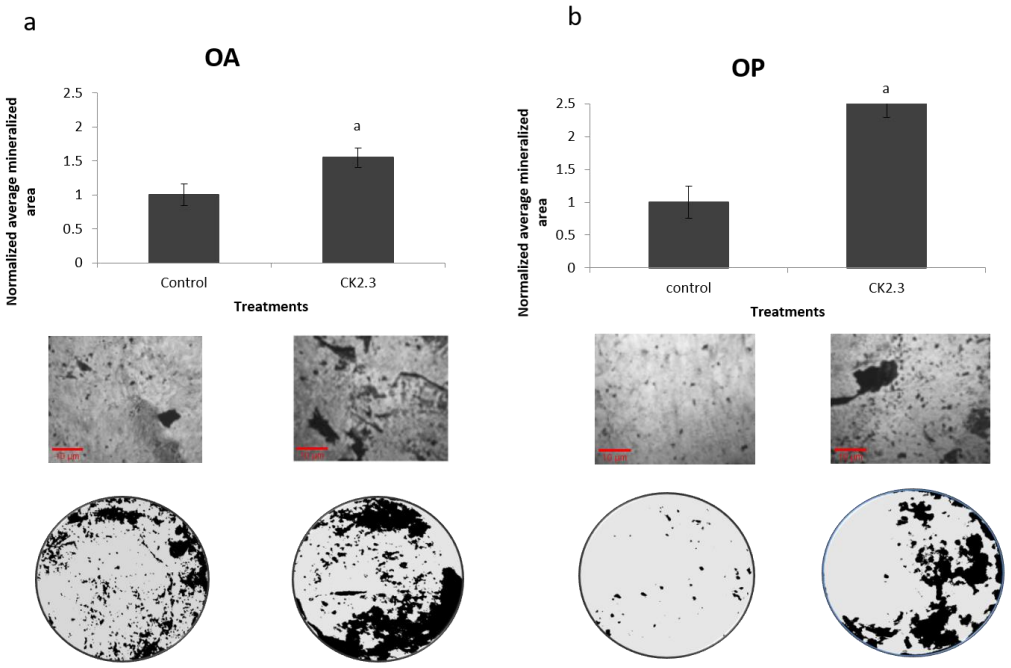

Figure 3.6. Cells isolated from both OA and OP patients increase their mineralization response to CK2.3 stimulation. (A) Cells extracted from five female OA patients were analyzed and significantly responded to CK2.3 stimulation when compared to US or control cells. (B) Cells extracted from five female OP patients were analyzed, and they significantly responded to CK2.3 treatment when compared to US or control cells. ($p<0.05$). Error bars represent SEM.

3.7 CK2.3 Increases Expression of Osteoblast Specific Marker in OP Cells from Patients

In order to observe the effects of BMP2 and CK2.3 stimulation on osteoblast expression in the cell population extracted from human femoral heads, three female OP patient cells (aged 60-80) were stained fluorescently for the osteoblast markers, ALP (red) and OC (green) as well as for the nucleus (blue). In all treatments, including control (or US), cells stained positive for both markers, (except the negative controls, which were only stained with the secondary antibody), which can be seen in Figure 3.7a. Cells also were counted for visible OC stain, ALP stain, both, or no stain (NS) in order to confirm equal seeding and population density. This was completed for cells stimulated with BMP2, CK2.3 or cells left US (control). The counts were divided by the nuclei count and multiplied by 100 to determine each stains population percentage (Figure 3.7b). Lastly, the intensity of the stains was quantified using ImageJ to determine whether treatments induced a stronger expression of OC or ALP. CK2.3 had significantly higher intensities of both OC and ALP (Figure 3.7c) when compared to control and BMP2 stimulated cells. This is indicative of increased osteoblast activity and differentiation when compared to BMP2 stimulation(186).

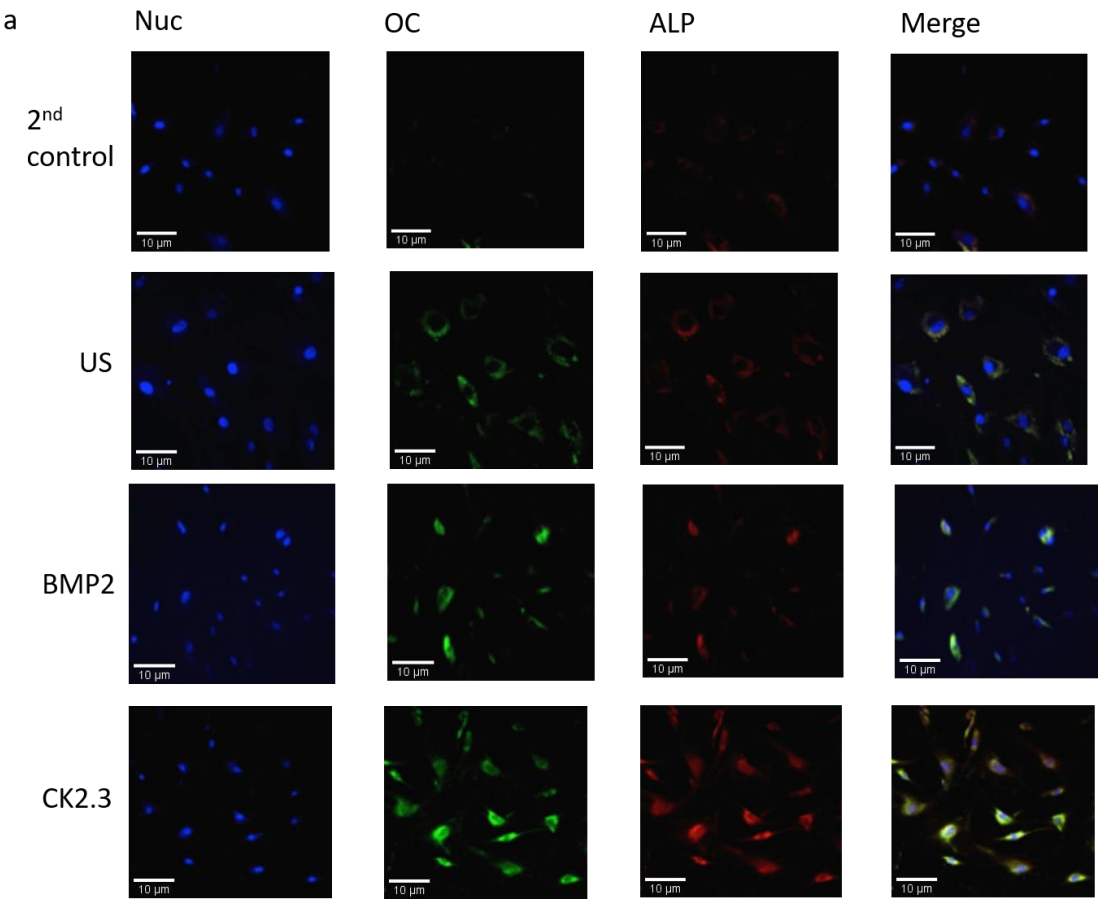
a
Nuc
OC
ALP
Merge
2nd control
US
BMP2
CK2.3
10 μm

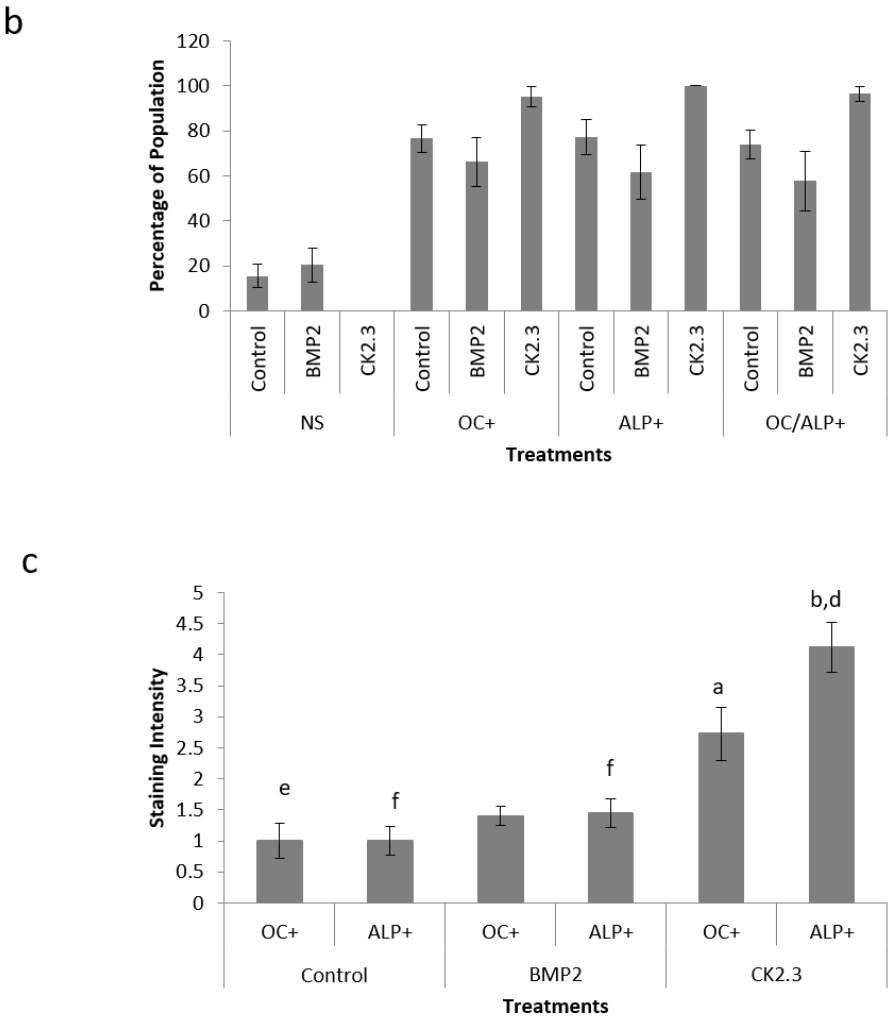

Figure 3.7. CK2.3 stimulation increases expression of both OC and ALP in primary human osteoblasts from OP patients. (A) Cells were stained fluorescently for the presence of osteoblast markers after treatment with BMP2, CK2.3, or left US. (B) Cells stained for OC, ALP, or both were counted and then divided by the total number of nuclei to obtain a stained cell percentage. All treatments resulted in an osteoblast phenotype. (C) The intensity of OC, ALP, or both were calculated through the "Color Histogram" function of ImageJ. CK2.3 had a significantly increased intensity of both OC and ALP when compared to BMP2 and control ($p<0.05$). Error bars represent SEM.

3.8 Trabecular Bone Explants as a Viable Bone Model System

I wanted to explore further how the native bone tissue reacted to stimulations with BMP2 and CK2.3, and to accomplish this I utilized an explant model. Explant models are beneficial models because you are employing the organ of interest and investigating the effects of stimulations or treatments on the native organ(189). It is important to note that OA patients will be referred to as control patients from herein, due to their positive and expected response to BMP2 stimulation (Figure 3.4a). To prep our samples for an explant study, the femoral heads (from both control and OP patients) were again cut down the midsagittal plane and the area of interest is indicated in Figure 3.8a. Control explants for the subsequent studies were isolated from patients aged 54-66 years old. OP explants were isolated from patients aged 79-87 years old. Bone fragments were fixed and stained for Calcein red-orange and Hoechst to determine efficacy and viability of the cells within the bone, and to test the model as a whole, Figure 3.8c. Calcein stains viable cells, while Hoechst is a nuclear stain that stains both live and dead cells. The bone fragments were imaged using confocal microscopy and the percent viability of the cells were determined. In both control and OP bone fragments, in all stimulations, cell viability was over 80%. This shows the efficacy of the trabecular bone model.

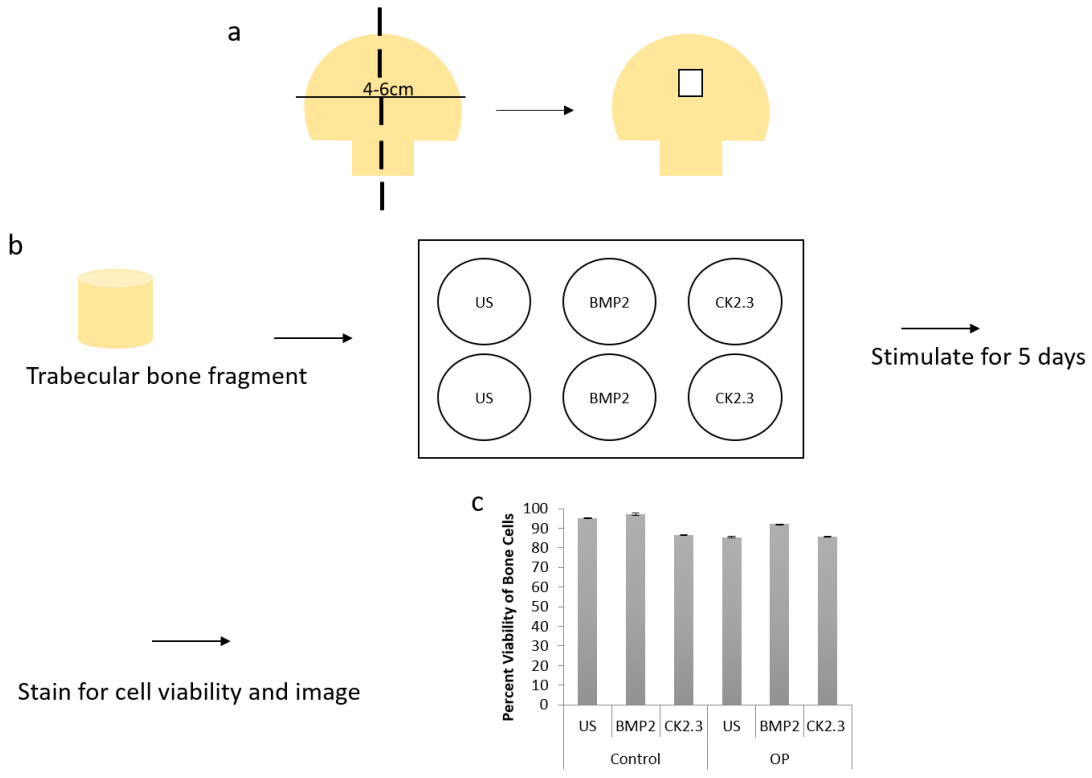

Figure 3.8. (A) A schematic representing how femoral heads were sliced down the midsagittal plane, and what region of interest was used for both the MMA experiments and the explant experiments. (B) Diagram showing the explant experimental set up. The trabecular bone fragment was removed from the femoral head, washed with PBS incubated with antibiotics/antimycotics for 10 minutes. The fragments were placed in a six well plate (one fragment per well) with DMEM. They were stimulated as designated for five days, following which they were either stained for cell viability and imaged or they were fixed with 4.4% PFA, fluorescently stained and then imaged. (C) Cell viability was assessed through a Calcein and Hoescht stain, and viable cells were counted. Under all stimulations and conditions cells were 80% or more viable within the explants. Error bars represent SEM.

3.9 BMP2 Stimulation Decreases OC and ALP Expression in OP Bone Explants when Compared to Control Explants

Once the explant model methodology was verified to be viable, I wanted to further validate its authenticity. Previously, I showed that primary osteoblasts isolated from OP patients had decreased expression of the osteoblast specific markers OC and ALP when stimulated with BMP2(158). I conducted the same study, except I used the explant model and included control patients as a comparison. The explants were stimulated with BMP2, CK2.3, or left US for five days. After the fifth day the explants were fixed in PFA and fluorescently labeled for OC (green) and ALP (red), Figure 3.9a and 3.9c. Representative images can be seen in Figures 3.9b and 3.9d, respectively. Again, BMP2 stimulation significantly decreased fluorescence of both OC and ALP in OP patients. However, CK2.3 significantly increased fluorescence of OC and ALP when compared to both BMP2 and US. Both BMP2 and CK2.3 significantly increased fluorescence of OC and ALP over US in control patients. This shows the validity of the trabecular bone explant model.

a

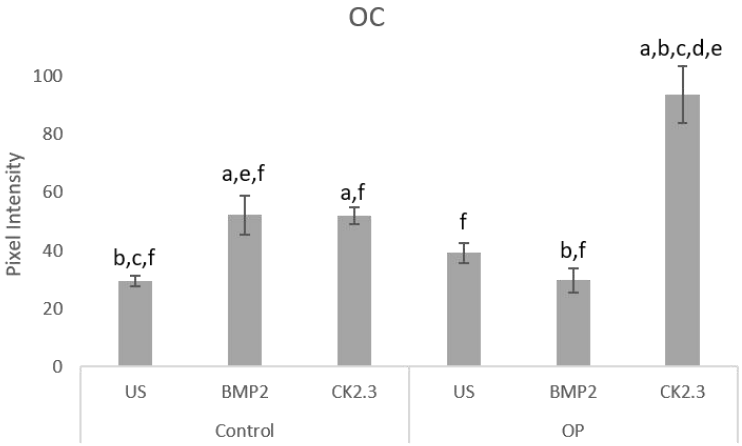
OC
Pixel Intensity
100
80
60
40
20
0
b,c,f
a,e,f
a,f
f
b,f
a,b,c,d,e
US
BMP2
CK2.3
US
BMP2
CK2.3
Control
OP

b

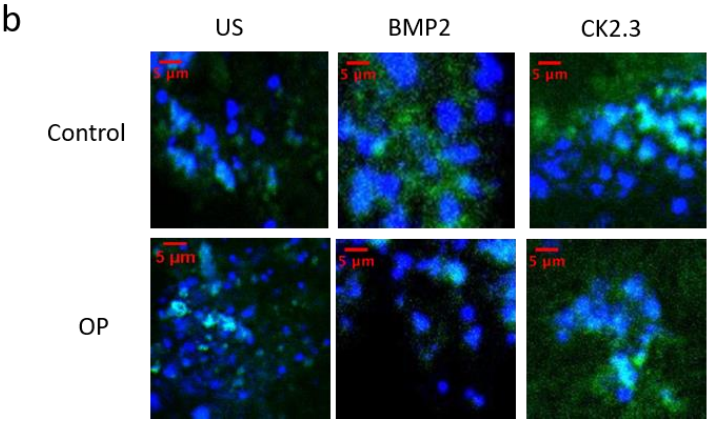
US
BMP2
CK2.3
Control
OP
5 µm

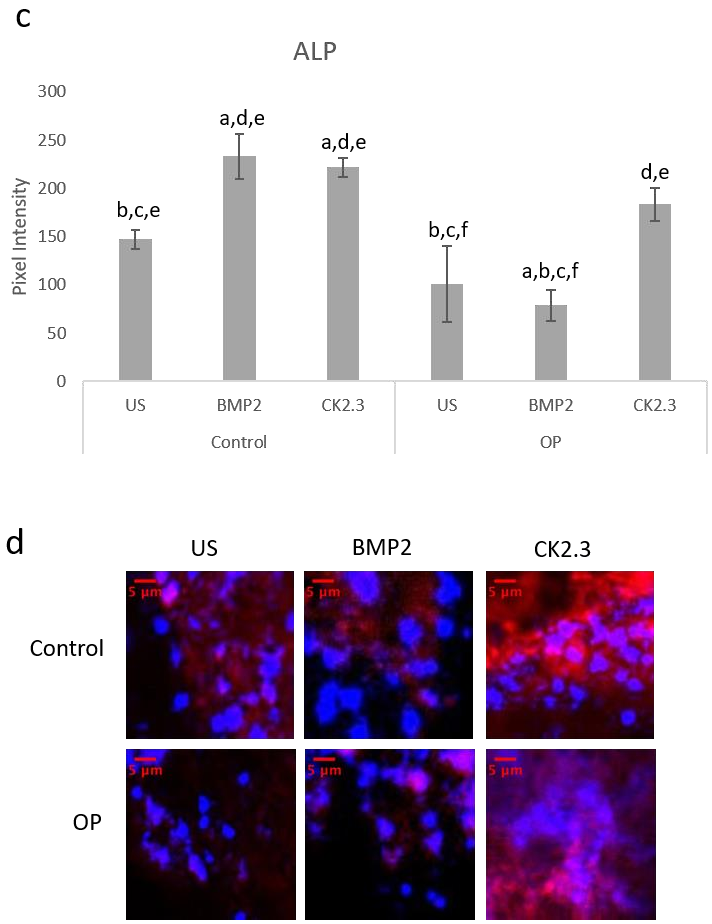

Figure 3.9. Explants from OP and control patients were prepared and stimulated with BMP2, CK2.3, or left US. After the fifth day the explants were fixed and stained for OC (green), ALP (red), and the nucleus (blue). (A) Control and OP explants stimulated with CK2.3 significantly increased expression of OC when compared to US and BMP2 stimulation. OP explants stimulated with BMP2 significantly decreased expression of OC. (B) Representative 2D images depicting the nuclear stain with the OC stain. (C) Both control and OP explants stimulated with CK2.3 significantly increased expression of ALP when compared to control and BMP2 stimulation. BMP2 stimulation significantly decreased ALP expression in both control and OP explants. (D) Representative 2D images depicting the nuclear stain overlay with the ALP stain. ($p<0.05$) Error bars represent SEM.

3.10 Increased Basal levels of BMPRIa and CK2α in Embedded Trabecular Bone Slices from OP patients

Due to the lack of BMP2 response previously shown in cells extracted from OP patients, receptor levels were investigated. Human femoral heads isolated from female patients diagnosed with OP, as well as control were again used. The specimens were preserved in 10% NBF solution within 48 hours of extraction. The samples were then cut down the midsagittal plane, and a 2mm bone fragment was removed and embedded in MMA to protect the normal integrity of the bone microenvironment. Other embedding methods, such as paraffin embedding, require bone demineralization before embedding, remove meaningful and important parameters when investigating skeletal based diseases, like OP(179). The embedded bone fragments were stained for BMPRIa (green) and CK2α (red), and increased fluorescence levels of both proteins were observed in the OP specimens, Figure 3.10. OP patients had significantly increased fluorescence of both BMPRIa and CK2α, when compared to control. This further indicates a signaling disparity within the BMP pathway that needs to be investigated.

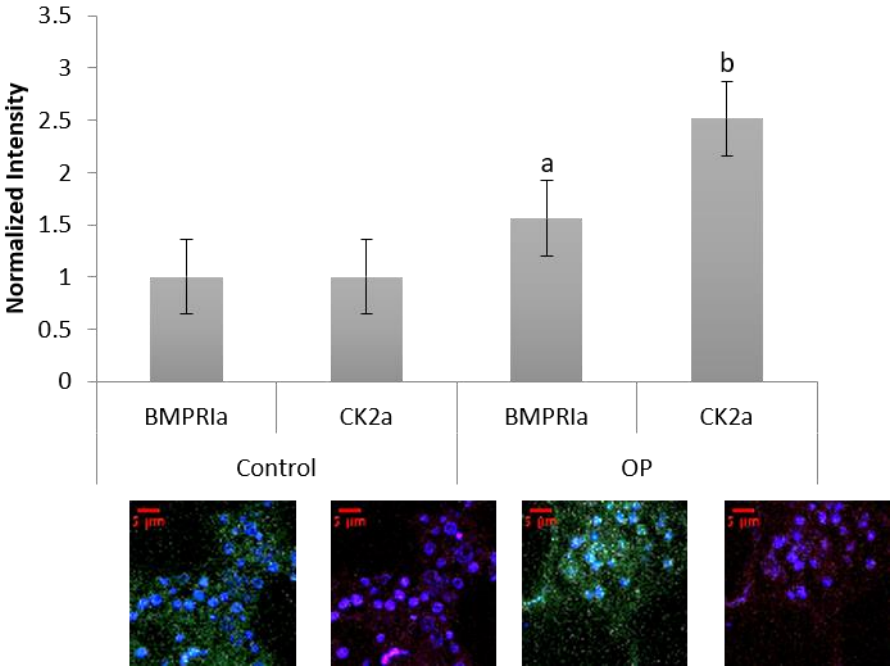

Figure 3.10.) Female OP and OA (control) trabecular bone slices were embedded in MMA and stained fluorescently for BMPRIa (green), CK2α (red), and the nucleus (blue). OP BMPRIa and CK2α expression was significantly higher than the expression levels in control bone slices. ($p<0.05$) Error bars depict SEM.

3.11 BMP2 Stimulation Decreases Expression of BMPRIa and CK2α in Explants Derived from OP Patients

The bone explant model was again utilized to study BMPRIa and CK2α expression after BMP2 and CK2.3 stimulation. Femoral heads from both control and OP samples were used and after the fifth day, once fixed, the samples were labeled fluorescently for BMPRIa (green) and CK2α(red). Representative images can be seen below each graph. In control samples there was a significant increase in BMPRIa fluorescence after both BMP2 and CK2.3 stimulation when compared to US, Figure 3.11a. In OP samples there was a significant decrease in BMPRIa fluorescence after BMP2 stimulation when compared to US and CK2.3 stimulated samples, Figure

3.11b. The fluorescence of BMPRIa in US explants was higher in explants from OP patients, when compared to the explants from OA patients. CK2α fluorescence followed the same pattern. In control patients, CK2α was increased significantly after both BMP2 and CK2.3 stimulation when compared to US explants, Figure 3.11c. BMP2 stimulation significantly decreased CK2α fluorescence in OP explants, when compared to US and CK2.3 stimulation, Figure 3.11d. Furthermore, both BMPRIa and CK2α fluorescent levels in US explants were significantly increased in explants isolated from OP patients when compared to control patients. For example, the pixel intensity of BMPRIa was around 300 in control explants, but was double that at 600 in OP explants, Figure 3.11a and 3.11b. This paralleled the response observed in the MMA trabecular bone slices, Figure 3.10, and further validates the experimental findings.

a

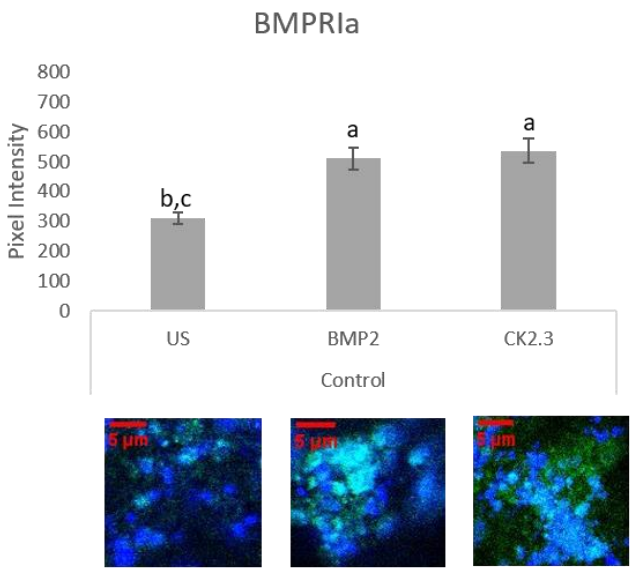
BMPRIa
Pixel Intensity
800
700
600
500
400
300
200
100
0
b,c
a
a
US
BMP2
CK2.3
Control
5 µm
5 µm
5 µm

b

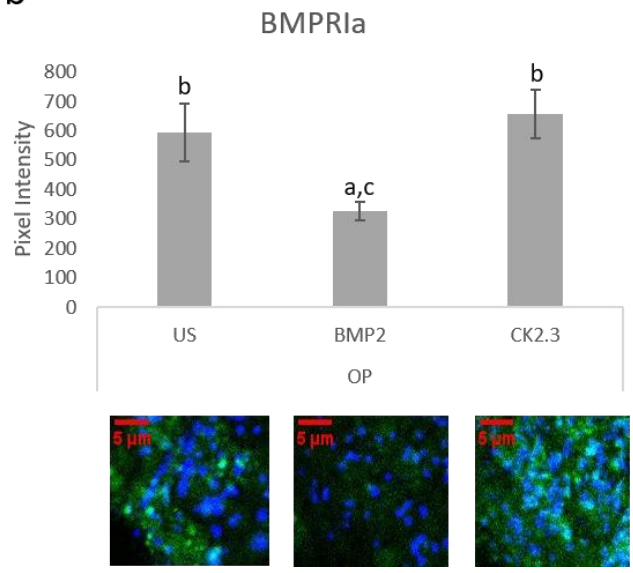
BMPRIa
Pixel Intensity
800
700
600
500
400
300
200
100
0
b
a,c
b
US
BMP2
CK2.3
OP
5 µm
5 µm
5 µm

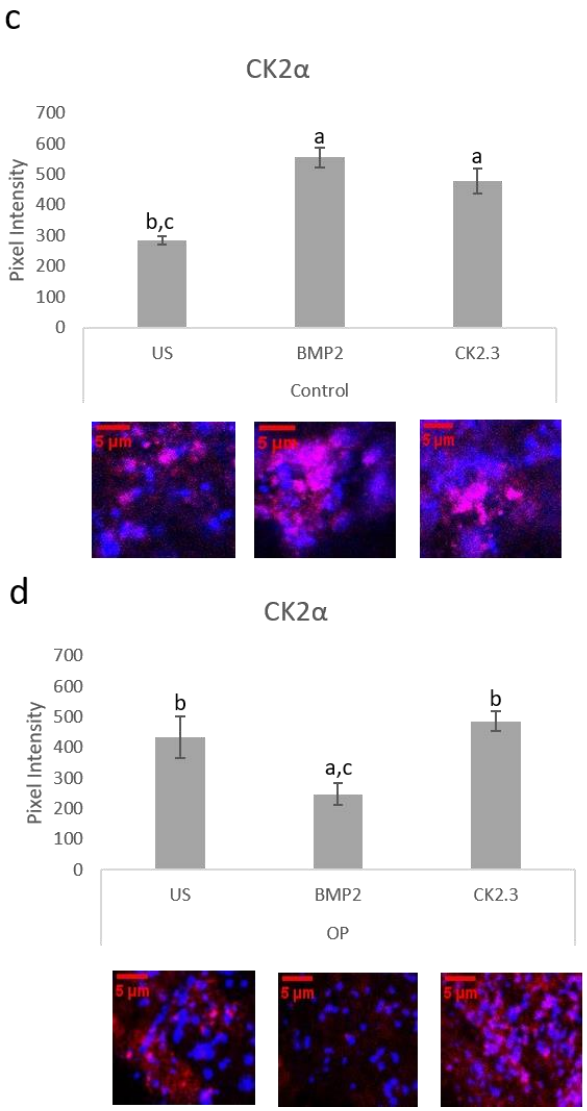

Figure 3.11. Trabecular bone slices were removed from isolated femoral heads. OP and control explants as described previously. Fixed explants were immunostained for BMPRIa (green), CK2α (red), and the nucleus (blue). (A) In control explants CK2.3 and BMP2 significantly increased BMPRIa expression when compared to US explants. (B) In OP explants, BMP2 significantly decreased BMPRIa expression when compared to CK2.3 and US explants. (C) In control explants, BMP2 and CK2.3 significantly increased expression of CK2α when compared to US explants. (D) In OP explants, BMP2 stimulation significantly decreased expression of CK2α when compared to US and CK2.3 stimulated explants. ($p<0.05$). Error bars represent SEM.

3.12 BMPRIa and CK2α expression levels in osteoblasts from OP patients

BMPRIa and CK2α expression levels were validated further in an *in vitro* model. Mature osteoblasts were isolated from five female OP patients (aged 60-87) as described previously. Cells were plated and stimulated with BMP2, CK2.3, or left US. After five days the cells were fixed and stained for BMPRIa (green), CK2α (red), and nucleus (blue). There was a significant increase in BMPRIa and CK2α fluorescence in CK2.3 stimulated cells when compared to BMP2 stimulation, Figure 3.12a and 3.12b. This paralleled the responses I had seen in both MMA embedded bone and the explant models. Next RNA was isolated from the cells and mRNA levels of *BMPRIa* and *CK2α* were detected through RT-PCR, Figure 3.12c. Again, BMP2 stimulation significantly decreased expression of BMPRIa when compared with US and CK2.3 stimulated cells. It is important to note that both BMP2 and CK2.3 stimulation did not increase BMPRIa immunofluorescence or steady-state mRNA levels over US levels. However, US BMPRIa immunofluorescence from embedded bone fragments from OP patients are increased when compared with US BMPRIa immunofluorescence levels in embedded bone fragments from OA patients. This further indicates a potentially BMP2 induced signaling disruption in OP as it parallels the responses seen in the MMA trabecular bone slices (Figure 3.10) and the bone explants (Figure 3.11). Taken together this indicates a major dysregulation in receptor expression in OP patients.

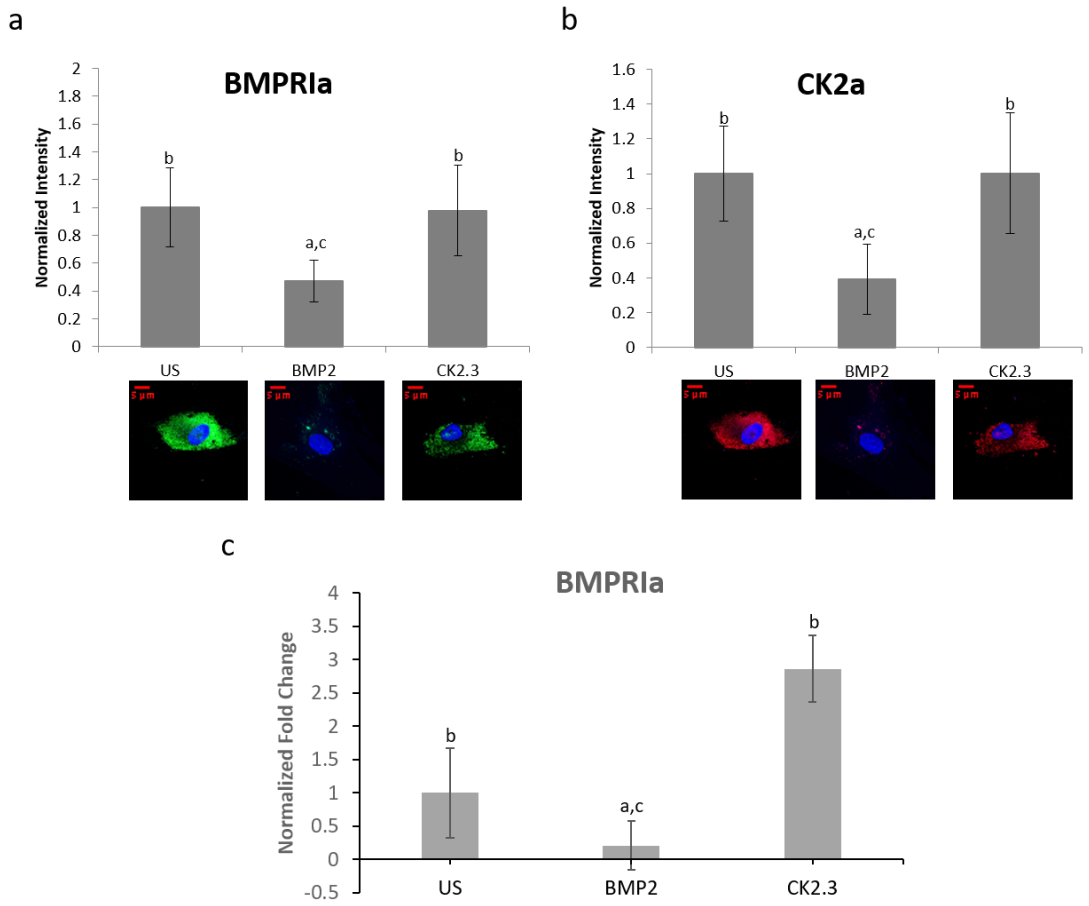

Figure 3.12. Osteoblasts extracted from OP patients were stimulated with BMP2, CK2.3, or left US for five days. After the fifth day the cells were fixed and immunostained for BMPRIa (green), CK2α (red), and the nucleus (blue). (A) CK2.3 and US cells significantly increased expression of BMPRIa when compared to BMP2 stimulation. (B) BMP2 stimulation significantly decreased expression of CK2α when compared to CK2.3 and US cells. (C) RNA was extracted from cells from OP patients after they were stimulated with BMP2, CK2.3, or left US for five days. BMP2 significantly decreased BMPRIa mRNA expression when compared to US and CK2.3 stimulated cells. ($p<0.05$) Error bars represent SEM.

3.13 BMP2 stimulation significantly decreases expression of pERK in osteoblasts from OP patients

Since BMP2 stimulation decreased expression of BMPRIa and CK2α, other downstream signaling proteins need to be investigated further to further elucidate where the BMP signaling disparity lies. The BMP2 signaling pathway is known to activate both SMAD signaling as well as SMAD independent signaling. SMAD independent signaling encompasses a variety of pathways, one of which is the ERK signaling pathway(55, 98). Therefore, mature osteoblasts isolated from five female OP patients (aged 60-87) were plated, grown, and stimulated with either BMP2, CK2.3 or left US. After the fifth day cells were immunostained for pERK (green), and the nucleus (blue), Figure 3.13a. Immunofluorescence of pERK, or activated ERK, was decreased significantly by BMP2 when compared to US and CK2.3 stimulated cells. These results were validated through immmunoblots. Briefly, patient cells were stimulated with BMP2, CK2.3 or left US for five days. On the fifth day whole cell lysates were collected, protein concentration was determined and normalized. Lysates were run on an SDS-PAGE gel, transferred to a PDVF membrane, and immunoblotted for pERK and β-actin. Protein expression of pERK was decreased signifcantly when compared to CK2.3 stimulated cells, Figure 3.13b. This indicates activated ERK signaling, or activated SMAD independent pathway, is disrupted in OP.

a

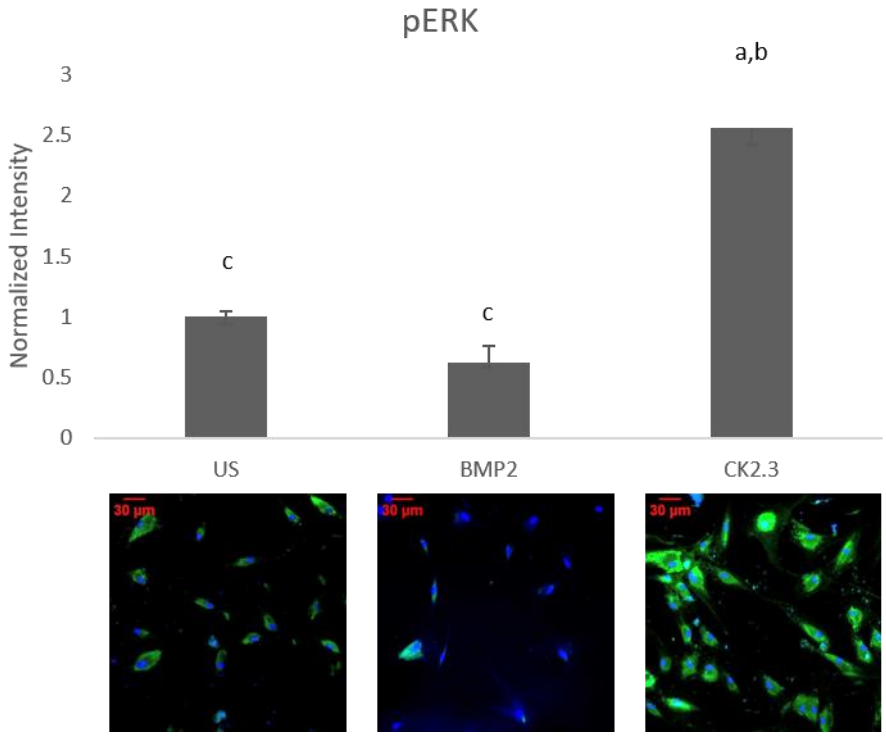
pERK
Normalized Intensity
3
2.5
2
1.5
1
0.5
0
c
c
a,b
US
BMP2
CK2.3
30 µm
30 µm
30 µm

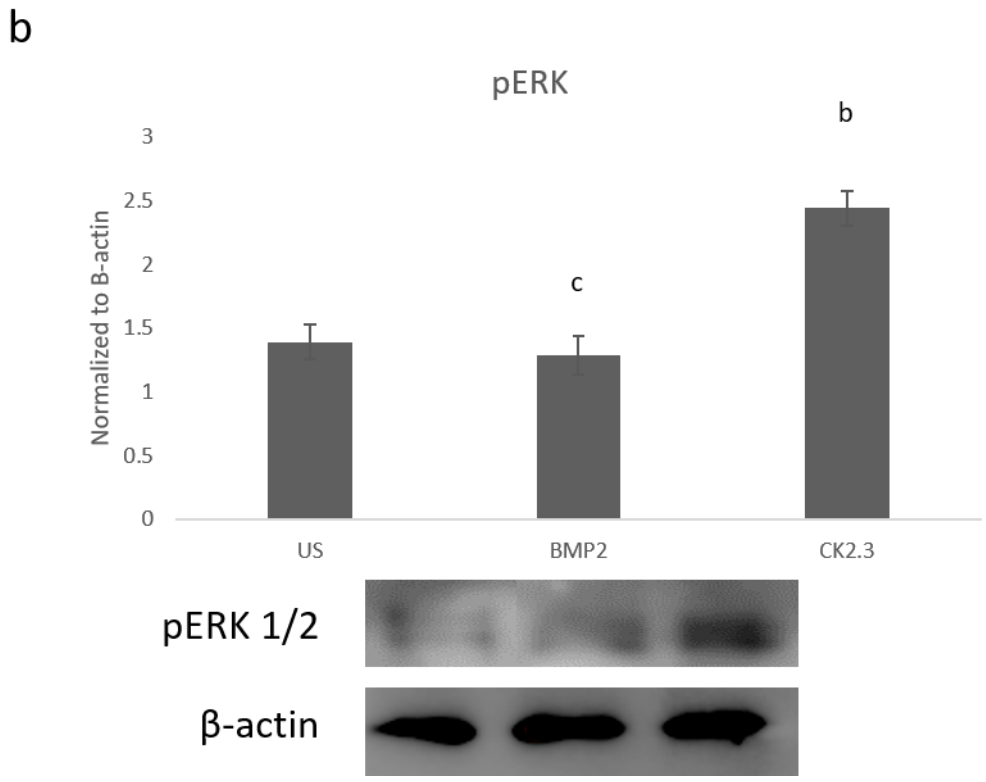

Figure 3.13. Mature osteoblasts were extracted from OP patients and stimulated with BMP2, CK2.3 or were left US for five days. On the fifth day cells were fixed and fluorescently stained for pERK (green) and the nucleus (blue). (A) CK2.3 significantly increase in fluorescence when compared to BMP2 and US cells. BMP2 stimulation significantly decreased fluorescent intensity when compared to CK2.3 stimulated cells. (B) Lysates were also collected from extract osteoblasts from OP patients and run on an SDS-Page gel to separate the proteins. The separated proteins were then transferred onto an immunoblot and pERK and β-actin protein levels were detected. Expression was detected by western blot and quantified through densiometric analysis. CK2.3 significantly increased expression of pERK when compared with US and BMP2 stimulated cells. ($p<0.05$) Error bars represent SEM.

3.14 pSMAD expression remains unchanged in osteoblasts from OP patients

Since ERK signaling was disrupted in OP patients, and is a part of SMAD independent signaling, SMAD dependent signaling also was investigated. Canonical SMAD signaling or SMAD dependent signaling is the most studied BMP signaling pathway(95, 96). The same five OP patient cells were stimulated with BMP2, CK2.3, or left US for five days. After the fifth day cells were immunolabeled for pSMAD (green), and the nucleus (blue), Figure 3.14a. While BMP2 stimulation seemed to decrease pSMAD (activated SMAD) fluorescent expression, it was not significant. These results were confirmed again through a western blot. The patient cells lysates were prepared as outlined above. Again, pSMAD expression did not change significantly under all stimulations, even though a slight decrease is observed following BMP2 stimulation Figure 3.14b. This indicates that the BMP signaling disparity is not within the SMAD dependent pathway.

a

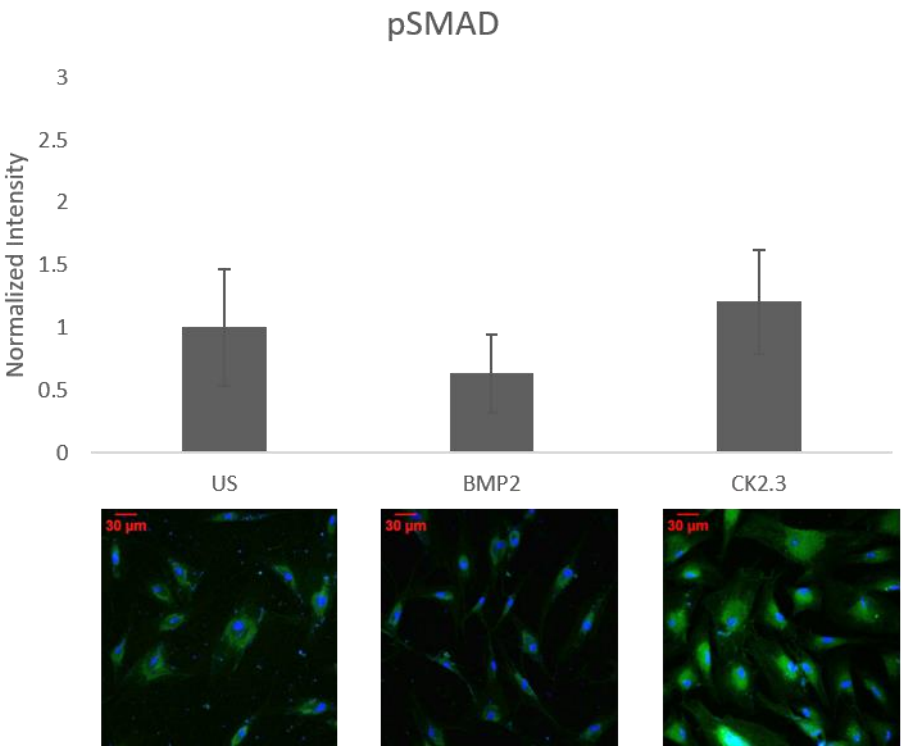
pSMAD
Normalized Intensity
3
2.5
2
1.5
1
0.5
0
US
BMP2
CK2.3
30 µm
30 µm
30 µm

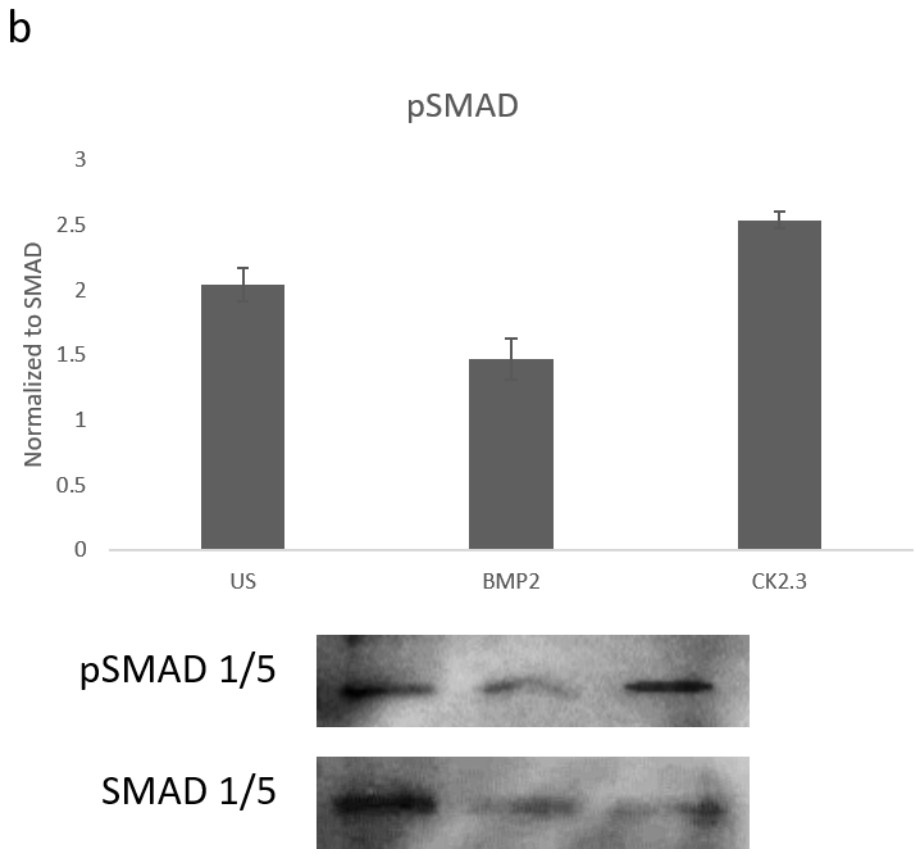

Figure 3.14. Mature osteoblasts were extracted from OP patients and stimulated with BMP2, CK2.3 or were left US for five days. On the fifth day cells were fixed and immunostained for pSMAD (green) and the nucleus (blue). (A) pSMAD immunofluorescence remains unchanged under all stimulations, while BMP2 stimulation indicates a slight decrease in expression, this was not significant. (B) Lysates also were collected from osteoblasts from OP patients and run on an SDS-Page gel to separate the proteins. The separated proteins were then transferred onto an immunoblot and pSMAD and SMAD protein levels were detected. Expression levels were determined through densiometric analysis BMP2 stimulation seems to decrease pSMAD expression, but this difference was not significant. Error bars represent SEM.

3.15 CK2 mediated colocalization with downstream BMP signaling proteins

If the BMP signaling disparity is not within the SMAD dependent pathway (but within the SMAD independent pathway) a mechanism of action needs to be investigated. Previously, it was shown the CK2 can bind to and activate ERK, helping to mediate its translocation into the nucleus and thus induce its pro-osteogenic effects(119). Therefore, pERK and CK2α interaction was investigated further through a co-localization study. The same five OP patient cells were stimulated with BMP2, CK2.3, or left US for five days. On the fifth day cells were fixed with PFA and labeled immunofluorescently for pERK (green), CK2α (red), and the nucleus (blue). BMP2 stimulation significantly decreased the number of pixel colocalization (Ncoloc) between pERK and CK2α when compared to both US and CK2.3 stimulated cells, Figure 3.15a. Representative images can be seen in Figure 3.15b, with a zoom 10 images showing cytoplasmic colocalization and overlay between pERK and CK2α. CK2.3 stimulation significantly increased pERK and CK2α Ncoloc when compared to US and BMP2 stimulated cells. This indicates that not only does BMP2 stimulation decrease the occurrence of pERK and CK2α interacting together, but that CK2.3 increases this interaction thus suggesting a potential mechanism of action for the novel peptide. As seen in Table 3.1, the Manders coefficients reported for CK2.3 stimulated cells are 0.843143 for Manders 1 and 0.769143 for Manders 2, indicating that increased pixel-pixel colocalization is observed. pSMAD and CK2α interaction was also investigated through a co-localization study. Patients cells were prepared as outlined above. They were labeled immunofluorescently for pSMAD (green), CK2α (red), and nucleus (blue), Figure 3.15c. Representative images can be seen in Figure 3.15d. No significant Ncoloc was observed in all stimulations between pSMAD and CK2α, indicating that CK2 does not mediate the direct activation of SMAD in OP

patients. As seen in Table 3.2, the Manders coefficients reported are all similar, around 0.8. This indicates that no increase or decrease in pixel-pixel colocalization was observed after stimulations with BMP2 or CK2.3.

a

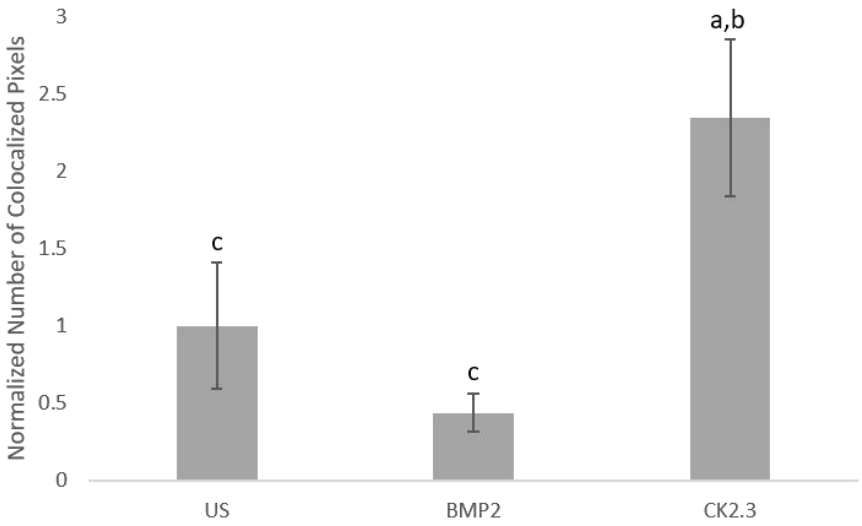
Normalized Number of Colocalized Pixels
3
2.5
2
1.5
1
0.5
0
c
c
a,b
US
BMP2
CK2.3

b

Zoom 10

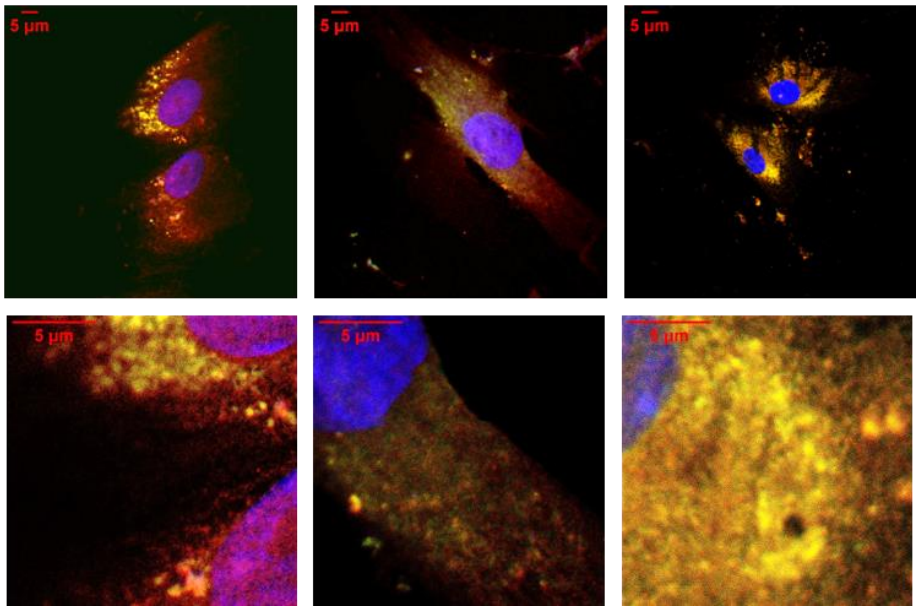
5 µm

c

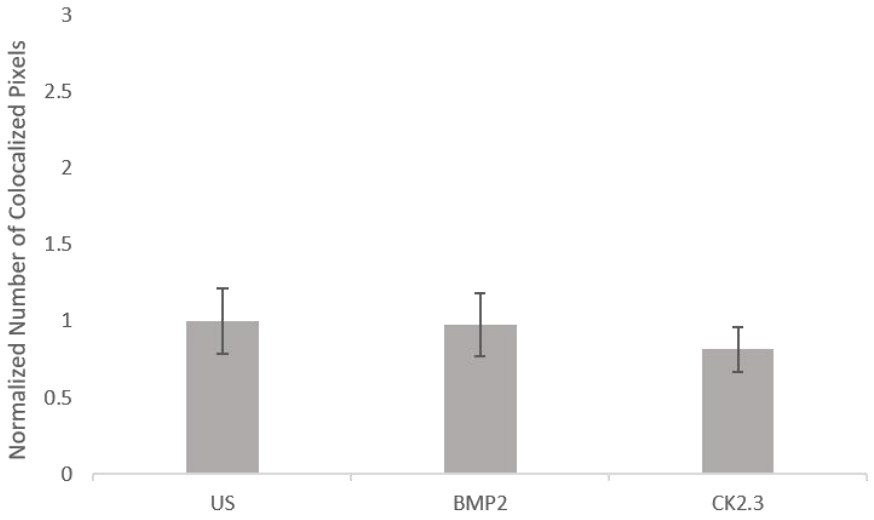
Normalized Number of Colocalized Pixels
3
2.5
2
1.5
1
0.5
0
US
BMP2
CK2.3

d

Zoom 10

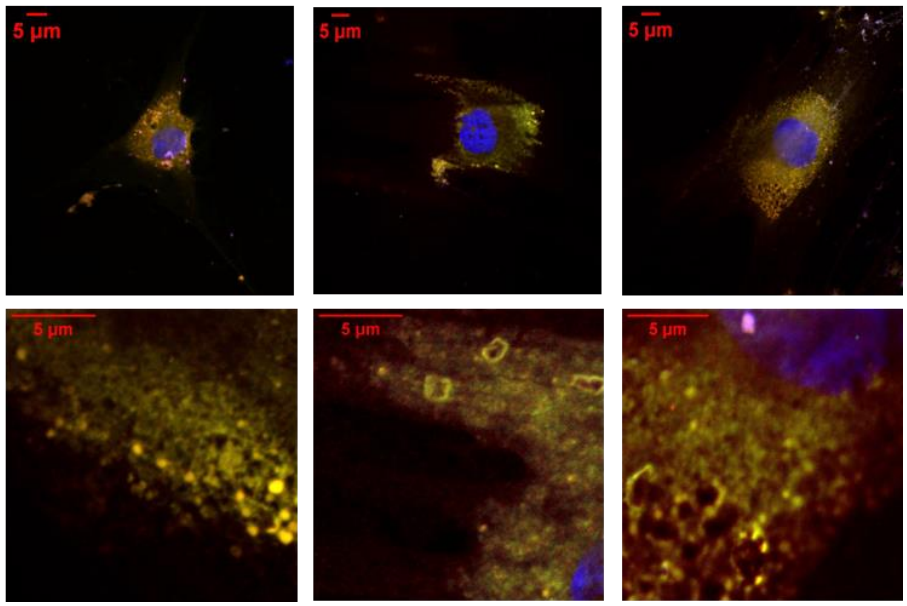
5 µm
5 µm
5 µm
5 µm
5 µm
5 µm

Figure 3.15. Mature osteoblasts were extracted from OP patients and stimulated with either BMP2, CK2.3, or left US for five days. On the fifth day the cells were fixed and immunofluorescently stained for pERK or pSMAD (green) and CK2α (red). (A) Decreased colocalized pixels between pERK and CK2α were observed after BMP2 stimulation, while CK2.3 stimulation significantly increased pixel colocalization. (B) Representative images with a zoom 10 panel showing enlarged portions of the cells' cytoplasm. (C) Pixel colocalization remained constant between pSMAD and CK2α under all conditions. (D) Representative images with a zoom 10 panel showing enlarged portions of the cell's cytoplasm. ($p<0.05$) Error bars represent SEM.

Table 3.1 Manders Coefficients for pERK and CK2α

Averaged Values	US	BMP2	CK2.3
Manders 1	0.667333	0.370273	0.843143
Standard Error	*0.272438*	*0.123424*	*0.243394*
Manders 2	0.355167	0.385818	0.769143
Standard Error	*0.144996*	*0.128606*	*0.222032*

Table 3.2 Manders Coefficients for pSMAD and CK2α

Averaged Values	US	BMP2	CK2.3
Manders 1	0.83333333	0.86627273	0.88009091
Standard Error	*0.03707837*	*0.01432369*	*0.0164537*
Manders 2	0.84455556	0.88172727	0.89263636
Standard Error	*0.03773854*	*0.00898897*	*0.00860259*

3.16 Preliminary BMP2 and CK2.3 Mineralization Concentration Curves

The BMP2 and CK2.3 concentrations used for all previous *in vitro* and *in vivo* work remained constant, as both have been shown to induce responses previously in

immortalized cell lines. However, this could explain the lack of response observed with BMP2 stimulation in the human OP cells. It is possible that the concentration of BMP2 used was too low and other concentrations needed to be further explored. Therefore, a von Kossa concentration curve was conducted on cells extracted from an OP patient after both various BMP2 and CK2.3 concentrations. The cells were stimulated with 25 nM, 40 nM, 100 nM, 200 nM, and 250 nM BMP2 or left US. While this experiment was conducted only in cells extracted from one patients, the trends observed indicate that even with an increase in BMP2 stimulation, OP cells do not mineralize in response to BMP2 stimulation, Figure 3.16a. It is important to note increased BMP2 concentration did overcome the mineralization suppression effect, by increasing mineralization back to US levels. A similar experiment was conducted with CK2.3, and the subsequent concentrations used were 50 nM, 75 nM, 100 nM, 200 nM, and 250 nM. Again, because this experiment was conducted only in cells extracted from one patients, significance could not be determined. However, the trends observed are interesting. With increasing CK2.3 concentration, there is an increase in mineralization when normalized to US cells, Figure 3.6b. More trials would need to be conducted in cells extracted from other OP patients to verify the trends observed. However, it is important to note that even with a drastic increase in BMP2 concentration, the cells from OP patients do not respond, further indicating aberrant BMP signaling in OP patients.

a

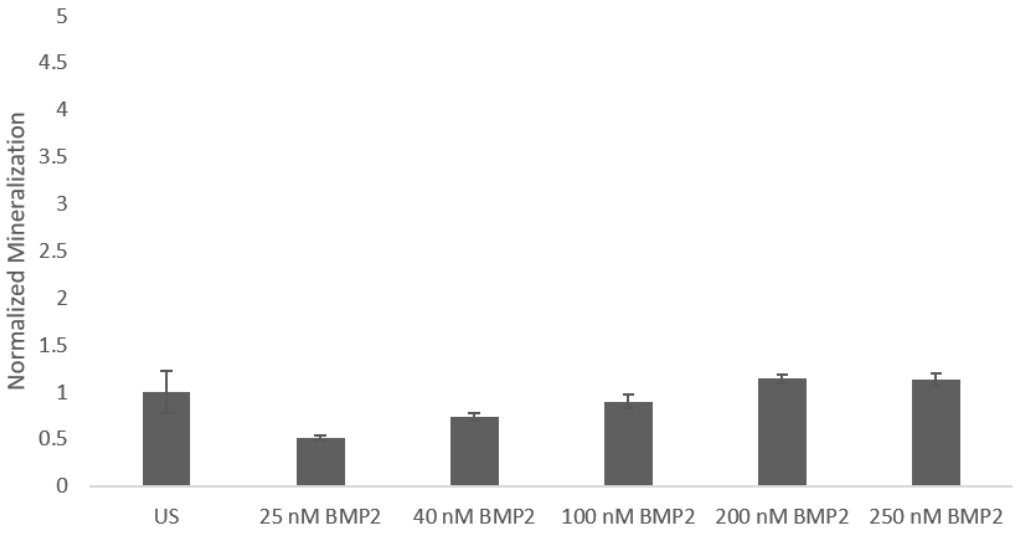
Normalized Mineralization
5
4.5
4
3.5
3
2.5
2
1.5
1
0.5
0
US
25 nM BMP2
40 nM BMP2
100 nM BMP2
200 nM BMP2
250 nM BMP2

b

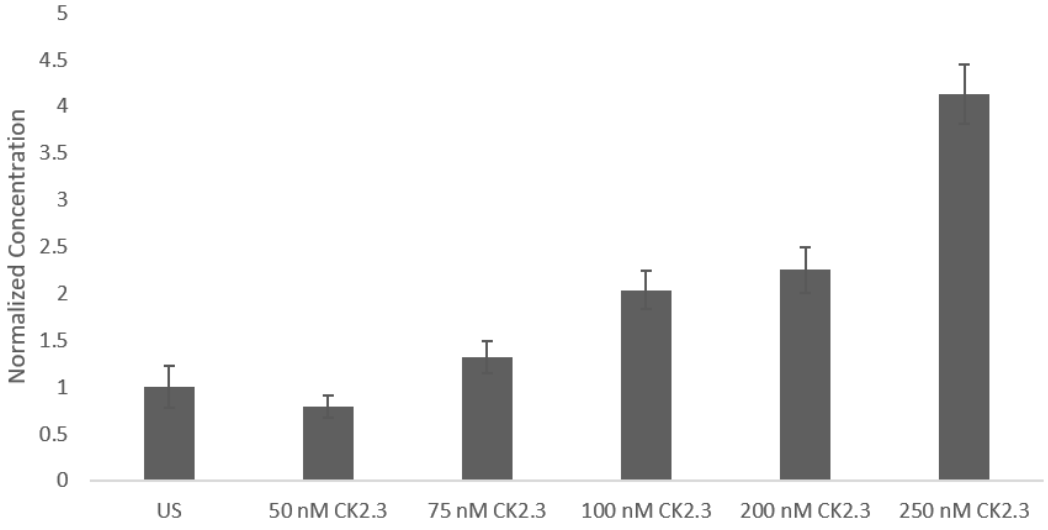
Normalized Concentration
5
4.5
4
3.5
3
2.5
2
1.5
1
0.5
0
US
50 nM CK2.3
75 nM CK2.3
100 nM CK2.3
200 nM CK2.3
250 nM CK2.3

Figure 3.16. Preliminary BMP2 and CK2.3 Concentration Curves. Cells extracted from a female 88-year-old OP patient were stimulated with the above designated concentrations of (A) BMP2 and (B) CK2.3 for five days. On the fifth day the cells were fixed in PFA and stained for mineralization through a von Kossa assay. This experiment needs to be completed again to verify the above trends observed.

Chapter 4

DISCUSSION

Bone is one of the most vital human organs. It protects, provides structure, support, locomotion, and mineral homeostasis to the human body. Continued maintenance of bone is critical for both structure and function(1). This maintenance is acquired through balanced activity of the cells involved in the bone remodeling cycle. The two major cell types responsible for maintaining bone are osteoblasts (bone forming cells) and osteoclasts (bone resorbing cells)(9). Dysregulation of this cycle lends itself to several bone diseases. The most common of these bone diseases in humans is OP, which occurs when there is too much osteoclast activity and too little osteoblast activity(6). This imbalance within the bone remodeling cycle leads to more porous or brittle bones that are susceptible to fractures. Bone fractures are extremely debilitating, and as OP is common in the older population where bone fractures are often life changing. While there are current therapeutics on the market to help treat OP, none of them are ideal as they produce several unwarranted side effects or can be taken only for a limited number of years(144). Currently, the best therapeutic option for OP is prevention, but this does not help those already diagnosed and struggling with this disease.

There are two types of OP treatments: antiresorptive and anabolic. Many of the current therapeutics are antiresorptive because they focus on decreasing osteoclast activity. Therapeutics that target osteoblast activity are called anabolic treatments, and there are very few on the market. Both osteoblasts and osteoclasts communicate with

one another when in the bone microenvironment. Therefore, it is detrimental for therapeutics to target one cell type over the other. A lot of the aforementioned side effects often entail a dramatic increase or decrease in the opposite cell type(144). Therefore, there is a great need to develop better OP therapeutics that are both antiresorptive and anabolic. This becomes even more critical as the older population continues to increase(6). In order to find new effective treatments, the exact molecular mechanisms of OP need to be further investigated.

BMP2 is a multipotent growth factor that is known to induce both osteoblasts and osteoclasts; therefore, it is a crucial factor to study when thinking about bone maintenance and OP. BMP2 has many uses in the clinic, in 2002 it was approved by the FDA for the healing of long bone fractures and spinal fusion surgeries. However, recently there has been some controversary surrounding the use of BMP2 itself in the clinic as many adverse side effects were reported(190). While BMP2 may not be an ideal therapeutic for OP, investigation of its signaling pathway is of interest since it can stimulate activity of the two major bone cells. Prolonged use of BMP2 has been linked to increased osteolysis or bone resorption therefore, it is not a viable treatment of OP(152, 190). Further research into the BMP pathway is of interest since it is known to activate and increase both osteoblast and osteoclast activity.

Multiple discrepancies have been noted with BMP2 and the BMP pathway in patients diagnosed with OP. These include different polymorphisms of the *BMP2* gene associated with osteoporotic parameters(156, 191) as well as a decrease in expression of key signaling proteins involved in BMP signaling (SMAD4, pSMAD1, pERK, RUNX2)(159). An interesting study was conducted in 2016 by Ehnert and colleagues that found that 30.9% of 110 total bone donors did not respond to BMP2 stimulation.

They also found that osteoblasts extracted from the bone specimens had high BAMBI expression and very low SOST expression. It is important to note that this particular study did not look into what skeletal diseases the donors had, and therefore it is hard to determine whether or not the population of individuals that did not respond to BMP2 stimulation had OP(166). However, several research groups have cited the decrease in BMP2 response in OP MSCs when assessed for mRNA expression of key osteogenic markers (like RUNX2, COL1A1, ALP, and OC)(162, 163). Additionally, MSC's derived from OP patients had significantly increased levels of BMPRIa when compared to control patients, pointing to a possible receptor distribution or recycling issue as a potential cause of aberrant BMP signaling(165). This increases interest in investigating this signaling pathway, not only for the development of new therapeutics, but to better understand the underlying molecular mechanisms leading to OP. Additionally, the Nohe lab has developed and discovered a novel peptide, CK2.3, that also utilizes the BMP signaling pathway in order to induce its signaling cascades (SMAD dependent and SMAD independent signaling). The Nohe lab has previously shown CK2.3's efficacy in multiple cell and animal models with its pro-osteoblast and anti-osteoclast effects(73, 97, 115-118). The effect of CK2.3 on cells extracted from OP patients had not been studied. My project was to investigate how cells extracted from OP and OA patients responded to CK2.3 stimulation, as well as BMP2 stimulation. I was interested in the mature osteoblast's response to both CK2.3 and BMP2 stimulation because there is not a lot of current research available on mature osteoblasts directly isolated from human patients. Most research focuses on BMSCs because they are easy to isolate and culture. Mature osteoblasts require several weeks

of culture before they are ready for plating and fixation, which makes this project novel.

For my project, I collected femoral heads from Christiana Care Hospital in Newark, DE after the patients underwent hip arthroplasty surgery. Before studying the direct effect of CK2.3 and BMP2 on cells extracted from femoral heads of OP and OA patients, the BMD of the femoral heads needed to be determined in order to confirm that the bone tissue localized within was osteoporotic or osteoarthritic. The BMD of the femoral heads was obtained through single photon absorptiometry (SPA), where a single light beam passes through the sample and onto a detector. The resulting radiographs were assessed in ImageJ to determine their BMD. Once determined these values were compared to TMD values, which were generated using microCT. This was done to determine the efficacy of determining BMD through SPA. There was a significant positive correlation between the TMD measurements and the BMD measurements, which can be seen in Figure 3.2a. The BMD remains unchanged in OA patients and decreases significantly in OP patients, as seen in Figure 3.2c and 3.2e, respectively. Representative radiographs can be seen in Figure 3.2b and 3.2d. Current research confirms that as the age of the patients increases, their BMD decreases, but OP patients had lower BMD when compared with OA patients(192). Ten years after menopause the BMD of women is three times less than what it was prior to menopause. The average age for a woman to undergo menopause is 51, meaning that the average age of lower BMD would be around 61(6). We found that around 60-70 years of age BMD decreases(192)(192)(192)(192)(192)(192)(192)(191)(190). Determining BMD helped confirm the extracted femoral heads were osteoporotic or osteoarthritic. We selected femoral heads closest to the trendline from the quantified

BMD where mature osteoblasts would be extracted for further investigation. In order to determine and confirm that the cells extracted from the femoral heads were indeed osteoblasts, the cells were stained immunofluorescently for two osteoblast markers, OC (green) and ALP (red), which can be seen in Figure 3.3. The positive staining for both in US cells confirmed I had successfully isolated a 99% pure and mature osteoblast culture from the femoral heads. While the proliferation rates of the extracted cells varied from patient to patient, analyzing their extracted osteoblasts' response to CK2.3 and BMP2 stimulation as it can lead to further understanding the molecular causes of OP.

Next, the extracted cells were assessed for mineralization using a Von Kossa assay. A Von Kossa assay was used because it measures and stains phosphate deposits. Phosphate is an important and prominent component of bone, which allows for a functional *in vitro* test to determine if bone formation is occurring(193). Osteoblasts from both OP and OA patients were assessed after stimulation with BMP2, CK2.3 or left US. However, prior to assessing mineralization after subsequent stimulation, the basal level mineralization potential was determined between both OP and OA cells. Cells extracted from OA patients had a significantly higher basal mineralization levels, when compared to cells extracted from OP patients, Figure 3.4. This was expected, as OP is a debilitating bone disease caused by a decrease in osteoblast activity, or bone formation and subsequent mineralization. We next wanted to determine the effect of both BMP2 and CK2.3 on cells isolated from OP and OA patients. CK2.3 already has been shown to increase mineralization in C2C12 cells and primary murine cells(116, 117). Cells extracted from OA patients and stimulated with BMP2 had significantly higher mineralization than US cells, Figure 3.5a. This

response mirrors previous results obtained from C2C12 cells, primary bovine cells, and primary murine cells. Interestingly, cells extracted from OP patients did not respond to BMP2 stimulation, Figure 3.5b. This mirrors previous results obtained from other research groups, where OP bone specimens, or cells did not respond to BMP2 stimulation, or have some type of dysregulation of the BMP signaling pathway(159, 165). Cells extracted from both skeletal diseases responded to CK2.3 stimulation by significantly increasing mineralization when compared to US cells, Figure 3.6a and 3.6b. Further, when CK2.3 mineralization levels were compared with BMP2 mineralization levels, CK2.3 had slightly elevated mineralization over BMP2. This difference was not statistically significant in cells extracted from OA patients, however CK2.3 significantly increased mineralization over BMP2 and US cells in cells extracted from OP patients. This shows a potential signaling bias occurring within the BMP pathway, since cells from OP patients did not respond to BMP2 stimulation but did respond to CK2.3 stimulation. CK2.3 acts through the BMP pathway; however, its exact method of action is unknown.

To further investigate this disparity cells were labeled immunofluorescently for osteoblast specific markers, OC (green) and ALP (red) to determine whether or not BMP2 and CK2.3 stimulated cells were active osteoblasts. With this experiment in particular, I was investigating the fluorescent intensity or fluorescent expression of OC and ALP as it relates to osteoblast activity. Additionally, I wanted to determine whether or not BMP2 or CK2.3 would increase or decrease the relative intensity of those same markers. CK2.3 significantly increased expression of the osteoblast markers ALP and OC when compared to US and BMP2 stimulated cells, as seen in Figure 3.7a. Cells were assessed for percentage stained for a specific biomarker's

staining intensity, in order to verify that all stimulations still retained the osteoblast phenotype. The cell population was determined to be uniform throughout stimulations, meaning at least 60% of cells were positively stained for OC, ALP, or both, Figure 3.7b. This indicates that the cells stained had maintained their osteoblasts phenotype, even under BMP2 stimulation. However, when assessing the stained cells for pixel or fluorescent intensity, OP cells did not increase expression of the osteoblast biomarkers after BMP2 stimulation. CK2.3, however, significantly increased staining expression of ALP and OC, further illustrating the effectiveness of CK2.3 in activating and increasing expression of osteoblasts, Figure 3.7c. This further indicates a potential disruption in BMP2 mediated signaling. It is important to note that CK2.3 is hypothesized to bind to the interacting protein CK2 and inhibit its binding to a specific phosphorylation site on BMPRIa, while BMP2 needs both receptors to elicit its osteogenic response. How those receptors are localized and activated subsequently decides the activated signaling cascade(101). CK2.3 induced a mineralization response in both sets of extracted cells, while BMP2 only induced a mineralization response in the OA population, which is the population whose BMD did not decrease with increasing age. CK2.3 acts through the BMP pathway and it has been shown to induce mineralization when BMP2 did not, further increasing interest as a potential OP therapeutic and further illustrating a signaling bias in the BMP pathway in those diagnosed with OP.

BMP2 is approved for fracture healing for osteoporotic patients by the FDA. However recently, it has been shown that prolonged treatment of BMP2 decreased OP patients BMD(190). Here I show that the BMD of OP patients decreased significantly in correlation with their increasing age. In addition, the cells isolated from OP patients

did not respond to BMP2 stimulation when assessed for mineralization. For BMP2 to elicit its mineralization response, it must bind to its two dimerized receptors (a type Ia and a type II receptor). BMP2 either will bind preferentially to the type 1 receptor and recruit the constituently active type II receptor or BMP2 will bind to an already dimerized complex of receptors (one type I and one type II)(116). The signaling pathways activated are dependent upon the location and dimerization of these receptors(70)

Next, I investigated important signaling proteins in the BMP pathway to further elucidate this signaling disparity. I started at the receptor level, since the BMP receptors can be localized in different areas within the plasma membrane, and their location dictates the pathways activated(70). Additionally, previous research groups had discovered an upregulation in BMPRIa expression in OP patients MSCs and bone specimens when compared to control patients(165). Therefore, BMPRIa and CK2α expression was investigated in three different models, and all produced the same results. Prior to assessing BMPRIa and CK2α levels after BMP2 and CK2.3 stimulation, basal level expression of these two key proteins was determined. To effectively study basal level expression of these two proteins, it is crucial to do so in a variety of models. First, I studied the expression in MMA embedded trabecular bone slices to study the native bone environment. MMA embedding was used because it does not require the decalcification process, like other embedding methods, and would be more indicative of protein expression levels in the bone microenvironment prior to treatments(179). Unfortunately, the OP patients and OA patients were not age matched, because I am reliant on the samples provided to me from Christiana Care. Moving forward with this project it would be important to age match the samples, as

variations in patient age could be a confounding variable when looking into BMP2 response, as other labs have cited age related changes in BMP2 serum concentration(159, 160). As seen in Figure 3.10, OP embedded bone slices had significantly higher basal expression of both BMPRIa and CK2α when compared to control bone slices, which coincides with the previous findings. While I am using the OA patients embedded bone samples as a control (because they responded positively to BMP2), I do expect the relative levels of BMPRIa and CK2α to be similar between OA and normal, healthy patients. This is because other research groups had found no change in BMPRIa (also known as Alk3) in normal patients. They did find that BMPRIb mRNA levels were extremely low in OP patients, and overexpression of BMPRIb did not change or alter BMP2 induced osteogenic potential (measured through ALP induction)(162). This further indicates the importance of studying BMPRIa levels in osteoblasts extracted from OP patients, to further determine if the BMP signaling disparity lies within type Ia receptor expression. It is important to note that those research groups only studied MSCs and not mature osteoblasts. Additionally, other research groups had discovered that BMPRIa levels were increased in ovarian cancer tissue, which increases interest in the BMP signaling pathway, as this could indicate dysregulation within the BMP pathway in other diseases(194).

After utilizing the embedded bone samples, I next wanted to assess how both BMP2 and CK2.3 stimulation affected BMPRIa and CK2α levels. I still wanted to utilize the native bone environment, as cell culture can sometimes misrepresent what would be occurring naturally in the bone microenvironment. Therefore, in these experiments I utilized an *ex vivo* trabecular bone explant model. Explant models have been used more and more frequently because they allow for the study of target cells

within their native environment(195). It is important to note that there are some drawbacks regarding the use of trabecular bone explants. Bone tissue itself is naturally fluorescent, which makes studying fluorescent intensities of proteins difficult within the bone microenvironment(196). Additionally, there is sample to sample variability – some explants may be more viable then other explants, which is why it is important to keep parameters consistent between each experiment. Explants were generated, stimulated, and assessed all from the same femoral head from the same patient. Three OP femoral head explants and three control femoral head explants, each from three different patients were studied to correct for this possible discrepancy. I verified the legitimacy of the explant model by assessing cell viability and immunofluorescent validity through a confirmation study. As seen in Figure 3.8c, increased cell viability was observed in both OP and control explants under all stimulations, validating and verifying the efficacy of this explant model of study. I wanted to further verify that the explant model could be utilized to study immunofluorescent levels of proteins within the bone. To verify this, I isolated, cultured, stimulated, fixed, and stained the explants for the key osteoblast biomarkers, OC and ALP. As seen in Figure 3.9, both OC and ALP expression were significantly increased in explants from OP patients after CK2.3 stimulation. BMP2 stimulation significantly decreased both osteogenic biomarkers expression when compared to US. This mirrors the previous *in vitro* study, where only CK2.3 significantly increased OC and ALP expression, while BMP2 decreased their expression. Interestingly, both BMP2 and CK2.3 significantly increased expression of OC and ALP in control patient explants when compared to US. This also increased the validity of using an explant model for studying immunofluorescence levels of proteins within the bone.

I again used the explant model to study the effect of BMPRIa and CK2α expression within the bone. Both BMPRIa and CK2α expression was significantly decreased under BMP2 stimulation in the OP models, when compared to CK2.3 and US explants, Figure 3.11. Additionally, control explants significantly responded to both BMP2 and CK2.3 stimulation through an increase in both BMPRIa expression and CK2α expression. It is important to note that the fluorescent intensity levels of both BMPRIa and CK2α is significantly increased in explants extracted from OP patients when compared to explants from control patients. This mirrors what was previously discovered in MSCs from OP patients as well as what I have previously shown in MMA embedded explants. Moreover, this again shows a decreased response to BMP2 in OP patients.

BMPRIa and CK2α fluorescent expression was observed in extracted cells from OP patients after stimulation with either BMP2, CK2.3 or left US. BMP2 significantly decreased fluorescent expression in both BMPRIa and CK2α when compared to US and CK2.3 stimulated cells, Figure 3.12a and 3.12b. Additionally, RNA was extracted from the patient derived osteoblasts and RT-PCR was conducted in order to asses steady-state RNA of *BMPRIa* following stimulation with either BMP2, CK2.3 or control (US). BMP2 significantly decreased steady-state mRNA expression of *BMPRIa* when compared with US and CK2.3 stimulations, Figure 3.12c. BMPRIa is a critical receptor in humans within the BMP pathway. BMP2 preferentially binds to BMPRIa, and the signaling cascade is activated. Therefore, a decrease in expression after BMP2 stimulation is concerning and further indicates dysregulation of the BMP pathway.

Since receptor levels of BMPRIa are decreased following BMP2 stimulation, downstream BMP signaling pathways were investigated. Specifically, SMAD dependent signaling and SMAD independent signaling (or ERK signaling) were investigated through immunofluorescent staining and western blotting. It is important to note that in the following western blot figures I am showing the normalized pERK densiometric increase or decrease compared to β actin and not total ERK. My original intent was to compare pERK with total ERK, like I have with pSMAD and total SMAD. Unfortunately, due to the novel coronavirus and various lab shut-downs, I was unable to obtain a total ERK blot. This should be completed in the future in order to properly compare activated ERK levels with total ERK levels, as they are currently being compared with β actin, which is not a phosphorylated protein. Interestingly, SMAD dependent signaling (or BMP canonical signaling) remained unchanged in both experiments, Figure 3.14. Even while BMP2 stimulation seemed to slightly decrease expression of pSMAD (or activated SMAD) when compared to US and CK2.3 stimulated cells; this was not significant. Since SMAD signaling is the canonical BMP signaling pathway, BMP2 stimulation should have increased significantly activated SMAD expression. However, once again BMP2 stimulation did not induce a signaling response. Interestingly, activated ERK (or pERK) expression was decreased significantly after BMP2 stimulation, which indicates that SMAD independent signaling is altered in OP, Figure 3.13a. CK2.3 has been shown to act through the ERK signaling pathway in C2C12 cells, and it also significantly increased expression of pERK in cells isolated from patients diagnosed with OP, Figure 3.13b. This suggests that CK2.3 acts through the ERK pathway in humans as well, and that

CK2.3 can rescue aberrant BMP signaling, however further investigation is required due to the aforementioned limitations.

Recently, it has been discovered that pERK can colocalize with and become phosphorylated (activated) by CK2 (113)(119). These previous findings indicate that ERK is possibly another substrate of CK2, and CK2 may change or alter the specificity of ERK. Therefore, colocalization between CK2 and both pERK and pSMAD were investigated, since the exact mechanism of how CK2.3 mediates CK2 activity or whether this colocalization occurs in human osteoblasts is unknown. Five female OP patient cells were fluorescently stained for pERK (green) or pSMAD (green), CK2α (red), and the nucleus (blue). The cells were stimulated with either BMP2, CK2.3, or left US. There was a significantly increased amount of pixel-pixel colocalization, or Ncoloc, observed between pERK and CK2, under CK2.3 stimulation when compared to both US and BMP2 stimulated cells, Figure 3.15a and 3.15b. In fact, BMP2 stimulation decreased the occurrence of pERK and CK2 colocalized pixels, which again suggests aberrant BMP signaling in osteoblasts extracted from OP patients. Additionally, the Manders coefficients reported in Table 3.1, show high values after CK2.3 stimulation, further indicating an increase in pixel-pixel colocalization. Manders coefficients are reported at Manders 1 and Manders 2. They refer to the amount of green pixels that colocalize with the red pixels, and the amount of red pixels that colocalize with the green pixels, respectively. No significant differences were observed between pSMAD and CK2 Ncoloc (Figure 3.15c and 3.15d). Interestingly, the Manders coefficients were all around the same value, about 0.8. This indicates that BMP2 and CK2.3 stimulation do not affect the pixel-pixel colocalization, however, because the Manders coefficient value is relatively close to 1,

this indicates that pSMAD and CK2 may remain close within the same location/ or colocalize together in osteoblasts extracted from OP patients, but this needs to be further investigated and addressed. It is possible that pSMAD may be another CK2 substrate, but this has not yet been reported in any cell line. It would seem as though CK2.3 is not mediating CK2 to directly interact with and activate the SMAD signaling pathway. All-together, this data highlights the importance of the ERK pathway, as well as CK2.3 mediated BMP signaling.

It is important to note that there are several limitations to this study. The cells were assessed for protein interaction after five days of treatment, which is a long time when looking into signaling protein interactions. This experiment needs to be repeated as a time course study in order to determine at what time the two proteins are interacting or colocalizing together. After the time frame is determined, more involved binding assays need to be completed to further delineate the level of interaction or binding between the two proteins. There are other explanations for why cells extracted form OP patients are not responding to BMP2, but are responding to CK2.3. The BMP receptors could be further up or downregulated on the plasma membrane surface, which could interfere with ligand binding and subsequent downstream signaling activation. Additionally, lots of other research groups are looking into the recycling mechanisms of BMPR mediated endocytosis(106). It is known that once BMP2 binds to both receptors, they may be endocytosed and it is hypothesized that they are recycled back to the plasma membrane, but this exact mechanism is not known and deserves further investigation.

Finally, preliminary work was completed regarding the effect differing concentrations of both BMP2 and CK2.3 on isolated human osteoblasts. Throughout

the project, 40nM of BMP2 and 100 nM of CK2.3 were used, as both of these concentrations have been shown to induce osteogenic responses in cell lines as well as *in vivo* models(73, 117, 118). It is unknown whether those concentrations are as effective in isolate human cells. Additionally, BMP2 concentration should be assessed, as its response in OP patient cells could be does-dependent. Therefore several concentrations of both BMP2 and CK2.3 were used to stimulate a single OP patient's extracted cells. The cells' mineralization was again assessed through a von Kossa assay. Even with increasing concentrations of BMP2, the cells seemed to have no response to increasing concentrations of BMP2, Figure 3.16a. Interestingly, with CK2.3 stimulation, the cells increased their mineralization response with corresponding increasing levels of CK2.3, Figure 3.16b. However, this experiment needs to be completed again in at least two different OP donors to determine significance and verify the aforementioned trends.

Taken together, BMP2 is not a viable treatment for OP as the signaling pathway is aberrant, however CK2.3 seemingly rescues BMP2 osteogenic mediated activity. Therefore, it has the potential to be a novel OP therapeutic.

Chapter 5

FUTURE DIRECTIONS

In the future more work needs to be completed to effectively determine the cause of aberrant BMP2 signaling in OP patients, as this could be the underlining cause of decreased BMD observed in those diagnosed with OP. BMP2 and CK2.3 concentration curves should be completed on at least three OP and OA patients in order to effectively determine the optimal concentration of CK2.3 that should be used for extracted primary patient cells, as well as to determine if OP cells would respond to a higher or lower BMP2 concentration. I have been using 40 nm BMP2 and 100 nM CK2.3 because they are the most effective concentrations for cell line and *in vivo* work. However, primary cells may require different doses of both BMP2 and CK2.3 than what was used previously, and this should be investigated. BMPRIa and CK2α protein expression levels should be determined through western blots. At least three OP and OA patient cell lysates should be used. This would verify the obtained immunofluorescent quantification and qPCR results as I would be looking into cellular distribution, steady-state mRNA levels and finally protein levels of BMPRIa and CK2α. Further colocalization studies would also be required to determine the exact dynamics between pERK and CK2α. A time course co-immunoprecipitation should be completed to determine the timing and level of interaction between these two proteins with BMP2 and CK2.3 stimulation.

Since *BMPRIa* steady-state mRNA levels were previously studied, it would be critical to also research *CK2α* gene expression following BMP2 and CK2.3

stimulations to determine if the same response pattern was observed. CK2.3 mediates CK2 activity and, based upon previous results, it would be expected to increase *CK2α* expression, while BMP2 would decrease *CK2α* gene expression. Steady-state mRNA levels of both *pERK*, and *pSMAD* after BMP2 and CK2.3 stimulation should also be investigated to confirm aberrant BMP signaling in cells extracted from OP patients. It is hypothesized that *pERK* expression would increase after CK2.3 stimulation but decrease after BMP2 stimulation. It is also predicted that *pSMAD* gene expression levels would remain relatively the same throughout all stimulations, except for a slight decrease following BMP2 stimulation.

Another important research avenue would be BMP receptor distribution on the membrane of osteoblasts extracted from OP patients. As previously mentioned, BMP receptors can oligomerize in different membrane locations. The receptors dimerization activity pre and post BMP2 stimulation affects the downstream pathways activated(70, 101, 180). All this previous work was completed only in mice cell lines, therefore it would be both interesting and critical to determine receptor localization and dynamics oo the plasma membrane within osteoblasts extracted from OP patients, as this could be a potential cause of aberrant BMP signaling. All my previous work focused solely on BMPRIa, due to our labs continued interest in the interaction between CK2 and the type Ia receptor. However, BMPRII receptor levels also should be investigated. BMPRII is required in order to activate the type Ia receptor through phosphorylation at the GS box. If BMPRII levels are decreased in cells extracted from OP patients, this could be a possible explanation for the cells decreased responsiveness to BMP2 stimulation. The osteoblasts did respond to CK2.3 stimulation, which could be due to the peptide bypassing the normal signaling cascade through internalization into the

cell through caveolae, and direct interaction with the downstream signaling protein CK2. However, it is not known whether CK2.3 needs BMPRII to induce its osteogenic response, which should be investigated in both cell lines and extracted patient cells. Taken together the findings discovered with this project have been substantial in the overall understanding of both the cause of OP, as well as for the development and use of other potential therapeutics, like CK2.3.

REFERENCES

1. Downey PA, PA Downey P, PhD, OCS, is Assistant Professor, Physical Therapy Program, Chatham College, Woodland Road, Pittsburgh, PA 15232 (USA), Siegel MI, MI Siegel P, is Professor, Department of Anthropology and Orthodontics, University of Pittsburgh, Pittsburgh, Pa. Bone Biology and the Clinical Implications for Osteoporosis. Physical Therapy. 2006;86(1):77-91. doi: 10.1093/ptj/86.1.77.
2. Buckwalter JA, Glimcher, M.J., Cooper, R.R., and Recker, R. Bone Biology. 1995(77):1256-75.
3. Pienkowski D, Pollack SR. The origin of stress-generated potentials in fluid-saturated bone. J Orthop Res. 1983;1(1):30-41. Epub 1983/01/01. doi: 10.1002/jor.1100010105. PubMed PMID: 6679573.
4. Currey JD. The Mechanical Adaptations of Bones: Princeton University Press; 1984.
5. (US) OotSG. The Basics of Bone in Health and Disease. 2004. doi: https://www.ncbi.nlm.nih.gov/books/NBK45504/.
6. (US) OotSG. Bone Health and Osteoporosis. 2004. doi: https://www.ncbi.nlm.nih.gov/books/NBK45513/.
7. Steele DG, and Bramblett, Claud A. The Anatomy and Biology of the Human Skeleton: Texas A&M University Press; 1988.
8. Burr DB. Basic and Applied Bone Biology: Academic Press; 2019.
9. Sims NA, Gooi, Jonathan H. Bone remodeling: Multiple cellular interactions required for coupling of bone formation and resorption. 2008;19(5):444-51.
10. Florencio-Silva R, Sasso GS, Sasso-Cerri E, Simões MJ, Cerri PS. Biology of Bone Tissue: Structure, Function, and Factors That Influence Bone Cells. Biomed Res Int. 2015;2015. doi: 10.1155/2015/421746. PubMed PMID: 26247020; PubMed Central PMCID: PMC4515490.
11. Andersen TL, Sondergaard, Teis Esben., Skorzynska, Katarzyna Ewa., Dagnaes-Hansen, Frederick., Plesner, Trine Lindhardt., Hauge, Ellen Margrethe.,Plesner, Torben., Delaisse, Jean-Marie. A Physical Mechanism for Coupling Bone Resorption and Formation in Adult Human Bone. 2009;174(1).
12. Dallas SL, Department of Oral and Craniofacial Sciences SoD, University of Missouri-Kansas City, Kansas City, Missouri 64108, Prideaux M, Department of Oral and Craniofacial Sciences SoD, University of Missouri-Kansas City, Kansas City, Missouri 64108, Bonewald LF, Department of Oral and Craniofacial Sciences SoD, University of Missouri-Kansas City, Kansas City, Missouri 64108. The Osteocyte: An

Endocrine Cell … and More. Endocrine Reviews. 2013;34(5):658-90. doi: 10.1210/er.2012-1026.
13. Boyce BF, Hughes DE, Wright KR, Xing L, Dai A. Recent advances in bone biology provide insight into the pathogenesis of bone diseases. Lab Invest. 1999;79(2):83-94. Epub 1999/03/06. PubMed PMID: 10068197.
14. Boyce BF, Xing L. Functions of RANKL/RANK/OPG in bone modeling and remodeling. Arch Biochem Biophys. 2008;473(2):139-46. doi: 10.1016/j.abb.2008.03.018. PubMed PMID: 18395508; PubMed Central PMCID: PMC2413418.
15. Mulari M, Vaaraniemi, Jukka., and Vaananen, H. Kalervo. Intracellular Membrane Trafficking in Bone Resorbing Osteoclasts. Microscopy Research and Technique. 2003;61(6):496-503.
16. Luxenburg C, Geblinger, Dafina., Klein, Eugenia., Anderson, Karen., Hanein, Dorit., Geiger, Benny., and Addadi Lia. The Architecture of the Adhesive Apparatus of Cultured Osteoclasts: From Podosome Formation to Sealing Zone Assembly. PLoS 1. 2007.
17. Young MF. Bone matrix proteins: their function, regulation, and relationship to osteoporosis. Osteoporosis International. 2003;14(3):35-42. doi: doi:10.1007/s00198-002-1342-7.
18. Capulli M, Paone R, Rucci N. Osteoblast and osteocyte: games without frontiers. Arch Biochem Biophys. 2014;561:3-12. Epub 2014/05/17. doi: 10.1016/j.abb.2014.05.003. PubMed PMID: 24832390.
19. Nakamura H. Morphology, Function, and Differentiation of Bone Cells. Journal of Hard Tissue Biology. 2007;16(1):15-22.
20. Fakhry M, Hamade E, Badran B, Buchet R, Magne D. Molecular mechanisms of mesenchymal stem cell differentiation towards osteoblasts. World J Stem Cells. 2013;5(4):136-48. doi: 10.4252/wjsc.v5.i4.136. PubMed PMID: 24179602; PubMed Central PMCID: PMC3812518.
21. Manolagas SC, Division of Endocrinology & Metabolism CfOMBD, University of Arkansas for Medical Sciences, and the Central Arkansas Veterans Healthcare System, Little Rock, Arkansas 72205, USA. Birth and Death of Bone Cells: Basic Regulatory Mechanisms and Implications for the Pathogenesis and Treatment of Osteoporosis. Endocrine Reviews. 2000;21(2):115-37. doi: 10.1210/edrv.21.2.0395.
22. Addison WN, Azari F, Sørensen ES, Kaartinen MT, McKee MD. Pyrophosphate Inhibits Mineralization of Osteoblast Cultures by Binding to Mineral, Up-regulating Osteopontin, and Inhibiting Alkaline Phosphatase Activity. 2007. doi: 10.1074/jbc.M701116200.
23. Boivin G, Bala Y, Doublier A, Farlay D, Ste-Marie LG, Meunier PJ, et al. The role of mineralization and organic matrix in the microhardness of bone tissue from controls and osteoporotic patients. Bone. 2008;43(3):532-8. Epub 2008/07/05. doi: 10.1016/j.bone.2008.05.024. PubMed PMID: 18599391.

24. Franz-Odendaal TA, Hall BK, Witten PE. Buried alive: how osteoblasts become osteocytes. Dev Dyn. 2006;235(1):176-90. Epub 2005/11/01. doi: 10.1002/dvdy.20603. PubMed PMID: 16258960.
25. Manolagas SC, Parfitt AM. WHAT OLD MEANS TO BONE. Trends Endocrinol Metab. 2010;21(6):369-74. doi: 10.1016/j.tem.2010.01.010. PubMed PMID: 20223679; PubMed Central PMCID: PMC2880220.
26. Rochefort GY, Pallu S, Benhamou CL. Osteocyte: the unrecognized side of bone tissue. Osteoporosis International. 2010;21(9):1457-69. doi: doi:10.1007/s00198-010-1194-5.
27. Schaffler MB, Cheung W-Y, Majeska R, Kennedy O. Osteocytes: Master Orchestrators of Bone. Calcified Tissue International. 2013;94(1):5-24. doi: doi:10.1007/s00223-013-9790-y.
28. Bonewald LF. The amazing osteocyte. J Bone Miner Res. 2011;26(2):229-38. Epub 2011/01/22. doi: 10.1002/jbmr.320. PubMed PMID: 21254230; PubMed Central PMCID: PMCPMC3179345.
29. Bileikian JP, Raisz, Lawrence G., and Martin, T. John. Principles of Bone Biology. 3 ed: Elsevier; 2008.
30. Noble BS, Stevens H, Loveridge N, Reeve J. Identification of apoptotic changes in osteocytes in normal and pathological human bone. Bone. 1997;20(3):273-82. Epub 1997/03/01. doi: 10.1016/s8756-3282(96)00365-1. PubMed PMID: 9071479.
31. Knothe Tate ML. "Whither flows the fluid in bone?" An osteocyte's perspective. J Biomech. 2003;36(10):1409-24. Epub 2003/09/23. doi: 10.1016/s0021-9290(03)00123-4. PubMed PMID: 14499290.
32. Xiao Z, Zhang S, Mahlios J, Zhou G, Magenheimer BS, Guo D, et al. Cilia-like Structures and Polycystin-1 in Osteoblasts/Osteocytes and Associated Abnormalities in Skeletogenesis and Runx2 Expression. 2006. doi: 10.1074/jbc.M604772200.
33. Santos A, Bakker AD, Zandieh-Doulabi B, de Blieck-Hogervorst JM, Klein-Nulend J. Early activation of the beta-catenin pathway in osteocytes is mediated by nitric oxide, phosphatidyl inositol-3 kinase/Akt, and focal adhesion kinase. Biochem Biophys Res Commun. 2010;391(1):364-9. Epub 2009/11/17. doi: 10.1016/j.bbrc.2009.11.064. PubMed PMID: 19913504.
34. Miller SC, de Saint-Georges L, Bowman BM, Jee WS. Bone lining cells: structure and function. Scanning Microsc. 1989;3(3):953-60; discussion 60-1. Epub 1989/09/01. PubMed PMID: 2694361.
35. Donahue HJ, McLeod KJ, Rubin CT, Andersen J, Grine EA, Hertzberg EL, et al. Cell-to-cell communication in osteoblastic networks: cell line-dependent hormonal regulation of gap junction function. J Bone Miner Res. 1995;10(6):881-9. Epub 1995/06/01. doi: 10.1002/jbmr.5650100609. PubMed PMID: 7572312.
36. Jin SW, Sim KB, Kim SD. Development and Growth of the Normal Cranial Vault : An Embryologic Review. J Korean Neurosurg Soc. 2016;59(3):192-6. Epub

2016/05/27. doi: 10.3340/jkns.2016.59.3.192. PubMed PMID: 27226848; PubMed Central PMCID: PMCPMC4877539.
37. Breeland G, Menezes RG. Embryology, Bone Ossification. 2019. doi: https://www.ncbi.nlm.nih.gov/books/NBK539718/.
38. Ortega N, Behonick DJ, Werb Z. Matrix remodeling during endochondral ossification. Trends Cell Biol. 2004;14(2):86-93. doi: 10.1016/j.tcb.2003.12.003. PubMed PMID: 15102440; PubMed Central PMCID: PMC2779708.
39. Mackie EJ, Ahmed YA, Tatarczuch L, Chen KS, Mirams M. Endochondral ossification: how cartilage is converted into bone in the developing skeleton. Int J Biochem Cell Biol. 2008;40(1):46-62. Epub 2007/07/31. doi: 10.1016/j.biocel.2007.06.009. PubMed PMID: 17659995.
40. Percival CJ, Richtsmeier JT. Angiogenesis and intramembranous osteogenesis. Dev Dyn. 2013;242(8):909-22. Epub 2013/06/06. doi: 10.1002/dvdy.23992. PubMed PMID: 23737393; PubMed Central PMCID: PMCPMC3803110.
41. Fractures (Broken Bones) - OrthoInfo - AAOS 2020. Available from: https://www.orthoinfo.org/en/diseases--conditions/fractures-broken-bones/.
42. Types: @StanfordHealth; 2020. Available from: https://stanfordhealthcare.org/medical-conditions/bones-joints-and-muscles/fracture/types.html.
43. Marsell R, Einhorn TA. THE BIOLOGY OF FRACTURE HEALING. Injury. 2011;42(6):551-5. doi: 10.1016/j.injury.2011.03.031. PubMed PMID: 21489527; PubMed Central PMCID: PMC3105171.
44. Einhorn TA, Gerstenfeld LC. Fracture healing: mechanisms and interventions. Nat Rev Rheumatol. 2015;11(1):45-54. doi: 10.1038/nrrheum.2014.164. PubMed PMID: 25266456; PubMed Central PMCID: PMC4464690.
45. Gerstenfeld LC, Cullinane DM, Barnes GL, Graves DT, Einhorn TA. Fracture healing as a post-natal developmental process: molecular, spatial, and temporal aspects of its regulation. J Cell Biochem. 2003;88(5):873-84. Epub 2003/03/05. doi: 10.1002/jcb.10435. PubMed PMID: 12616527.
46. Green E, Lubahn JD, Evans J. Risk factors, treatment, and outcomes associated with nonunion of the midshaft humerus fracture. J Surg Orthop Adv. 2005;14(2):64-72. Epub 2005/08/24. PubMed PMID: 16115430.
47. Gerstenfeld LC, Alkhiary YM, Krall EA, Nicholls FH, Stapleton SN, Fitch JL, et al. Three-dimensional reconstruction of fracture callus morphogenesis. J Histochem Cytochem. 2006;54(11):1215-28. Epub 2006/07/26. doi: 10.1369/jhc.6A6959.2006. PubMed PMID: 16864894.
48. Cho TJ, Gerstenfeld LC, Einhorn TA. Differential temporal expression of members of the transforming growth factor beta superfamily during murine fracture healing. J Bone Miner Res. 2002;17(3):513-20. Epub 2002/03/05. doi: 10.1359/jbmr.2002.17.3.513. PubMed PMID: 11874242.
49. Yang W, Guo D, Harris MA, Cui Y, Gluhak-Heinrich J, Wu J, et al. Bmp2 in osteoblasts of periosteum and trabecular bone links bone formation to vascularization and mesenchymal stem cells. J Cell Sci. 2013;126(Pt 18):4085-98. Epub 2013/07/12.

doi: 10.1242/jcs.118596. PubMed PMID: 23843612; PubMed Central PMCID: PMCPMC3772385.
50. Granero-Molto F, Weis JA, Miga MI, Landis B, Myers TJ, O'Rear L, et al. Regenerative effects of transplanted mesenchymal stem cells in fracture healing. Stem Cells. 2009;27(8):1887-98. Epub 2009/06/23. doi: 10.1002/stem.103. PubMed PMID: 19544445; PubMed Central PMCID: PMCPMC3426453.
51. Kitaori T, Ito H, Schwarz EM, Tsutsumi R, Yoshitomi H, Oishi S, et al. Stromal cell-derived factor 1/CXCR4 signaling is critical for the recruitment of mesenchymal stem cells to the fracture site during skeletal repair in a mouse model. Arthritis Rheum. 2009;60(3):813-23. Epub 2009/02/28. doi: 10.1002/art.24330. PubMed PMID: 19248097.
52. Bais MV, Wigner N, Young M, Toholka R, Graves DT, Morgan EF, et al. BMP2 is essential for post natal osteogenesis but not for recruitment of osteogenic stem cells. Bone. 2009;45(2):254-66. Epub 2009/04/29. doi: 10.1016/j.bone.2009.04.239. PubMed PMID: 19398045; PubMed Central PMCID: PMCPMC2745982.
53. Tsuji K, Bandyopadhyay A, Harfe BD, Cox K, Kakar S, Gerstenfeld L, et al. BMP2 activity, although dispensable for bone formation, is required for the initiation of fracture healing. Nat Genet. 2006;38(12):1424-9. Epub 2006/11/14. doi: 10.1038/ng1916. PubMed PMID: 17099713.
54. Dimitriou R, Tsiridis E, Giannoudis PV. Current concepts of molecular aspects of bone healing. Injury. 2005;36(12):1392-404. Epub 2005/08/17. doi: 10.1016/j.injury.2005.07.019. PubMed PMID: 16102764.
55. Ai-Aql ZS, Alagl AS, Graves DT, Gerstenfeld LC, Einhorn TA. Molecular mechanisms controlling bone formation during fracture healing and distraction osteogenesis. J Dent Res. 2008;87(2):107-18. Epub 2008/01/26. doi: 10.1177/154405910808700215. PubMed PMID: 18218835; PubMed Central PMCID: PMCPMC3109437.
56. Tsiridis E, Upadhyay N, Giannoudis P. Molecular aspects of fracture healing: which are the important molecules? Injury. 2007;38 Suppl 1:S11-25. Epub 2007/03/27. doi: 10.1016/j.injury.2007.02.006. PubMed PMID: 17383481.
57. Shapiro F. Cortical bone repair. The relationship of the lacunar-canalicular system and intercellular gap junctions to the repair process. J Bone Joint Surg Am. 1988;70(7):1067-81. Epub 1988/08/01. PubMed PMID: 3042791.
58. R D, PV G. Discovery and Development of BMPs. Injury. 2005;36 Suppl 3. doi: 10.1016/j.injury.2005.07.031. PubMed PMID: 16188546.
59. Lavery K, Swain P, Falb D, Alaoui-Ismaili MH. BMP-2/4 and BMP-6/7 Differentially Utilize Cell Surface Receptors to Induce Osteoblastic Differentiation of Human Bone Marrow-derived Mesenchymal Stem Cells. 2008. doi: 10.1074/jbc.M800850200.
60. Chen D, Zhao M, Mundy GR. Bone morphogenetic proteins. Growth Factors. 2004;22(4):233-41. Epub 2004/12/29. doi: 10.1080/08977190412331279890. PubMed PMID: 15621726.

61. Mazerbourg S, Division of Reproductive Biology DoOaG, Stanford University School of Medicine, Stanford, CA, USA, Hsueh AJW, Division of Reproductive Biology DoOaG, Stanford University School of Medicine, Stanford, CA, USA. Genomic analyses facilitate identification of receptors and signalling pathways for growth differentiation factor 9 and related orphan bone morphogenetic protein/growth differentiation factor ligands. Human Reproduction Update. 2006;12(4):373-83. doi: 10.1093/humupd/dml014.
62. Bragdon B, Moseychuk O, Saldanha S, King D, Julian J, Nohe A. Bone morphogenetic proteins: a critical review. Cell Signal. 2011;23(4):609-20. Epub 2010/10/21. doi: 10.1016/j.cellsig.2010.10.003. PubMed PMID: 20959140.
63. Sieber C, Kopf J, Hiepen C, Knaus P. Recent advances in BMP receptor signaling. Cytokine Growth Factor Rev. 2009;20(5-6):343-55. Epub 2009/11/10. doi: 10.1016/j.cytogfr.2009.10.007. PubMed PMID: 19897402.
64. Nohe A, Keating E, Knaus P, Petersen NO. Signal transduction of bone morphogenetic protein receptors. Cell Signal. 2004;16(3):291-9. Epub 2003/12/23. doi: 10.1016/j.cellsig.2003.08.011. PubMed PMID: 14687659.
65. Cui Y, Hackenmiller R, Berg L, Jean F, Nakayama T, Thomas G, et al. The activity and signaling range of mature BMP-4 is regulated by sequential cleavage at two sites within the prodomain of the precursor. Genes Dev. 2001;15(21):2797-802. Epub 2001/11/03. doi: 10.1101/gad.940001. PubMed PMID: 11691831; PubMed Central PMCID: PMCPMC312809.
66. Nahar NN, Missana LR, Garimella R, Tague SE, Anderson HC. Matrix vesicles are carriers of bone morphogenetic proteins (BMPs), vascular endothelial growth factor (VEGF), and noncollagenous matrix proteins. Journal of Bone and Mineral Metabolism. 2008;26(5):514-9. doi: doi:10.1007/s00774-008-0859-z.
67. Kodaira K, Imada M, Goto M, Tomoyasu A, Fukuda T, Kamijo R, et al. Purification and identification of a BMP-like factor from bovine serum. Biochem Biophys Res Commun. 2006;345(3):1224-31. Epub 2006/05/24. doi: 10.1016/j.bbrc.2006.05.045. PubMed PMID: 16716261.
68. Avsian-Kretchmer O, Hsueh AJ. Comparative genomic analysis of the eight-membered ring cystine knot-containing bone morphogenetic protein antagonists. Mol Endocrinol. 2004;18(1):1-12. Epub 2003/10/04. doi: 10.1210/me.2003-0227. PubMed PMID: 14525956.
69. Rosen V. BMP and BMP inhibitors in bone. Ann N Y Acad Sci. 2006;1068:19-25. Epub 2006/07/13. doi: 10.1196/annals.1346.005. PubMed PMID: 16831902.
70. Nohe A, Hassel S, Ehrlich M, Neubauer F, Sebald W, Henis YI, et al. The Mode of Bone Morphogenetic Protein (BMP) Receptor Oligomerization Determines Different BMP-2 Signaling Pathways. 2002. doi: 10.1074/jbc.M102750200.
71. Pomeraniec L, Hector-Greene M, Ehrlich M, Blobe GC, Henis YI. Regulation of TGF-β receptor hetero-oligomerization and signaling by endoglin. Mol Biol Cell. 262015. p. 3117-27.

72. Urist MR. Bone: formation by autoinduction. Science. 1965;150(3698):893-9. Epub 1965/11/12. doi: 10.1126/science.150.3698.893. PubMed PMID: 5319761.
73. Vrathasha V, Weidner H, Nohe A. Mechanism of CK2.3, a Novel Mimetic Peptide of Bone Morphogenetic Protein Receptor Type IA, Mediated Osteogenesis. International Journal of Molecular Sciences. 2019;20(10):2500. doi: 10.3390/ijms20102500.
74. Shu B, Zhang M, Xie R, Wang M, Jin H, Hou W, et al. BMP2, but not BMP4, is crucial for chondrocyte proliferation and maturation during endochondral bone development. J Cell Sci. 2011;124(Pt 20):3428-40. Epub 2011/10/11. doi: 10.1242/jcs.083659. PubMed PMID: 21984813; PubMed Central PMCID: PMCPMC3196857.
75. Tannoury CA, An HS. Complications with the use of bone morphogenetic protein 2 (BMP-2) in spine surgery. Spine J. 2014;14(3):552-9. Epub 2014/01/15. doi: 10.1016/j.spinee.2013.08.060. PubMed PMID: 24412416.
76. Burkus JK, Gornet MF, Dickman CA, Zdeblick TA. Anterior lumbar interbody fusion using rhBMP-2 with tapered interbody cages. J Spinal Disord Tech. 2002;15(5):337-49. Epub 2002/10/24. doi: 10.1097/00024720-200210000-00001. PubMed PMID: 12394656.
77. Burkus JK, Dorchak JD, Sanders DL. Radiographic assessment of interbody fusion using recombinant human bone morphogenetic protein type 2. Spine (Phila Pa 1976). 2003;28(4):372-7. Epub 2003/02/19. doi: 10.1097/01.brs.0000048469.45035.b9. PubMed PMID: 12590213.
78. Smoljanovic T, Bojanic I, Dokuzovic S. Re: Mindea SA, Shih P, Song JK. Recombinant human bone morphogenetic protein-2-induced radiculitis in elective minimally invasive transforaminal lumbar interbody fusions: a series review. Spine 2009;34:1480-5. Spine (Phila Pa 1976). 35. United States2010. p. 929.
79. Mindea SA, Shih P, Song JK. Recombinant human bone morphogenetic protein-2-induced radiculitis in elective minimally invasive transforaminal lumbar interbody fusions: a series review. Spine (Phila Pa 1976). 2009;34(14):1480-4; discussion 5. Epub 2009/06/16. doi: 10.1097/BRS.0b013e3181a396a1. PubMed PMID: 19525840.
80. Tumialan LM, Pan J, Rodts GE, Mummaneni PV. The safety and efficacy of anterior cervical discectomy and fusion with polyetheretherketone spacer and recombinant human bone morphogenetic protein-2: a review of 200 patients. J Neurosurg Spine. 2008;8(6):529-35. Epub 2008/06/04. doi: 10.3171/spi/2008/8/6/529. PubMed PMID: 18518673.
81. Shields LB, Raque GH, Glassman SD, Campbell M, Vitaz T, Harpring J, et al. Adverse effects associated with high-dose recombinant human bone morphogenetic protein-2 use in anterior cervical spine fusion. Spine (Phila Pa 1976). 2006;31(5):542-7. Epub 2006/03/02. doi: 10.1097/01.brs.0000201424.27509.72. PubMed PMID: 16508549.
82. McClellan JW, Mulconrey DS, Forbes RJ, Fullmer N. Vertebral bone resorption after transforaminal lumbar interbody fusion with bone morphogenetic

protein (rhBMP-2). J Spinal Disord Tech. 2006;19(7):483-6. Epub 2006/10/06. doi: 10.1097/01.bsd.0000211231.83716.4b. PubMed PMID: 17021411.
83. Lewandrowski KU, Nanson C, Calderon R. Vertebral osteolysis after posterior interbody lumbar fusion with recombinant human bone morphogenetic protein 2: a report of five cases. Spine J. 2007;7(5):609-14. Epub 2007/05/29. doi: 10.1016/j.spinee.2007.01.011. PubMed PMID: 17526434.
84. Zhang H, Bradley A. Mice deficient for BMP2 are nonviable and have defects in amnion/chorion and cardiac development. Development. 1996;122(10):2977-86. Epub 1996/10/01. PubMed PMID: 8898212.
85. Nakase T, Yoshikawa H. Potential roles of bone morphogenetic proteins (BMPs) in skeletal repair and regeneration. J Bone Miner Metab. 2006;24(6):425-33. Epub 2006/10/31. doi: 10.1007/s00774-006-0718-8. PubMed PMID: 17072733.
86. Heng S, Paule S, Hardman B, Li Y, Singh H, Rainczuk A, et al. Posttranslational activation of bone morphogenetic protein 2 is mediated by proprotein convertase 6 during decidualization for pregnancy establishment. Endocrinology. 2010;151(8):3909-17. Epub 2010/06/18. doi: 10.1210/en.2010-0326. PubMed PMID: 20555025.
87. Heldin CH, Miyazono K, ten Dijke P. TGF-beta signalling from cell membrane to nucleus through SMAD proteins. Nature. 1997;390(6659):465-71. Epub 1997/12/11. doi: 10.1038/37284. PubMed PMID: 9393997.
88. Horbelt D, Denkis A, Knaus P. A portrait of Transforming Growth Factor beta superfamily signalling: Background matters. Int J Biochem Cell Biol. 2012;44(3):469-74. Epub 2012/01/10. doi: 10.1016/j.biocel.2011.12.013. PubMed PMID: 22226817.
89. Klages J, Kotzsch A, Coles M, Sebald W, Nickel J, Müller T, et al. The Solution Structure of BMPR-IA Reveals a Local Disorder-to-Order Transition upon BMP-2 Binding†‡. 2008. doi: 10.1021/bi801059j.
90. Heinecke K, Seher A, Schmitz W, Mueller TD, Sebald W, Nickel J. Receptor oligomerization and beyond: a case study in bone morphogenetic proteins. BMC Biol. 2009;7:59. Epub 2009/09/09. doi: 10.1186/1741-7007-7-59. PubMed PMID: 19735544; PubMed Central PMCID: PMCPMC2749821.
91. Gilboa L, Nohe A, Geissendorfer T, Sebald W, Henis YI, Knaus P. Bone morphogenetic protein receptor complexes on the surface of live cells: a new oligomerization mode for serine/threonine kinase receptors. Mol Biol Cell. 2000;11(3):1023-35. Epub 2000/03/11. doi: 10.1091/mbc.11.3.1023. PubMed PMID: 10712517; PubMed Central PMCID: PMCPMC14828.
92. Gomez-Puerto MC, Iyengar PV, Garcia de Vinuesa A, Ten Dijke P, Sanchez-Duffhues G. Bone morphogenetic protein receptor signal transduction in human disease. J Pathol. 2019;247(1):9-20. Epub 2018/09/25. doi: 10.1002/path.5170. PubMed PMID: 30246251; PubMed Central PMCID: PMCPMC6587955.
93. Xu SC, Harris MA, Rubenstein JL, Mundy GR, Harris SE. Bone morphogenetic protein-2 (BMP-2) signaling to the Col2alpha1 gene in chondroblasts requires the homeobox gene Dlx-2. DNA Cell Biol. 2001;20(6):359-65. doi: 10.1089/10445490152122479. PubMed PMID: 11445007.

94. Zhou N, Li Q, Lin X, Hu N, Liao JY, Lin LB, et al. BMP2 induces chondrogenic differentiation, osteogenic differentiation and endochondral ossification in stem cells. Cell Tissue Res. 2016;366(1):101-11. Epub 2016/04/17. doi: 10.1007/s00441-016-2403-0. PubMed PMID: 27083447.
95. Bruderer M, Richards RG, Alini M, Stoddart MJ. Role and regulation of RUNX2 in osteogenesis. Eur Cell Mater. 2014;28:269-86. Epub 2014/10/24. doi: 10.22203/ecm.v028a19. PubMed PMID: 25340806.
96. Sinha KM, Zhou X. Genetic and molecular control of osterix in skeletal formation. J Cell Biochem. 2013;114(5):975-84. Epub 2012/12/12. doi: 10.1002/jcb.24439. PubMed PMID: 23225263; PubMed Central PMCID: PMCPMC3725781.
97. Bragdon B, Thinakaran S, Moseychuk O, King D, Young K, Litchfield D, et al. Casein Kinase 2 β-Subunit Is a Regulator of Bone Morphogenetic Protein 2 Signaling. Biophys J. 992010. p. 897-904.
98. Zhang YE. Non-Smad Signaling Pathways of the TGF-beta Family. Cold Spring Harb Perspect Biol. 2017;9(2). Epub 2016/11/20. doi: 10.1101/cshperspect.a022129. PubMed PMID: 27864313; PubMed Central PMCID: PMCPMC5287080.
99. Bragdon B, D'Angelo A, Gurski L, Bonor J, Schultz KL, Beamer WG, et al. Altered plasma membrane dynamics of bone morphogenetic protein receptor type Ia in a low bone mass mouse model. Bone. 2012;50(1):189-99. Epub 2011/10/22. doi: 10.1016/j.bone.2011.10.016. PubMed PMID: 22036911; PubMed Central PMCID: PMCPMC3651650.
100. Bragdon B, Bonor J, Shultz KL, Beamer WG, Rosen CJ, Nohe A. Bone morphogenetic protein receptor type Ia localization causes increased BMP2 signaling in mice exhibiting increased peak bone mass phenotype. J Cell Physiol. 2012;227(7):2870-9. doi: 10.1002/jcp.23028. PubMed PMID: 22170575; PubMed Central PMCID: PMCPMC3309108.
101. Bonor J, Adams EL, Bragdon B, Moseychuk O, Czymmek KJ, Nohe A. Initiation of BMP2 Signaling in Domains on the Plasma Membrane. J Cell Physiol. 2012;227(7):2880-8. doi: 10.1002/jcp.23032. PubMed PMID: 21938723; PubMed Central PMCID: PMC3310286.
102. Saldanha S, Bragdon B, Moseychuk O, Bonor J, Dhurjati P, Nohe A. Caveolae regulate Smad signaling as verified by novel imaging and system biology approaches. J Cell Physiol. 2013;228(5):1060-9. Epub 2012/10/09. doi: 10.1002/jcp.24253. PubMed PMID: 23041979.
103. Bragdon B, Thinakaran S, Bonor J, Underhill TM, Petersen NO, Nohe A. FRET Reveals Novel Protein-Receptor Interaction of Bone Morphogenetic Proteins Receptors and Adaptor Protein 2 at the Cell Surface. Biophys J. 972009. p. 1428-35.
104. Durrington HJ, Upton PD, Hoer S, Boname J, Dunmore BJ, Yang J, et al. Identification of a lysosomal pathway regulating degradation of the bone morphogenetic protein receptor type II. J Biol Chem. 2010;285(48):37641-9. Epub

2010/09/24. doi: 10.1074/jbc.M110.132415. PubMed PMID: 20870717; PubMed Central PMCID: PMCPMC2988369.
105. Murakami K, Etlinger JD. Role of SMURF1 ubiquitin ligase in BMP receptor trafficking and signaling. Cell Signal. 2019;54:139-49. Epub 2018/11/03. doi: 10.1016/j.cellsig.2018.10.015. PubMed PMID: 30395943.
106. Hartung A, Bitton-Worms K, Rechtman MM, Wenzel V, Boergermann JH, Hassel S, et al. Different routes of bone morphogenic protein (BMP) receptor endocytosis influence BMP signaling. Mol Cell Biol. 2006;26(20):7791-805. Epub 2006/08/21. doi: 10.1128/MCB.00022-06. PubMed PMID: 16923969; PubMed Central PMCID: PMCPMC1636853.
107. Lozeman FJ, Litchfield DW, Piening C, Takio K, Walsh KA, Krebs EG. Isolation and characterization of human cDNA clones encoding the alpha and the alpha' subunits of casein kinase II. Biochemistry. 1990;29(36):8436-47. Epub 1990/09/11. doi: 10.1021/bi00488a034. PubMed PMID: 2174700.
108. Litchfield DW, Lozeman FJ, Piening C, Sommercorn J, Takio K, Walsh KA, et al. Subunit structure of casein kinase II from bovine testis. Demonstration that the alpha and alpha' subunits are distinct polypeptides. J Biol Chem. 1990;265(13):7638-44. Epub 1990/05/05. PubMed PMID: 2159007.
109. Glover CV, 3rd. On the physiological role of casein kinase II in Saccharomyces cerevisiae. Prog Nucleic Acid Res Mol Biol. 1998;59:95-133. Epub 1998/01/15. doi: 10.1016/s0079-6603(08)61030-2. PubMed PMID: 9427841.
110. Litchfield DW, Bosc DG, Canton DA, Saulnier RB, Vilk G, Zhang C. Functional specialization of CK2 isoforms and characterization of isoform-specific binding partners. Molecular and Cellular Biochemistry. 2001;227(1):21-9. doi: doi:10.1023/A:1013188101465.
111. Shi X, Potvin B, Huang T, Hilgard P, Spray DC, Suadicani SO, et al. A novel casein kinase 2 alpha-subunit regulates membrane protein traffic in the human hepatoma cell line HuH-7. J Biol Chem. 2001;276(3):2075-82. Epub 2000/10/20. doi: 10.1074/jbc.M008583200. PubMed PMID: 11038365.
112. Pinna LA. Casein kinase 2: an 'eminence grise' in cellular regulation? Biochim Biophys Acta. 1990;1054(3):267-84. Epub 1990/09/24. doi: 10.1016/0167-4889(90)90098-x. PubMed PMID: 2207178.
113. Marin O, Meggio F, Sarno S, Cesaro L, Pagano MA, Pinna LA. Tyrosine versus serine/threonine phosphorylation by protein kinase casein kinase-2. A study with peptide substrates derived from immunophilin Fpr3. J Biol Chem. 1999;274(41):29260-5. Epub 1999/10/03. doi: 10.1074/jbc.274.41.29260. PubMed PMID: 10506183.
114. Litchfield DW. Protein kinase CK2: structure, regulation and role in cellular decisions of life and death. Biochem J. 2003;369(Pt 1):1-15. Epub 2002/10/25. doi: 10.1042/bj20021469. PubMed PMID: 12396231; PubMed Central PMCID: PMCPMC1223072.
115. Bragdon B, Thinakaran S, Moseychuk O, Gurski L, Bonor J, Price C, et al. Casein kinase 2 regulates in vivo bone formation through its interaction with bone

morphogenetic protein receptor type Ia. Bone. 2011;49(5):944-54. Epub 2011/07/19. doi: 10.1016/j.bone.2011.06.037. PubMed PMID: 21763800.
116. Moseychuk O, Akkiraju H, Dutta J, D'Angelo A, Bragdon B, Duncan RL, et al. Inhibition of CK2 binding to BMPRIa induces C2C12 differentiation into osteoblasts and adipocytes. J Cell Commun Signal. 72013. p. 265-78.
117. Akkiraju H, Bonor J, Olli K, Bowen C, Bragdon B, Coombs H, et al. Systemic injection of CK2.3, a novel peptide acting downstream of Bone Morphogenetic Protein receptor BMPRIa, leads to increased trabecular bone mass. J Orthop Res. 2015;33(2):208-15. doi: 10.1002/jor.22752. PubMed PMID: 25331517; PubMed Central PMCID: PMC4304894.
118. Nguyen J, Weidner H, Schell LM, Sequeira L, Kabrick R, Dharmadhikari S, et al. Synthetic Peptide CK2.3 Enhances Bone Mineral Density in Senile Mice. Journal of Bone Research. 2018;6(2):1-7. doi: 10.4172/2572-4916.1000190.
119. Plotnikov A, Chuderland D, Karamansha Y, Livnah O, Seger R. Nuclear ERK Translocation is Mediated by Protein Kinase CK2 and Accelerated by Autophosphorylation. Cell Physiol Biochem. 2019;53(2):366-87. Epub 2019/08/07. doi: 10.33594/000000144. PubMed PMID: 31385665.
120. (US) OotSG. Diseases of Bone. 2004. doi: https://www.ncbi.nlm.nih.gov/books/NBK45506/.
121. Whyte M. Sclerosing bone disorders. Washington DC: American Society for Bone and Mineral Research; 2003. p. 449-66.
122. Rauch F, Glorieux FH. Osteogenesis imperfecta. Lancet. 2004;363(9418):1377-85. Epub 2004/04/28. doi: 10.1016/s0140-6736(04)16051-0. PubMed PMID: 15110498.
123. Chesney RW. Vitamin D deficiency and rickets. Rev Endocr Metab Disord. 2001;2(2):145-51. Epub 2001/11/14. doi: 10.1023/a:1010071426415. PubMed PMID: 11705320.
124. Pettifor JM. Rickets. Calcif Tissue Int. 2002;70(5):398-9. Epub 2002/04/18. doi: 10.1007/s00223-001-0046-x. PubMed PMID: 11960205.
125. Elder G. Pathophysiology and recent advances in the management of renal osteodystrophy. J Bone Miner Res. 2002;17(12):2094-105. Epub 2002/12/10. doi: 10.1359/jbmr.2002.17.12.2094. PubMed PMID: 12469904.
126. Bikle D. Vitamin D: Production, Metabolism, and Mechanisms of Action. 2017. doi: https://www.ncbi.nlm.nih.gov/books/NBK278935/.
127. Cunningham J, Sprague SM, Cannata-Andia J, Coco M, Cohen-Solal M, Fitzpatrick L, et al. Osteoporosis in chronic kidney disease. Am J Kidney Dis. 2004;43(3):566-71. Epub 2004/02/26. doi: 10.1053/j.ajkd.2003.12.004. PubMed PMID: 14981616.
128. Martin KJ, Olgaard K, Coburn JW, Coen GM, Fukagawa M, Langman C, et al. Diagnosis, assessment, and treatment of bone turnover abnormalities in renal osteodystrophy. Am J Kidney Dis. 2004;43(3):558-65. Epub 2004/02/26. doi: 10.1053/j.ajkd.2003.12.003. PubMed PMID: 14981615.

129. SJ W, SW D. Parathyroid Hormone for Bone Regeneration. Journal of orthopaedic research : official publication of the Orthopaedic Research Society. 2018;36(10). doi: 10.1002/jor.24075. PubMed PMID: 29926970.
130. Shaker JL. Paget's Disease of Bone: A Review of Epidemiology, Pathophysiology and Management. Ther Adv Musculoskelet Dis. 12009. p. 107-25.
131. Osteoarthritis: Arthritis Foundation; 2020. Available from: https://www.arthritis.org/diseases/osteoarthritis.
132. Seeman E. Invited Review: Pathogenesis of osteoporosis. J Appl Physiol (1985). 2003;95(5):2142-51. Epub 2003/10/14. doi: 10.1152/japplphysiol.00564.2003. PubMed PMID: 14555675.
133. Riggs BL, Khosla S, Melton LJ, 3rd. Sex steroids and the construction and conservation of the adult skeleton. Endocr Rev. 2002;23(3):279-302. Epub 2002/06/07. doi: 10.1210/edrv.23.3.0465. PubMed PMID: 12050121.
134. Ahlborg HG, Johnell O, Turner CH, Rannevik G, Karlsson MK. Bone loss and bone size after menopause. N Engl J Med. 2003;349(4):327-34. Epub 2003/07/25. doi: 10.1056/NEJMoa022464. PubMed PMID: 12878739.
135. Khosla S, Lufkin EG, Hodgson SF, Fitzpatrick LA, Melton LJ, 3rd. Epidemiology and clinical features of osteoporosis in young individuals. Bone. 1994;15(5):551-5. Epub 1994/09/01. doi: 10.1016/8756-3282(94)90280-1. PubMed PMID: 7980966.
136. Stein E, Shane E. Secondary osteoporosis. Endocrinol Metab Clin North Am. 2003;32(1):115-34, vii. Epub 2003/04/18. doi: 10.1016/s0889-8529(02)00062-2. PubMed PMID: 12699295.
137. Ott SM, Aitken ML. Osteoporosis in patients with cystic fibrosis. Clin Chest Med. 1998;19(3):555-67. Epub 1998/10/06. doi: 10.1016/s0272-5231(05)70100-3. PubMed PMID: 9759556.
138. Wynne AG, van Heerden J, Carney JA, Fitzpatrick LA. Parathyroid carcinoma: clinical and pathologic features in 43 patients. Medicine (Baltimore). 1992;71(4):197-205. Epub 1992/07/01. PubMed PMID: 1518393.
139. Dauty M, Perrouin Verbe B, Maugars Y, Dubois C, Mathe JF. Supralesional and sublesional bone mineral density in spinal cord-injured patients. Bone. 2000;27(2):305-9. Epub 2000/07/29. doi: 10.1016/s8756-3282(00)00326-4. PubMed PMID: 10913927.
140. Robbins J, Hirsch C, Whitmer R, Cauley J, Harris T. The association of bone mineral density and depression in an older population. J Am Geriatr Soc. 2001;49(6):732-6. Epub 2001/07/17. doi: 10.1046/j.1532-5415.2001.49149.x. PubMed PMID: 11454111.
141. van Staa TP, Leufkens HG, Cooper C. The epidemiology of corticosteroid-induced osteoporosis: a meta-analysis. Osteoporos Int. 2002;13(10):777-87. Epub 2002/10/16. doi: 10.1007/s001980200108. PubMed PMID: 12378366.
142. Bone Density Test, Osteoporosis Screening & T-score Interpretation 2018. Available from: https://www.nof.org/patients/diagnosis-information/bone-density-examtesting/.

143. Tu KN, Lie JD, Wan CKV, Cameron M, Austel AG, Nguyen JK, et al. Osteoporosis: A Review of Treatment Options. P T. 432018. p. 92-104.
144. Osteoporosis Treatment Drugs, Side Effects, Guidelines, Diet 2018. Available from: https://www.emedicinehealth.com/treatment_of_osteoporosis/article_em.htm.
145. Camacho PM, Petak SM, Binkley N, Clarke BL, Harris ST, Hurley DL, et al. AMERICAN ASSOCIATION OF CLINICAL ENDOCRINOLOGISTS AND AMERICAN COLLEGE OF ENDOCRINOLOGY CLINICAL PRACTICE GUIDELINES FOR THE DIAGNOSIS AND TREATMENT OF POSTMENOPAUSAL OSTEOPOROSIS - 2016. Endocr Pract. 2016;22(Suppl 4):1-42. Epub 2016/09/24. doi: 10.4158/ep161435.gl. PubMed PMID: 27662240.
146. Miller PD. Safety of parathyroid hormone for the treatment of osteoporosis. Curr Osteoporos Rep. 2008;6(1):12-6. Epub 2008/04/24. PubMed PMID: 18430395.
147. Miller PD, Hattersley G, Riis BJ, Williams GC, Lau E, Russo LA, et al. Effect of Abaloparatide vs Placebo on New Vertebral Fractures in Postmenopausal Women With Osteoporosis: A Randomized Clinical Trial. Jama. 2016;316(7):722-33. Epub 2016/08/18. doi: 10.1001/jama.2016.11136. PubMed PMID: 27533157.
148. Neer RM, Arnaud CD, Zanchetta JR, Prince R, Gaich GA, Reginster JY, et al. Effect of parathyroid hormone (1-34) on fractures and bone mineral density in postmenopausal women with osteoporosis. N Engl J Med. 2001;344(19):1434-41. Epub 2001/05/11. doi: 10.1056/nejm200105103441904. PubMed PMID: 11346808.
149. Cosman F, Crittenden DB, Adachi JD, Binkley N, Czerwinski E, Ferrari S, et al. Romosozumab Treatment in Postmenopausal Women with Osteoporosis. N Engl J Med. 2016;375(16):1532-43. Epub 2016/11/01. doi: 10.1056/NEJMoa1607948. PubMed PMID: 27641143.
150. FDA approves romosozumab for osteoporosis: @GoHealio; 2020. Available from: https://www.healio.com/endocrinology/bone-mineral-metabolism/news/online/{46cf9eb4-b0ed-4b7d-a4a2-f8eba9b0301b}/fda-approves-romosozumab-for-osteoporosis.
151. Romosozumab Side Effects: Common, Severe, Long Term - Drugs.com. 2020.
152. Jensen ED, Pham L, Billington CJ, Espe K, Carlson AE, Westendorf JJ, et al. BONE MORPHOGENIC PROTEIN 2 DIRECTLY ENHANCES DIFFERENTIATION OF MURINE OSTEOCLAST PRECURSORS. J Cell Biochem. 2010;109(4):672-82. doi: 10.1002/jcb.22462. PubMed PMID: 20039313; PubMed Central PMCID: PMC2836597.
153. Itoh K, Udagawa N, Katagiri T, Iemura S, Ueno N, Yasuda H, et al. Bone morphogenetic protein 2 stimulates osteoclast differentiation and survival supported by receptor activator of nuclear factor-kappaB ligand. Endocrinology. 2001;142(8):3656-62. Epub 2001/07/19. doi: 10.1210/endo.142.8.8300. PubMed PMID: 11459815.
154. Kanatani M, Sugimoto T, Kaji H, Kobayashi T, Nishiyama K, Fukase M, et al. Stimulatory effect of bone morphogenetic protein-2 on osteoclast-like cell formation and bone-resorbing activity. J Bone Miner Res. 1995;10(11):1681-90. Epub 1995/11/01. doi: 10.1002/jbmr.5650101110. PubMed PMID: 8592944.

155. Kaneko H, Arakawa T, Mano H, Kaneda T, Ogasawara A, Nakagawa M, et al. Direct stimulation of osteoclastic bone resorption by bone morphogenetic protein (BMP)-2 and expression of BMP receptors in mature osteoclasts. Bone. 2000;27(4):479-86. Epub 2000/10/18. PubMed PMID: 11033442.
156. Styrkarsdottir U, Cazier J-B, Kong A, Rolfsson O, Larsen H, Bjarnadottir E, et al. Linkage of Osteoporosis to Chromosome 20p12 and Association to BMP2. PLOS Biology. 2003;10(1371). doi: 10.1371/journal.pbio.0000069.
157. Medici M, van Meurs JB, Rivadeneira F, Zhao H, Arp PP, Hofman A, et al. BMP-2 gene polymorphisms and osteoporosis: the Rotterdam Study. J Bone Miner Res. 2006;21(6):845-54. Epub 2006/06/07. doi: 10.1359/jbmr.060306. PubMed PMID: 16753015.
158. Weidner H, Gao VY, Dibert D, McTague S, Eskander M, Duncan R, et al. CK2.3, a Mimetic Peptide of the BMP Type I Receptor, Increases Activity in Osteoblasts over BMP2. International Journal of Molecular Sciences. 2019;20(23):5877. doi: 10.3390/ijms20235877.
159. Liu DB, Sui C, Wu TT, Wu LZ, Zhu YY, Ren ZH. Association of Bone Morphogenetic Protein (BMP)/Smad Signaling Pathway with Fracture Healing and Osteogenic Ability in Senile Osteoporotic Fracture in Humans and Rats. Med Sci Monit. 242018. p. 4363-71.
160. Liang C, Peng S, Li J, Lu J, Guan D, Jiang F, et al. Inhibition of osteoblastic Smurf1 promotes bone formation in mouse models of distinctive age-related osteoporosis. Nat Commun. 2018;9(1):3428. Epub 2018/08/26. doi: 10.1038/s41467-018-05974-z. PubMed PMID: 30143635; PubMed Central PMCID: PMCPMC6109183.
161. Prall WC, Haasters F, Heggebo J, Polzer H, Schwarz C, Gassner C, et al. Mesenchymal stem cells from osteoporotic patients feature impaired signal transduction but sustained osteoinduction in response to BMP-2 stimulation. Biochem Biophys Res Commun. 2013;440(4):617-22. Epub 2013/10/09. doi: 10.1016/j.bbrc.2013.09.114. PubMed PMID: 24099772.
162. Osyczka AM, Diefenderfer DL, Bhargave G, Leboy PS. Different Effects of BMP-2 on Marrow Stromal Cells from Human and Rat Bone. Cells Tissues Organs. 2004;176(1-3):109-19. doi: 10.1159/000075032. PubMed PMID: 14745240.
163. Diefenderfer DL, Osyczka AM, Reilly GC, Leboy PS. BMP responsiveness in human mesenchymal stem cells. Connect Tissue Res. 2003;44 Suppl 1:305-11. Epub 2003/09/04. PubMed PMID: 12952214.
164. Benisch P, Schilling T, Klein-Hitpass L, Frey SP, Seefried L, Raaijmakers N, et al. The transcriptional profile of mesenchymal stem cell populations in primary osteoporosis is distinct and shows overexpression of osteogenic inhibitors. PLoS One. 2012;7(9):e45142. Epub 2012/10/03. doi: 10.1371/journal.pone.0045142. PubMed PMID: 23028809; PubMed Central PMCID: PMCPMC3454401.
165. Donoso O, Pino AM, Seitz G, Osses N, Rodriguez JP. Osteoporosis-associated alteration in the signalling status of BMP-2 in human MSCs under adipogenic

conditions. J Cell Biochem. 2015;116(7):1267-77. Epub 2015/02/03. doi: 10.1002/jcb.25082. PubMed PMID: 25640452.
166. Ehnert S, Aspera-Werz RH, Freude T, Reumann MK, Ochs BG, Bahrs C, et al. Distinct Gene Expression Patterns Defining Human Osteoblasts' Response to BMP2 Treatment: Is the Therapeutic Success All a Matter of Timing? Eur Surg Res. 2016;57(3-4):197-210. Epub 2016/11/05. doi: 10.1159/000447089. PubMed PMID: 27441597.
167. Liporace FA, Breitbart EA, Yoon RS, Doyle E, Paglia DN, Lin S. The effect of locally delivered recombinant human bone morphogenetic protein-2 with hydroxyapatite/tri-calcium phosphate on the biomechanical properties of bone in diabetes-related osteoporosis. J Orthop Traumatol. 2015;16(2):151-9. Epub 2014/11/26. doi: 10.1007/s10195-014-0327-6. PubMed PMID: 25421865; PubMed Central PMCID: PMCPMC4441641.
168. Zarrinkalam MR, Schultz CG, Ardern DW, Vernon-Roberts B, Moore RJ. Recombinant human bone morphogenetic protein-type 2 (rhBMP-2) enhances local bone formation in the lumbar spine of osteoporotic sheep. J Orthop Res. 2013;31(9):1390-7. Epub 2013/06/06. doi: 10.1002/jor.22387. PubMed PMID: 23737220.
169. Matsubara T, Kida K, Yamaguchi A, Hata K, Ichida F, Meguro H, et al. BMP2 regulates Osterix through Msx2 and Runx2 during osteoblast differentiation. J Biol Chem. 2008;283(43):29119-25. Epub 2008/08/16. doi: 10.1074/jbc.M801774200. PubMed PMID: 18703512; PubMed Central PMCID: PMCPMC2662012.
170. Ghosh-Choudhury N, Abboud SL, Nishimura R, Celeste A, Mahimainathan L, Choudhury GG. Requirement of BMP-2-induced phosphatidylinositol 3-kinase and Akt serine/threonine kinase in osteoblast differentiation and Smad-dependent BMP-2 gene transcription. J Biol Chem. 2002;277(36):33361-8. Epub 2002/06/27. doi: 10.1074/jbc.M205053200. PubMed PMID: 12084724.
171. Lai CF, Cheng SL. Signal transductions induced by bone morphogenetic protein-2 and transforming growth factor-beta in normal human osteoblastic cells. J Biol Chem. 2002;277(18):15514-22. Epub 2002/02/21. doi: 10.1074/jbc.M200794200. PubMed PMID: 11854297.
172. Gautschi OP, Frey SP, Zellweger R. Bone morphogenetic proteins in clinical applications. ANZ J Surg. 2007;77(8):626-31. Epub 2007/07/20. doi: 10.1111/j.1445-2197.2007.04175.x. PubMed PMID: 17635273.
173. Duncan JS, Litchfield DW. Too much of a good thing: the role of protein kinase CK2 in tumorigenesis and prospects for therapeutic inhibition of CK2. Biochim Biophys Acta. 2008;1784(1):33-47. Epub 2007/10/13. doi: 10.1016/j.bbapap.2007.08.017. PubMed PMID: 17931986.
174. Vilk G, Weber JE, Turowec JP, Duncan JS, Wu C, Derksen DR, et al. Protein kinase CK2 catalyzes tyrosine phosphorylation in mammalian cells. Cell Signal. 2008;20(11):1942-51. Epub 2008/07/30. doi: 10.1016/j.cellsig.2008.07.002. PubMed PMID: 18662771.

175. Zhu L, Schwegler-Berry D, Castranova V, He P. Internalization of caveolin-1 scaffolding domain facilitated by Antennapedia homeodomain attenuates PAF-induced increase in microvessel permeability. Am J Physiol Heart Circ Physiol. 2004;286(1):H195-201. Epub 2003/08/30. doi: 10.1152/ajpheart.00667.2003. PubMed PMID: 12946927.
176. Soğur E, esogur@yahoo.com, Department of Oral Diagnosis and Radiology SoD, Ege University, Izmir, Turkey, Baksı BG, Department of Oral Diagnosis and Radiology SoD, Ege University, Izmir, Turkey, Gröndahl H-G, et al. Pixel Intensity and Fractal Dimension of Periapical Lesions Visually Indiscernible in Radiographs. Journal of Endodontics. 2013;39(1):16-9. doi: 10.1016/j.joen.2012.10.016. PubMed PMID: 23228251.
177. Lofman O, Larsson L, Toss G. Bone mineral density in diagnosis of osteoporosis: reference population, definition of peak bone mass, and measured site determine prevalence. J Clin Densitom. 2000;3(2):177-86. Epub 2000/06/29. PubMed PMID: 10871911.
178. Bilbrey GL, Weix J, Kaplan GD. Value of single photon absorptiometry in osteoporosis screening. Clin Nucl Med. 1988;13(1):7-12. Epub 1988/01/01. PubMed PMID: 3349709.
179. Akkiraju H, Bonor J, Nohe A. An Improved Immunostaining and Imaging Methodology to Determine Cell and Protein Distributions within the Bone Environment. J Histochem Cytochem. 642016. p. 168-78.
180. Nohe A, Keating E, Underhill TM, Knaus P, Petersen NO. Dynamics and interaction of caveolin-1 isoforms with BMP-receptors. 2005. doi: 10.1242/jcs.01402.
181. Nohe A, Petersen NO. Image Correlation Spectroscopy. 2007. doi: 10.1126/stke.4172007pl7.
182. Pawley JB. Points, Pixels, and Gray Levels: Digitizing Image Data | SpringerLink. 2006. doi: 10.1007/978-0-387-45524-2_4.
183. JA P, IB S, JZ R, JK H. Quantifying Receptor Trafficking and Colocalization With Confocal Microscopy. Methods (San Diego, Calif). 2017;115. doi: 10.1016/j.ymeth.2017.01.005. PubMed PMID: 28131869.
184. A R, R A, B H, JB L, JL S, GS S, et al. Epigenetic Control of the Bone-master Runx2 Gene During Osteoblast-lineage Commitment by the Histone Demethylase JARID1B/KDM5B. The Journal of biological chemistry. 2015;290(47). doi: 10.1074/jbc.M115.657825. PubMed PMID: 26453309.
185. KJ L, TD S. Analysis of Relative Gene Expression Data Using Real-Time Quantitative PCR and the 2(-Delta Delta C(T)) Method. Methods (San Diego, Calif). 2001;25(4). doi: 10.1006/meth.2001.1262. PubMed PMID: 11846609.
186. Weidner H, Yuan Gao V, Dibert D, McTague S, Eskander M, Duncan R, et al. CK2.3, a Mimetic Peptide of the BMP Type I Receptor, Increases Activity in Osteoblasts over BMP2. International Journal of Molecular Sciences. 2019;20(23):5877. doi: 10.3390/ijms20235877.
187. Qin Y, Guan J, Zhang C. Mesenchymal stem cells: mechanisms and role in bone regeneration. Postgrad Med J. 902014. p. 643-7.

188. Lee SH. The advantages and limitations of mesenchymal stem cells in clinical application for treating human diseases. Osteoporos Sarcopenia. 42018. p. 150.
189. Marino S, Staines KA, Brown G, Howard-Jones RA, Adamczyk M. Models of ex vivo explant cultures: applications in bone research. Bonekey Rep. 52016.
190. James AW, LaChaud G, Shen J, Asatrian G, Nguyen V, Zhang X, et al. A Review of the Clinical Side Effects of Bone Morphogenetic Protein-2. Tissue Eng Part B Rev. 2016;22(4):284-97. Epub 2016/02/10. doi: 10.1089/ten.TEB.2015.0357. PubMed PMID: 26857241; PubMed Central PMCID: PMCPMC4964756.
191. Ichikawa S, Johnson, Michelle L., Koller DL, Lai D, Xuei X, Edenberg HJ, Hui SL, et al. Polymorphisms in the bone morphogenetic protein 2 (BMP2) gene do not affect bone mineral density in white men or women | SpringerLink. Osteoporosis International. 2006;17(4):587-92. doi: 10.1007/s00198-005-0018-5.
192. Warming L, Hassager C, Christiansen C. Changes in bone mineral density with age in men and women: a longitudinal study. Osteoporos Int. 2002;13(2):105-12. Epub 2002/03/22. doi: 10.1007/s001980200001. PubMed PMID: 11905520.
193. Rungby J, Kassem M, Fink Eriksen E, Danscher G. The von Kossa reaction for calcium deposits: silver lactate staining increases sensitivity and reduces background. The Histochemical Journal. 1993;25(6):446-51. doi: doi:10.1007/BF00157809.
194. Y M, L M, Q G, S Z. Expression of Bone Morphogenetic protein-2 and Its Receptors in Epithelial Ovarian Cancer and Their Influence on the Prognosis of Ovarian Cancer Patients. Journal of experimental & clinical cancer research : CR. 2010;29(1). doi: 10.1186/1756-9966-29-85. PubMed PMID: 20587070.
195. CM D, DB J, MJ S, K K, E S, CW A, et al. Mechanically Loaded Ex Vivo Bone Culture System 'Zetos': Systems and Culture Preparation. European cells & materials. 2006;11. doi: 10.22203/ecm.v011a07. PubMed PMID: 16612792.
196. CH B, EH E. Fluorescence of Bone. Nature. 1965;206(991). doi: 10.1038/2061328a0. PubMed PMID: 5838243.

APPENDIX A

A.1 IRB/ HUMAN SUBJECTS APPROVAL

CHRISTIANA CARE

Institutional Review Board
FWA00006557

Helen F. Graham Cancer Center
West Pavilion - Suite 2350
4701 Ogletown Stanton Road
Newark, DE 19713

302-623-4983 phone
302-623-4989 phone
302-623-6863 fax

MEMORANDUM

DATE: April 11, 2013

TO: Mark Eskander, MD
Orthopedics Research
Christiana Hospital

FROM: Sonia Martinez-Colon

RE: *CCC# 33053* - **The Efficacy of Treatment with the Novel Peptide CK2.3 in Inducing Mineralization in Human Osteoblasts in Relation to the Subjects' Prior Bone Mineral Density: (DDD# 602228)**

This is to officially inform you that your protocol was reviewed and determined to be exempt from Institutional Review Board oversight per *45 CFR 46.101(b) (4)* by Jerry Castellano, Pharm.D, CIP, Corporate Director of Christiana Care Health System Institutional Review Board, on **04/10/2013**.

Please note that if there are any changes to this protocol, such changes may alter the protocol's exemption status. If you need to make any amendments to your study or if you have any questions or concerns, please contact the IRB Office.

Thank you.

This approval verifies that the IRB operates in Accordance with applicable ICH, federal, local and institutional regulations, and with all GCP Guidelines that govern institutional IRB operation.

APPENDIX B

A.2 PERMISSIONS

International Journal of Molecular Sciences (MDPI), rights link.

https://www.mdpi.com/authors/rights